Robust stabilization of a system with distributed pumping

Electronic Systems, GR-1028, 05-2024

Master Thesis

AALBORG UNIVERSITY

STUDENT REPORT

Electronic Systems
Aalborg University
https://www.aau.dk

Title:
Robust stabilization of a system with distributed pumping

Theme:
Master thesis

Project Period:
Spring 2024

Project Group:
GR-1028

Participant(s):
Mikkel Schjøtt Pedersen
Rasmus Vestergaard Johansen

Supervisor(s):
Carsten Callesø
John-Josef Leth

Copies: Available online

Page Numbers: 94

Date of Completion:
31-05-2024

Abstract:

In this project, a cooling system using distributed pumps was analysed and examined for the possibility of designing robust controllers that can operate with uncertainty in the hydraulic connection. The cooling system consist of four different air handling units, containing pumps, which share the same cooling water through a hydraulic connection. To this extend a model was derived for the system, where the uncertainty was described using both norm-bounded and polytopic interpretations. The distribution of the pumps in the network required a specific structure of the controller, to which Linear Matrix Inequality based methods was used.
Based on the requirements on the controller, an examination was performed to find a possible design procedure that could handle the uncertainty in the hydraulic network.
The examinations found methods for designing state feedback and static output feedback controllers, which was robustly stable towards the uncertainties, while also fulfilling specific response requirements.

Rasmus Vestergaard Johansen
<rjohan19@student.aau.dk>

Mikkel Schjøtt Pedersen
<mipede19@student.aau.dk>

Preface

This report was written during the 4^{th} semester of the master's program *Electronic Systems* in spring 2024.

Reading guide

The report contains references as hyperlinks to elements in the bibliography, which can be found at the end of the report, before the appendices. The references are formatted using the Vancouver method, such that the sources in the text are framed as "[No.]" and numbered chronologically, such that the first source shown in the report will be [1]. The bibliography is, likewise, numbered in this order. In the bibliography, the sources are specified with author, title, publication month, year, and, if relevant, link and date of visit. In cases where the date of publication is unavailable, instead, the date of access is used. Immediately after the bibliography is the appendices, which are numbered using Roman numerals.

External appendices like MATLAB-scripts can be found on GitHub:
https://github.com/RasmusvJohansen/P10-Thesis-Matlab.

The figures, tables, etc. within this report are numbered in order of appearance and where in the report they are placed. For instance, figure 3.2 will be the second figure found within chapter 3. Figure captions are written beneath the figures, while table captions can be found above.

The report is written in accordance with the ISO 80000 standard. Matrices are denoted with bold upper-case letters, while vectors are denoted with bold lower-case letters. The notation $(\mathbf{M})_{\text{ij}}$ indicates the i,j entry of $\mathbf{M}$. $\mathbf{0}_{\text{n}\times\text{m}}$ is the $n \times m$ zero matrix and $\mathbf{1}_{\text{n}\times\text{m}}$ is the $n \times m$ matrix of ones, with $\mathbf{1}_n$ being a vector of ones. The identity matrix of size n is denoted $\mathbf{I}_{\text{n}}$. In some summations, matrices can be denoted $\mathbf{A}_{0\times 0}$. This is to be understood as the matrix does not exist. A $\star$ can occur in a matrix and is used to imply the value needed to make the matrix symmetric:

$$\begin{bmatrix} \mathbf{A} & \mathbf{B} \\ \star & \mathbf{C} \end{bmatrix} = \begin{bmatrix} \mathbf{A} & \mathbf{B} \\ \mathbf{B}^{\text{T}} & \mathbf{C} \end{bmatrix}$$

$\mathbf{vert}(\Delta)$ is the set of vertices of a convex polytope Δ.

Contents

Summary 1

This project examines the possibility of guaranteeing robust stability towards uncertainties in the hydraulic network of a heating ventilation and air condition (HVAC) system with distributed pumping. To this end, a model of the HVAC system was derived, with pumps in the individual air handling units (AHU), which is distributed throughout the system. Using the derived model state feedback (SF) and static output feedback (SOF) controllers was synthesised to achieve robust stability.

As the HVAC system utilizes distributed pumping, this introduced a requirement on the allowed structure of the controller. Specifically the controller had to have a block diagonal structure, which implied the pump only has measurements from its own AHU. To fulfill this requirement, linear matrix inequalities (LMIs) was utilized, as these are based on an optimisation problem, which allows for constraints and structure to be included.

In the case of SF, the uncertainties was defined as norm-bounded uncertainties, which implied synthesis could be performed based on the small gain theorem. The small gain theorem utilize the general control configuration in frequency domain, and as such it was necessary to relate to statespace which was achieved using bounded real lemma.

For SOF the uncertainties was redefined to be polytopic, which resulted in the system becoming a linear parameter varying (LPV) system, with the uncertainty being the parameter that varies. Utilizing that the uncertainties is time-invariant and described a convex hull, robust stability of such a LPV system was achieved by guaranteeing stability at each vertex. To achieve this, two different methods was investigated.

The design procedure for SF and SOF, resulted in controllers which could guarantee robust stability for their respective uncertainties. Furthermore, the design procedures was extended such that the system behaved according to a desired response using frequency weighted model matching.

Introduction 2

Today, Heating Ventilation and Air Conditioning (HVAC) systems are an important factor for providing comfort for occupants in a building, however HVAC is also among the largest consumers of energy in buildings. Especially in commercial buildings where almost 50% of the energy is used for cooling [1]. In 2016 cooling of buildings consumed just below 12.000 GW, with half of this being consumed by commercial buildings [2]. This number is expected to increase due to rising temperatures, as a results of climate changes and a growing middle class in developing countries, resulting in more households able to afford cooling. This would suggest that commissioning of HVAC is an important factor in the design process. However, it has been a problem in the building sector, and it is often not done to the necessary extend, primarily due to costs [2].

In addition, when the HVAC system is designed, it is often designed to work during normal operation, that being when every room of the system is active. However, when the system is deployed, it is practical to turn on the rooms independently, which could potentially lead to an unstable systems [3]. For this reason it would be practical, if the designed control scheme was stable in the both cases. Designing a single controller capable of this becomes complicated due to the connections of the HVAC system. HVAC systems typically consists of a hydraulic network, where a chiller is connected to a number of Air Handling Units (AHU)s, through a number of pipes which are shared between the AHUs as illustrated on figure 2.1.

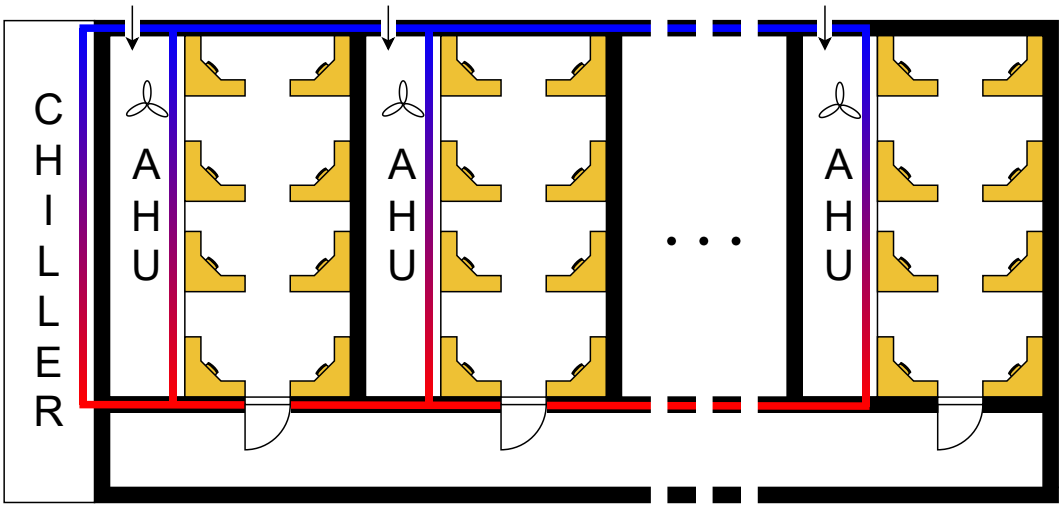

Figure 2.1: Illustration of the general structure of a HVAC system. Each AHU is connected in parallel with the chiller through pipes. The arrows indicate the inflow of air to the AHU, which is then chilled before entering the room.

Such a system can have different configurations, however, a new approach is to have pumps distributed at each AHU. Having a pump at the individual AHU also significantly reduces the price of both installing and operating the HVAC system [2]. The design structure also implies that each AHU is responsible for controlling its own temperature, usually through a PI controller [3]. This design is practical for the case of controlling the temperature for a single room, however when the entire system is considered, this design choice becomes problematic, as each AHU only has knowledge of its own temperatures and flows, which means the coupling of the hydraulic network is unaccounted for. An alternative design option could be that each AHU has knowledge of measurements from every AHU. This would require a centralized controller, which would eliminate the option of controlling each AHU individually. Additionally, having a centralized structure would also require communication between each AHUs sensor and the centralized controller, which would increase complexity.

Instead, it is investigated if a decentralized controller can be designed, using the existing structure, which can stabilize the individual AHUs, while being robust towards the influence from the changes caused by the other AHUs.

Requirements 3

To design a controller capable of fulfilling the specification introduced in chapter 2, the control scheme must be able to stabilize the decoupled system and be robust towards the uncertainties introduced in the hydraulic connection. Additionally it is required that the designed controller be decentralized, meaning an AHU can only react on changes measured by its own sensors. This implies that the designed controller must have a block diagonal structure.

Table 3.1: List of requirements

Requirement	Description
R.1	The designed controller must stabilize the decoupled system
R.2	The designed controller must be robust towards the uncertainties introduced by the hydraulic network.
R.3	The designed controller must have a block diagonal structure

Modelling 4

The HVAC system used in the project is based on a new design proposed in [2], where the hydraulic system has been modified to have dedicated pumps at the AHU, as opposed to control valves. An illustration of the system can be seen on figure 4.1.

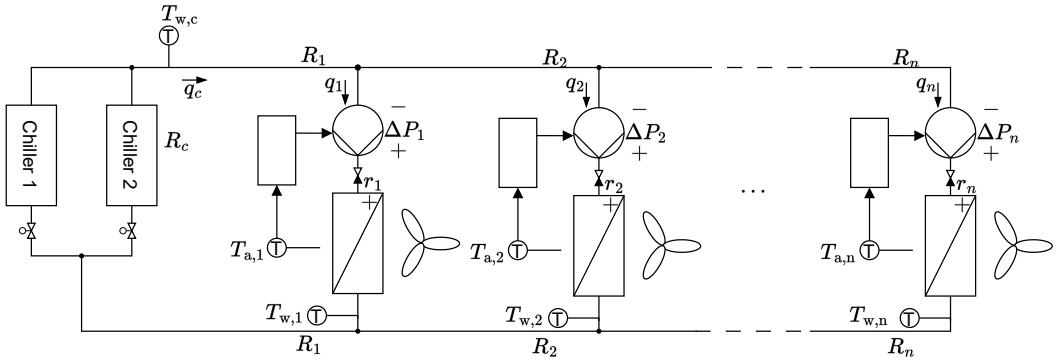

Figure 4.1: Illustration of the HVAC system used in the project [2].

To the left on figure 4.1 a pair of chillers can be seen, their responsibility is to cool the returning water, the chillers in the system are assumed to be designed and regulated such that a constant inlet water temperature $T_{\mathrm{w,c}}$ is maintained. Placed parallel to the chillers are n AHUs, which are responsible for adjusting the air temperature. To adjust the air temperature, each AHU use a pump in combination with sensors measuring the output temperature of the water and air in a Water to Air Heat Exchanger (WAHE). In addition, a one-way valve blocks the flow of water from returning to the pump, which implies the flow being in the clockwise direction on figure 4.1. The WAHE is the element responsible for the heat transfer between the chilled water and air, and is illustrated on figure 4.2.

On figure 4.2 the waterflow (q_{i}) is shown to flow left to right, while the airflow (Q_{i}) flows from bottom to the top. The middle part is the actual WAHE, where transfer of heat between the water and air occurs through convection. Convection describes heat transfer between two materials, due to a fluid or gas being moved. Generally convection can be

split into two categories, one called natural convection, where the convection happens due to natural reasons, such as when the heat transfers from a radiator to the air. The other category is forced convection, where the flow is induced by some mechanical actuation such as a pump.

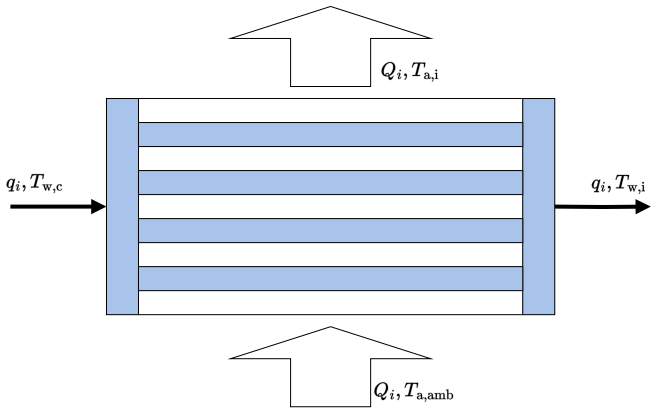

Figure 4.2: Illustration of the i'th WAHE, the blue area illustrates water volume, while the white is the air volume [3].

As the WAHE is a closed system, the flows in and out are the same, however due to the convection, the temperatures at the inlet and outlet of the water and air can be different. For the given system, the flowrate of air (Q_{i}) is assumed to be constant, as the fan moving the air is rotating at a constant angular velocity.

4.1 Thermodynamics

The WAHE depicted in figure 4.2 is modelled using a control volume approach, where the temperature dynamics of the air and water in the WAHE are described. The control volume approach is used, as the energy transfer in the WAHE is seen as homogeneous, implying that the temperature at the output is the same as within the WAHE. A one phase energy balance can be used as the phase of both the air and water remains the same, which means they can be expressed by:

$$\frac{c_{\mathrm{CV}} M_{\mathrm{CV}}(t) dT_{\mathrm{CV}}(t)}{dt} = P_{ext}(t) + cm_{\mathrm{in}}(t) T_{in}(t) - cm_{\mathrm{out}}(t) T_{out}(t) \tag{4.1}$$

Where:

c_{CV}	$\in \mathbb{R}$	specific heat capacity of control volume	$\left[\frac{\text{J}}{\text{KgK}}\right]$
M_{CV}	$\in \mathbb{R}$	Mass in control volume	[Kg]
T_{CV}	$\in \mathbb{R}$	Temperature in control volume	[K]
$\mathcal{P}_{\text{ext}}$	$\in \mathbb{R}$	External power in the system	[W]
c	$\in \mathbb{R}$	specific heat capacity of the material in the control volume	$\left[\frac{\text{J}}{\text{KgK}}\right]$
m_{in}	$\in \mathbb{R}$	mass flow into control volume	$\left[\frac{\text{Kg}}{\text{s}}\right]$
m_{out}	$\in \mathbb{R}$	mass flow out of control volume	$\left[\frac{\text{Kg}}{\text{s}}\right]$
T_{in}	$\in \mathbb{R}$	Temperatur into control volume	[K]
T_{out}	$\in \mathbb{R}$	Temperatur out of control volume	[K]

As the WAHE is homogeneous, the temperature of the control volume is the same as the outlet temperature, thereby $T_{\text{CV}}(t) = T_{\text{out}}(t)$. In (4.1) the energy balance is expressed in terms of the mass and massflows, however these parameters are unknown. Instead a representation in terms of the volume, density, and flowrate can be used as:

$$M_{\text{a}} = \rho_{\text{a}} V_{\text{a}} \qquad M_{\text{w}} = \rho_{\text{w}} V_{\text{w}} \tag{4.2}$$

$$m_{\text{a}} = Q\rho_{\text{a}} \qquad m_{\text{w}} = q(t)\rho_{\text{w}} \tag{4.3}$$

Where:

ρ_{w}	$\in \mathbb{R}$	Density of water	$\left[\frac{\text{Kg}}{\text{m}^3}\right]$
ρ_{a}	$\in \mathbb{R}$	Density of air	$\left[\frac{\text{Kg}}{\text{m}^3}\right]$
V_{w}	$\in \mathbb{R}$	Volume of water	$\left[\text{m}^3\right]$
V_{a}	$\in \mathbb{R}$	Volume of air	$\left[\text{m}^3\right]$
$q(t)$	$\in \mathbb{R}$	Flowrate of water	$\left[\frac{\text{m}^3}{\text{s}}\right]$
Q	$\in \mathbb{R}$	Flowrate of air	$\left[\frac{\text{m}^3}{\text{s}}\right]$

With this reformulation, the only remaining unknown is the external power, which is the transfer of energy between the water and air in the WAHE through convection, where the transferred power from material a to b can be described by:

$$P_{\text{convection},a\to b}(t) = A\alpha(T_{\text{a}}(t) - T_{\text{b}}(t)) \tag{4.4}$$

Where:

A	$\in \mathbb{R}$	Surface area of contact between the two materials transferring heat energy	$[\mathrm{m}^2]$
α	$\in \mathbb{R}$	Heat transfer coefficient of the two materials	$[\frac{\mathrm{W}}{\mathrm{m}^2\mathrm{K}}]$
T_a	$\in \mathbb{R}$	Temperature of material a	[K]
T_b	$\in \mathbb{R}$	Temperature of material b	[K]

The WAHE is assumed to absorb a negligible amount of energy from the convection between water and air. Therefore, the convection path can be reduced to, the convection from water to air, and air to water in the control volumes. As such, the convection can be described, based on the temperatures of water and air in the control volumes:

$$P_{\text{convection,w}\to\text{a}} = A\alpha(T_\mathrm{w} - T_\mathrm{a}) \tag{4.5}$$

$$P_{\text{convection,a}\to\text{w}} = A\alpha(T_\mathrm{a} - T_\mathrm{w}) \tag{4.6}$$

Where:

$T_\mathrm{w}(t)$	$\in \mathbb{R}$	The output temperature of the water control volume	[K]
$T_\mathrm{a}(t)$	$\in \mathbb{R}$	The output temperature of the air control volume	[K]

By pre-multiplying -1 in (4.6), both equations become identical, with only a change in sign. The constant $A\alpha$ can be combined to a single constant, describing the energy transfer from a know surface area.

$$B = A\alpha \tag{4.7}$$

Where:

B	$\in \mathbb{R}$	Heat transfer constant between air and water in a WAHE	$[\frac{\mathrm{W}}{\mathrm{K}}]$

The energy balance for water and air in a WAHE can then be described using (4.1), (4.2), (4.3), (4.5), and (4.7) as:

$$C_\mathrm{w}\rho_\mathrm{w}V_\mathrm{w}\frac{dT_\mathrm{w}(t)}{dt} = C_\mathrm{w}\rho_\mathrm{w}q(t)(T_{\mathrm{w,c}}(t) - T_\mathrm{w}(t)) - B(T_\mathrm{w}(t) - T_\mathrm{a}(t)) \tag{4.8}$$

$$C_\mathrm{a}\rho_\mathrm{a}V_\mathrm{a}\frac{dT_\mathrm{a}(t)}{dt} = C_\mathrm{a}\rho_\mathrm{a}Q(T_{\mathrm{a,amb}} - T_\mathrm{a}(t)) + B(T_\mathrm{w}(t) - T_\mathrm{a}(t)) \tag{4.9}$$

Where:

C_{w}	$\in \mathbb{R}$	Specific heat capacity of water	$\left[\frac{\mathrm{J}}{\mathrm{KgK}}\right]$
C_{a}	$\in \mathbb{R}$	Specific heat capacity of air	$\left[\frac{\mathrm{J}}{\mathrm{KgK}}\right]$
$T_{\mathrm{w,c}}$	$\in \mathbb{R}$	Temperature of the water entering the WAHE	[K]
$T_{\mathrm{a,amb}}$	$\in \mathbb{R}$	Temperature of the ambient air entering the WAHE	[K]

The input air temperature in the air energy balance of (4.9) use a constant temperature $T_{\mathrm{a,amb}}$. This choice is based on the assumption that the change of outdoor air temperature occurs slowly, and may therefore be seen as constant. As the HVAC system consists of n WAHE's the two expressions, (4.8) and (4.9), are extended to describe the i'th WAHE's energy balance, to this extend, the parameters $T_{\mathrm{a,amb}}$,$T_{\mathrm{w,c}}$, C_{A}, ρ_{A}, C_{W} and ρ_{W} does not change, as these are constant with respect to the specific HVAC system. The i'th WAHE energy balance can therefore be expressed as:

$$\begin{aligned} C_{\mathrm{w}}\rho_{\mathrm{w}}V_{\mathrm{w,i}}\frac{dT_{\mathrm{w,i}}(t)}{dt} &= C_{\mathrm{w}}\rho_{\mathrm{w}}q_{\mathrm{i}}(t)(T_{\mathrm{w,c}}(t) - T_{\mathrm{w,i}}(t)) - B_{\mathrm{i}}(T_{\mathrm{w,i}}(t) - T_{\mathrm{a,i}}(t)) \\ C_{\mathrm{a}}\rho_{\mathrm{a}}V_{\mathrm{a,i}}\frac{dT_{\mathrm{a,i}}(t)}{dt} &= C_{\mathrm{a}}\rho_{\mathrm{a}}Q_{\mathrm{i}}(T_{\mathrm{a,amb}} - T_{\mathrm{a,i}}(t)) + B_{\mathrm{i}}(T_{\mathrm{w,i}}(t) - T_{\mathrm{a,i}}(t)) \end{aligned} \tag{4.10}$$

4.2 Hydraulics

The dynamics found in (4.10) assumes that the input is the flow of water (q_{i}) in the individual AHU. However, no direct way of controlling the flow exists, instead the flow can be found from the angular velocity of the pump, which can be controlled. For this, a relation between the angular velocity of the pump and the waterflow must be derived. This can be achieved by modeling the dynamics of the hydraulic system.

Firstly the individual elements of the system from figure 4.1 is modelled. From a hydraulic modelling perspective, the chiller, WAHE, and pipes can all be modeled as a pipe with the equation:

$$\Delta P = \frac{L\rho}{A}\frac{dq}{dt} + R|q|q \tag{4.11}$$

Where:

ΔP	$\in \mathbb{R}$	Pressure difference	[Pa]
L	$\in \mathbb{R}$	Length of the pipe	[m]
A	$\in \mathbb{R}$	Cross-sectional area of the pipe	$\left[\mathrm{m}^2\right]$
R	$\in \mathbb{R}$	Resistance of the pipe	$\left[\frac{\mathrm{Pa\ s}}{\mathrm{m}^3}\right]$

(4.11) has the term $|q|q$ to describe the direction of flow, however as the system on figure 4.1 incorporates a one-way valve in every loop, this expression can be written as q^2.

To model the chiller using (4.11), the flow q_c must first be derived as it is not available. The flow can be found by using KCL on the hydraulic network illustrated on figure 4.1. Applying this, the flow into an vertex must be equal to the flow out, which by extending through the system results in the that flow from the chillers must be equal to the sum of flows from all n pumps. This means the chiller can be modelled as:

$$\Delta P_\mathrm{c} = \frac{L_\mathrm{c}\rho}{A_\mathrm{c}} \frac{d\sum_{\mathrm{k}=1}^{n} q_\mathrm{k}}{dt} + R_\mathrm{c}\left(\sum_{\mathrm{k}=1}^{n} q_\mathrm{k}\right)^2 \tag{4.12}$$

The flow though the WAHE in the i'th AHU is simply the flow generated by the pump in the respective AHU. This means that the WAHE can be modelled as:

$$\Delta P_{\mathrm{W,i}} = \frac{L_{\mathrm{r,i}}\rho}{A_{\mathrm{r,i}}} \frac{dq_\mathrm{i}}{dt} + r_\mathrm{i} q_\mathrm{i}^2 \tag{4.13}$$

When modelling the pipes, the flow though the different pipe sections change, the further down the network the pipe is located. Nevertheless, using KCL, similar to the chiller, it is known that the flows in a section of pipe, must be equal to the total flow of all AHU further down the network. This results in the model for the i'th pipe segment as:

$$\Delta P_{\mathrm{R,i}} = \frac{L_{\mathrm{R,i}}\rho}{A_{\mathrm{R,i}}} \frac{d\sum_{\mathrm{k}=\mathrm{i}}^{n} q_\mathrm{k}}{dt} + R_\mathrm{i}\left(\sum_{\mathrm{k}=\mathrm{i}}^{n} q_\mathrm{k}\right)^2 \tag{4.14}$$

The last element in the network is the pump. The pump used in the system is a centrifugal pump, which can be modelled as [2]:

$$\Delta P_\mathrm{p},i = -a_\mathrm{i} q_\mathrm{i}^2 + b_\mathrm{i}\omega_\mathrm{i}^2 \tag{4.15}$$

With a model for the different elements of the hydraulic network derived, a model for the individual loops can be derived using KVL. To do this, the pressure change of the i'th loop can be expressed as a sum of the pressure changes over the chiller, i'th WAHE, i'th pump, and two times the sum of the pipes from the chiller down to the i'th AHU. This results in the expression:

$$\Delta P_\mathrm{i} = \underbrace{\frac{L_\mathrm{c}\rho}{A_\mathrm{c}} \frac{d\sum_{\mathrm{k}=1}^{n} q_\mathrm{k}}{dt} + R_\mathrm{c}\left(\sum_{\mathrm{k}=1}^{n} q_\mathrm{k}\right)^2}_{\text{Chiller}} + \underbrace{\frac{L_{\mathrm{r,i}}\rho}{A_{\mathrm{r,i}}} \frac{dq_\mathrm{i}}{dt} + r_\mathrm{i} q_\mathrm{i}^2}_{\text{WAHE}} - \underbrace{(-a_\mathrm{i} q_\mathrm{i}^2 + b_\mathrm{i}\omega_\mathrm{i}^2)}_{\text{Pump}} + \underbrace{2\sum_{\mathrm{m}=1}^{i}\left(\frac{L_{\mathrm{R,i}}\rho}{A_{\mathrm{R,i}}} \frac{d\sum_{\mathrm{k}=\mathrm{m}}^{n} q_\mathrm{k}}{dt} + R_\mathrm{m}\left(\sum_{\mathrm{k}=\mathrm{m}}^{n} q_\mathrm{k}\right)^2\right)}_{\text{Pipe}} \tag{4.16}$$

This expression can be isolated for the changes in flow ($\frac{dq}{dt}$), to express the dynamics of the hydraulic network. These dynamics can then be used in combination with the dynamics of the thermodynamics from (4.10) to describe the dynamics of the HVAC system. However, as the changes in the hydraulic network is much faster than the thermodynamics and the network is stable, (4.16) can be modelled using only the static components [3]. This results in a static expression for the relation between the flowrate and angular velocity of the i'th pump as:

$$\Delta P_{\mathrm{i}} = \underbrace{r_{\mathrm{i}} q_{\mathrm{i}}^2}_{\text{WAHE}} + \underbrace{R_{\mathrm{c}} \left(\sum_{\mathrm{k}=1}^{n} q_{\mathrm{k}} \right)^2}_{\text{Chiller}} - \underbrace{(-a_{\mathrm{i}} q_{\mathrm{i}}^2 + b_{\mathrm{i}} \omega_{\mathrm{i}}^2)}_{\text{Pump}} + \underbrace{2 \sum_{\mathrm{m}=1}^{i} R_{\mathrm{m}} \left(\sum_{\mathrm{k}=\mathrm{m}}^{n} q_{\mathrm{k}} \right)^2}_{\text{Pipe}} \tag{4.17}$$

KVL dictates that the total pressure change of the closed loop must be equal to 0, which means the angular velocity can be isolated:

$$\omega_{\mathrm{i}}^2 = \frac{a_{\mathrm{i}} + r_{\mathrm{i}}}{b_{\mathrm{i}}} q_{\mathrm{i}}^2 + \frac{R_{\mathrm{c}}}{b_{\mathrm{i}}} \left(\sum_{\mathrm{k}=1}^{n} q_{\mathrm{k}} \right)^2 + 2 \sum_{\mathrm{m}=1}^{i} \frac{R_{\mathrm{m}}}{b_{\mathrm{i}}} \left(\sum_{\mathrm{k}=\mathrm{m}}^{n} q_{\mathrm{k}} \right)^2 \tag{4.18}$$

This expression can now be used in (4.10) to express the flowrate in terms of the pumps angular velocity. However, (4.18) shows that a coupling exists between the individual pumps and the flowrates throughout the system, which implies that changing the angular velocity of one pump affects the flowrate of the entire network.

4.3 System representation

With the thermodynamics and hydraulics expressed, a system representation can be made. Firstly, since the normal structure uses PI, an additional integral state is added for the temperature of the air. This assures that the desired air temperature is reached. With this state and the thermodynamics from (4.10) the system dynamics can be expressed as:

$$\begin{aligned} \dot{T}_{\mathrm{w,i}}(t) &= \frac{q_{\mathrm{i}}(t)}{V_{\mathrm{w,i}}} \left(T_{\mathrm{w,c}} - T_{\mathrm{w,i}}(t) \right) - \frac{B_{\mathrm{i}}}{C_{\mathrm{w}} \rho_{\mathrm{w}} V_{\mathrm{w,i}}} \left(T_{\mathrm{w,i}}(t) - T_{\mathrm{a,i}}(t) \right) \\ \dot{T}_{\mathrm{a,i}}(t) &= \frac{Q_{\mathrm{i}}}{V_{\mathrm{a,i}}} \left(T_{\mathrm{a,amb}} - T_{\mathrm{a,i}}(t) \right) + \frac{B_{\mathrm{i}}}{C_{\mathrm{a}} \rho_{\mathrm{a}} V_{\mathrm{a,i}}} \left(T_{\mathrm{w,i}}(t) - T_{\mathrm{a,i}}(t) \right) \\ \dot{\delta}_{\mathrm{i}} &= T_{\mathrm{a,i}} - T_{\mathrm{ref,i}} \end{aligned} \tag{4.19}$$

Where:

$T_{\mathrm{ref,i}}$	$\in \mathbb{R}$	is the reference for the WAHE output air temperature	[K]
δ_{i}	$\in \mathbb{R}$	is the integral state	[K]

Before any additional derivations is performed, the controllability of the individual WAHE is investigated. For the system to be controllable, the controllability matrix must have full rank. The controllability matrix is however only defined for linear system, and therefore (4.19) is linearised using a first order Taylor approximation, which is defined as:

$$\mathbf{f}(\mathbf{x},\mathbf{u}) \approx \mathbf{f}(\mathbf{x}^*,\mathbf{u}^*) + \left.\frac{\partial \mathbf{f}(\mathbf{x},\mathbf{u})}{\partial \mathbf{x}}\right|_{\substack{\mathbf{x}=\mathbf{x}^* \\ \mathbf{u}=\mathbf{u}^*}} (\mathbf{x}-\mathbf{x}^*) + \left.\frac{\partial \mathbf{f}(\mathbf{x},\mathbf{u})}{\partial \mathbf{u}}\right|_{\substack{\mathbf{x}=\mathbf{x}^* \\ \mathbf{u}=\mathbf{u}^*}} (\mathbf{u}-\mathbf{u}^*) \tag{4.20}$$

This linearisation method requires an operating point ($\mathbf{x}^*$,$\mathbf{u}^*$). When defining an operating point, it is desirable that the system is in steady state, which for (4.19) means the temperatures and flow do not change. The point at which this is the case can be calculated by defining $T^*_{\mathrm{a,i}} = T_{\mathrm{ref,i}}$, which reduced the remaining equations to:

$$\begin{aligned} T^*_{\mathrm{w,i}} &= \frac{B_{\mathrm{i}} T^*_{\mathrm{a,i}} - C_{\mathrm{a}}\rho_{\mathrm{a}} Q_{\mathrm{i}} \left(T_{\mathrm{a,amb}} - T^*_{\mathrm{a,i}}\right)}{B_{\mathrm{i}}} \\ q^*_{\mathrm{i}} &= \frac{B_{\mathrm{i}} \left(T^*_{\mathrm{w,i}} - T^*_{\mathrm{a,i}}\right)}{C_{\mathrm{w}}\rho_{\mathrm{w}} \left(T_{\mathrm{w,c}} - T^*_{\mathrm{w,i}}\right)} \end{aligned} \tag{4.21}$$

This operating point (q^*_{i},$T^*_{\mathrm{w,i}}$,$T^*_{\mathrm{a,i}}$, 0) can then be used in the first order Taylor approximation (4.20) to derive a linearised model where $\mathbf{x} = \begin{bmatrix} T_{\mathrm{w,i}} & T_{\mathrm{a,i}} & \delta_{\mathrm{i}} \end{bmatrix}^{\mathrm{T}}$ and $u = q_{\mathrm{i}}$. Since the operating point is found at a steady state, $\mathbf{f}(\mathbf{x}^*,u^*) = \mathbf{0}$, as a result the linearised model becomes:

$$\dot{\mathbf{x}} = \underbrace{\left.\frac{\partial \mathbf{f}(\mathbf{x},\mathbf{u})}{\partial \mathbf{x}}\right|_{\substack{\mathbf{x}=\mathbf{x}^* \\ u=u^*}}}_{\mathbf{A}} (\mathbf{x}-\mathbf{x}^*) + \underbrace{\left.\frac{\partial \mathbf{f}(\mathbf{x},\mathbf{u})}{\partial \mathbf{u}}\right|_{\substack{\mathbf{x}=\mathbf{x}^* \\ u=u^*}}}_{\mathbf{B}} (u-u^*) \tag{4.22}$$

with

$$\begin{aligned} \left.\frac{\partial f(\mathbf{x},\mathbf{u})}{\partial \mathbf{x}}\right|_{\substack{\mathbf{x}=\mathbf{x}^* \\ \mathbf{u}=\mathbf{u}^*}} &= \begin{bmatrix} -\left(\frac{q^*_{\mathrm{i}}}{V_{\mathrm{w,i}}} + \frac{B_{\mathrm{i}}}{C_{\mathrm{w}}\rho_{\mathrm{w}}V_{\mathrm{w,i}}}\right) & \frac{B_{\mathrm{i}}}{C_{\mathrm{w}}\rho_{\mathrm{w}}V_{\mathrm{w,i}}} & 0 \\ \frac{B_{\mathrm{i}}}{C_{\mathrm{a}}\rho_{\mathrm{a}}V_{\mathrm{a,i}}} & -\left(\frac{Q_{\mathrm{i}}}{V_{\mathrm{a,i}}} + \frac{B_{\mathrm{i}}}{C_{\mathrm{a}}\rho_{\mathrm{a}}V_{\mathrm{a,i}}}\right) & 0 \\ 0 & 1 & 0 \end{bmatrix} \\ \left.\frac{\partial f(\mathbf{x},\mathbf{u})}{\partial \mathbf{u}}\right|_{\substack{\mathbf{x}=\mathbf{x}^* \\ \mathbf{u}=\mathbf{u}^*}} &= \begin{bmatrix} \left(\frac{T_{\mathrm{w,c}} - T^*_{\mathrm{w,i}}}{V_{\mathrm{w,i}}}\right) \\ 0 \\ 0 \end{bmatrix} \end{aligned} \tag{4.22a}$$

These matrices are used in appendix I to derive the determinant of the controllability matrix as:

$$\det(\boldsymbol{\mathcal{C}}) = \left(\frac{T_{\mathrm{w,c}} - T^*_{\mathrm{w,i}}}{V_{\mathrm{w,i}}}\right)^3 \left(\frac{B_{\mathrm{i}}}{C_{\mathrm{a}}\rho_{\mathrm{a}}V_{\mathrm{a,i}}}\right)^2 \tag{4.23}$$

For a system to be controllable, the determinant must be different from zero. From (4.23) the specific heat capacity (C_a) and density (ρ_a) are physical constants which are different from zero, in addition the heat transfer coefficient (B_i) is different from zero. The presence of the WAHE implies the volumes $V_\mathrm{w,i}$ and $V_\mathrm{a,i}$ are different from zero, which means that that the determinant is different from zero when the temperature of the water is different from the temperature of the chiller. As shown in appendix I, the singularity is linked to the choice of air temperature reference, it is therefore possible to avoid this singularity through the choice of the reference.

With controllability handled, an expression for the entire system is derived. From (4.19), it is apparent that the equations can be restructured into a bilinear expression in terms of the states and input. This expression can be written in matrix form as:

$$\dot{\mathbf{z}}_\mathrm{i} = \mathbf{F}_\mathrm{i}\mathbf{z}_\mathrm{i} + \mathbf{M}_\mathrm{i}\mathbf{z}_\mathrm{i}q_\mathrm{i} + \mathbf{G}_\mathrm{i}q_\mathrm{i} + \mathbf{E}_\mathrm{i} \tag{4.24}$$

with

$$\begin{aligned}
\mathbf{z}_\mathrm{i} &= \begin{bmatrix} T_\mathrm{w,i} \\ T_\mathrm{a,i} \\ \delta_\mathrm{i} \end{bmatrix}, \qquad \mathbf{F}_\mathrm{i} = \begin{bmatrix} \frac{-B_\mathrm{i}}{C_\mathrm{w}\rho_\mathrm{w}V_\mathrm{w,i}} & \frac{B_\mathrm{i}}{C_\mathrm{w}\rho_\mathrm{w}V_\mathrm{w,i}} & 0 \\ \frac{B_\mathrm{i}}{C_\mathrm{a}\rho_\mathrm{a}V_\mathrm{a,i}} & -\left(\frac{Q_\mathrm{i}}{V_\mathrm{a,i}} + \frac{B_\mathrm{i}}{C_\mathrm{a}\rho_\mathrm{a}V_\mathrm{a,i}}\right) & 0 \\ 0 & 1 & 0 \end{bmatrix} \\
\mathbf{M}_\mathrm{i} &= \begin{bmatrix} -\frac{1}{V_\mathrm{w,i}} & 0 & 0 \\ 0 & 0 & 0 \\ 0 & 0 & 0 \end{bmatrix}, \qquad \mathbf{G}_\mathrm{i} = \begin{bmatrix} \frac{T_\mathrm{w,c}}{V_\mathrm{w,i}} \\ 0 \\ 0 \end{bmatrix}, \qquad \mathbf{E}_\mathrm{i} = \begin{bmatrix} 0 \\ \frac{Q_\mathrm{i}T_\mathrm{a,amb}}{V_\mathrm{a,i}} \\ -T_\mathrm{ref,i} \end{bmatrix}
\end{aligned} \tag{4.24a}$$

Where:

$\mathbf{z}_\mathrm{i}$	$\in \mathbb{R}^{3\times1}$	is the states of the i'th WAHE
$\mathbf{F}_\mathrm{i}$	$\in \mathbb{R}^{3\times3}$	is a matrix describing the dynamics relating to only the states
$\mathbf{M}_\mathrm{i}$	$\in \mathbb{R}^{3\times3}$	is a matrix describing the dynamics relating to both states and inputs
$\mathbf{G}_\mathrm{i}$	$\in \mathbb{R}^{3\times1}$	is a vector describing the dynamics relating to only the inputs
$\mathbf{E}_\mathrm{i}$	$\in \mathbb{R}^{3\times1}$	is a vector describing the dynamics not dependent on state or input.

This describes the dynamics of the i'th WAHE, however a description for the entire system is desired. Such a description can be derived by expanding (4.24) to n WAHEs, by combining the matrices as block diagonals. Additionally, it is assumed every state is directly measurable at the output, which in results in the system:

$$\begin{aligned} \dot{\boldsymbol{\xi}} &= \boldsymbol{\mathcal{F}}\boldsymbol{\xi} + \mathbf{H}(\boldsymbol{\xi})\mathbf{q} + \boldsymbol{\mathcal{G}}\mathbf{q} + \boldsymbol{\mathcal{E}} \\ \mathbf{y} &= \mathbf{C}\boldsymbol{\xi} \end{aligned} \tag{4.25}$$

Where:

$\boldsymbol{\mathcal{F}}$	$\in \mathbb{R}^{3n\times 3n}$	is the block diagonal matrix diag $(\mathbf{F}_1, \ldots, \mathbf{F}_\mathrm{n})$
$\mathbf{H}(\boldsymbol{\xi})$	$\in \mathbb{R}^{3n\times n}$	is the block diagonal matrix diag $(\mathbf{M}_1\mathbf{z}_1, \ldots, \mathbf{M}_\mathrm{n}\mathbf{z}_\mathrm{n})$
$\boldsymbol{\mathcal{G}}$	$\in \mathbb{R}^{3n\times n}$	is the block diagonal matrix diag $(\mathbf{G}_1, \ldots, \mathbf{G}_\mathrm{n})$
$\boldsymbol{\mathcal{E}}$	$\in \mathbb{R}^{3n\times 1}$	is the vector $\begin{bmatrix} \mathbf{E}_1 & \ldots & \mathbf{E}_\mathrm{n} \end{bmatrix}^\mathrm{T}$
$\boldsymbol{\xi}$	$\in \mathbb{R}^{3n\times 1}$	is the vector $\begin{bmatrix} \mathbf{z}_1 & \ldots & \mathbf{z}_\mathrm{n} \end{bmatrix}^\mathrm{T}$
$\mathbf{q}$	$\in \mathbb{R}^{n\times 1}$	is the vector $\begin{bmatrix} q_1 & \ldots & q_\mathrm{n} \end{bmatrix}^\mathrm{T}$
n	$\in \mathbb{R}$	is the number of WAHE's in the system
$\mathbf{C}$	$\in \mathbb{R}^{12\times 12}$	is the output matrix defined as $\mathbf{I}_{12}$

With the thermodynamics of the entire system described in terms of the flow, this expression is altered to be described in terms of the pumps angular velocity as expressed in (4.17). However, as the the designed controller must be stable in both the case where every AHU is on and only one is on, two different models are needed. One model which takes the coupling of the hydraulics into account and one that ignores it. These two different models are denoted *coupled* and *decoupled*-model and are derived in the following sections.

4.3.1 Decoupled model

In the decoupled model, the hydraulic coupling is ignored, which means that the flows not originating form the i'th pump are ignored. This is equivalent to $q_\mathrm{j} = 0$ for $j \neq i$, which means (4.17) reduces to:

$$\omega_\mathrm{i}^2 = \left(\frac{a_\mathrm{i} + r_\mathrm{i}}{b_\mathrm{i}} + \frac{R_\mathrm{c}}{b_\mathrm{i}} + \sum_{m=1}^{i} 2\frac{R_\mathrm{m}}{b_\mathrm{i}} \right) q_\mathrm{i}^2 \tag{4.26}$$

Due to the physical construction of the system, the direction of flow is the same as the direction of the angular velocity, this implies that $\mathrm{sign}(\omega_\mathrm{i}) = \mathrm{sign}(q_\mathrm{i})$, which further implies (4.26), can be written as:

$$\omega_{\mathrm{i}} = \sqrt{\frac{a_{\mathrm{i}} + r_{\mathrm{i}}}{b_{\mathrm{i}}} + \frac{R_{\mathrm{c}}}{b_{\mathrm{i}}} + \sum_{m=1}^{i} 2\frac{R_{\mathrm{m}}}{b_{\mathrm{i}}}}\, q_{\mathrm{i}} \tag{4.27}$$

As the terms in the square root is constant, these can be defined as a $\bar{\alpha}_{\mathrm{i}}$. In addition, (4.27) can be extended to every WAHE and isolated for the flow as:

$$\mathbf{q} = \bar{\mathbf{\Lambda}}^{-1}\boldsymbol{\omega} \tag{4.28}$$

Where:

$\bar{\mathbf{\Lambda}}$	$\in \mathbb{R}^{n\times n}$	is the diagonal matrix diag $(\bar{\alpha}_1, \ldots, \bar{\alpha}_{\mathrm{n}})$
$\boldsymbol{\omega}$	$\in \mathbb{R}^{n\times 1}$	is the vector $\begin{bmatrix}\omega_1 & \ldots & \omega_{\mathrm{n}}\end{bmatrix}^{\mathrm{T}}$

Substituting (4.28) into (4.25) results in:

$$\dot{\boldsymbol{\xi}} = \bar{\mathbf{\Phi}}(\boldsymbol{\xi},\boldsymbol{\omega}) = \boldsymbol{\mathcal{F}}\boldsymbol{\xi} + \mathbf{H}(\boldsymbol{\xi})\bar{\mathbf{\Lambda}}^{-1}\boldsymbol{\omega} + \boldsymbol{\mathcal{G}}\bar{\mathbf{\Lambda}}^{-1}\boldsymbol{\omega} + \boldsymbol{\mathcal{E}} \tag{4.29}$$

This model describes the dynamics of the thermodynamic system without considering the coupling introduced by the hydraulic connections.

4.3.2 Coupled model

In the coupled model the hydraulic coupling described in (4.17) must be considered. This definition can be reformulated into a quadratic expression as [3]:

$$\omega_{\mathrm{i}}^2 = \mathbf{q}^{\mathrm{T}}(\mathbf{\Lambda}_{\mathrm{i}} + \mathbf{\Psi}_{\mathrm{i}} + \mathbf{\Gamma}_{\mathrm{i}})\mathbf{q} = \mathbf{q}^{\mathrm{T}}\mathbf{S}_{\mathrm{i}}\mathbf{q} \tag{4.30}$$

with

$$(\mathbf{\Lambda}_{\mathrm{i}})_{\mathrm{jl}} = \begin{cases} \alpha_{\mathrm{i}} \triangleq \frac{r_{\mathrm{i}}+a_{\mathrm{i}}}{b_{\mathrm{i}}}, & j = l = i \\ 0, & \text{otherwise} \end{cases}$$

$$\mathbf{\Psi}_{\mathrm{i}} = \frac{R_{\mathrm{c}}}{b_{\mathrm{i}}}\mathbf{1}_{n\times n} \triangleq \psi_{\mathrm{i}}\mathbf{1}_{n\times n} \tag{4.30a}$$

$$\mathbf{\Gamma}_{\mathrm{i}} = \sum_{m=1}^{i} 2\frac{R_{\mathrm{m}}}{b_{\mathrm{i}}}\mathrm{diag}\left(\mathbf{0}_{(m-1)\times(m-1)}, \mathbf{1}_{(n-m+1)\times(n-m+1)}\right)$$

Using this formulation for the pump, a function relating the angular velocity of the pumps to the flows can be formulated as:

$$\boldsymbol{\omega} = \mathbf{f}(\mathbf{q}) = \begin{bmatrix} \sqrt{\mathbf{q}^{\mathrm{T}}\mathbf{S}_1\mathbf{q}} \\ \vdots \\ \sqrt{\mathbf{q}^{\mathrm{T}}\mathbf{S}_{\mathrm{n}}\mathbf{q}} \end{bmatrix} \tag{4.31}$$

It is, however, the inverse of this function, if it exists, that is desired, since this would describe the flow in terms of the angular velocity. To determine if an inverse exists the inverse function theorem is used. This theorem states that if $\mathbf{f}(\mathbf{x})$ is differentiable at a point $\mathbf{x}$ and its derivative $\frac{\partial \mathbf{f}}{\partial \mathbf{x}}(\mathbf{x})$ is continuous and non singular at $\mathbf{x}$, then there exists a local inverse function $\mathbf{f}^{-1}(\mathbf{x})$ which is also differentiable. Firstly the derivative $\frac{\partial \mathbf{f}}{\partial \mathbf{q}}(\mathbf{q})$ is found from (4.31). Note that since the water can only flow in the positive direction $\mathbf{q} > 0$ then $\mathbf{q}^{\mathrm{T}}\mathbf{S}_{\mathrm{i}}\mathbf{q} > 0$.

$$\frac{\partial \mathbf{f}(\mathbf{q})}{\partial \mathbf{q}} = \begin{bmatrix} \rho_1(\mathbf{q})\mathbf{S}_1\mathbf{q} & \dots & \rho_{\mathrm{n}}(\mathbf{q})\mathbf{S}_{\mathrm{n}}\mathbf{q} \end{bmatrix}^{\mathrm{T}} \tag{4.32}$$

with

$$\rho_{\mathrm{i}}(\mathbf{q}) = \frac{1}{\sqrt{\mathbf{q}^{\mathrm{T}}\mathbf{S}_{\mathrm{i}}\mathbf{q}}} > 0 \tag{4.32a}$$

In this projects it is assumed that the Jacobian (4.32) is non singular at $\mathbf{q}$ and an inverse always exists. In fact, the inverse exists in almost every case, and the simulations performed could calculate the inverse. As such the inverse is defined as:

$$\mathbf{g}(\boldsymbol{\omega}) = \mathbf{f}(\mathbf{q})^{-1} \tag{4.33}$$

Inserting this function into (4.25), results in a description of the coupled system as:

$$\dot{\boldsymbol{\xi}} = \boldsymbol{\Phi}(\boldsymbol{\xi},\boldsymbol{\omega}) = \boldsymbol{\mathcal{F}}\boldsymbol{\xi} + \mathbf{H}(\boldsymbol{\xi})\mathrm{g}(\boldsymbol{\omega}) + \boldsymbol{\mathcal{G}}\mathrm{g}(\boldsymbol{\omega}) + \boldsymbol{\mathcal{E}} \tag{4.34}$$

With a model describing the dynamics of both the coupled and decoupled system, these can now be used to design a control scheme, which stabilizes both the decoupled and coupled dynamics.

Uncertainty modelling and control schemes 5

Based on the requirements from chapter 3, this project aims at deriving a design procedure for a controller, which can guarantee robust stability towards uncertainty in the inputs, the model derived in the previous chapter must first be expanded to include these uncertainties. As such, the first part of this chapter explores uncertainty modelling and robust control. Furthermore, it is necessary to limit the synthesised controller to be block diagonal. This is important, as the designed controller can only operate on a given AHU and that AHUs measurements. This limits the design approaches, as traditional control schemes such as pole placement and Linear Quadratic Regulator both design a full feedback matrix. Instead, to ensure that the feedback matrix has a block diagonal structure, control schemes using optimisation are investigated, as these has the possibility to apply a constraint on the structure of the feedback matrix. Specifically, an alternative control scheme using Linear Matrix Inequalities (LMI)s is investigated, as this offers the necessary constraints on the feedback matrix. Control design using LMI requires a linear model, and therefore the two models are first linearised.

5.1 Linearisation and state feedback

As the control should take into account the coupled and decoupled model, both models are linearised. The models are linearised using a first order Taylor approximation as shown in (4.20). In addition to the linearisation, the control, in terms of state feedback, is also applied to the models (4.29) and (4.34). State feedback is defined as $\mathbf{u} = \mathbf{K}\mathbf{x}$, however as the models are linearised $\mathbf{u} = (\boldsymbol{\omega} - \boldsymbol{\omega}^*)$, where $\boldsymbol{\omega}^*$ is the operating point for the angular velocities. With this linearisation, the state feedback becomes:

$$\begin{aligned} (\boldsymbol{\omega} - \boldsymbol{\omega}^*) &= \mathbf{K}\mathbf{x} \\ \boldsymbol{\omega} &= \mathbf{K}\mathbf{x} + \boldsymbol{\omega}^* \end{aligned} \tag{5.1}$$

The operating point $\boldsymbol{\omega}^*$ is different for the coupled and decoupled model. These different operating points are hereafter denoted $\bar{\boldsymbol{\omega}}^*$ for the decoupled model and $\boldsymbol{\omega}^*$ for the coupled model.

5.1.1 Decoupled model

The decoupled model (4.29) is linearised around the states $\boldsymbol{\xi}^*$, which are the states at the operating point from (4.21), and the inputs $\bar{\boldsymbol{\omega}}^*$ which gives the linearised model:

$$\dot{\boldsymbol{\xi}} = \left(\boldsymbol{\mathcal{F}} + \mathbf{H}(\bar{\boldsymbol{\Lambda}}^{-1}\bar{\boldsymbol{\omega}}^*)\right)(\boldsymbol{\xi} - \boldsymbol{\xi}^*) + \left(\mathbf{H}(\boldsymbol{\xi}^*)\bar{\boldsymbol{\Lambda}}^{-1} + \boldsymbol{\mathcal{G}}\bar{\boldsymbol{\Lambda}}^{-1}\right)(\boldsymbol{\omega} - \bar{\boldsymbol{\omega}}^*) \tag{5.2}$$

Applying the state feedback from (5.1) and defining $\mathbf{x} = (\boldsymbol{\xi} - \boldsymbol{\xi}^*)$ results in the linear state space model:

$$\dot{\mathbf{x}} = \left(\underbrace{\boldsymbol{\mathcal{F}} + \mathbf{H}(\bar{\boldsymbol{\Lambda}}^{-1}\bar{\boldsymbol{\omega}}^*)}_{\bar{\mathbf{A}}} + \underbrace{\left(\mathbf{H}(\boldsymbol{\xi}^*) + \boldsymbol{\mathcal{G}}\right)\bar{\boldsymbol{\Lambda}}^{-1}}_{\bar{\mathbf{B}}}\mathbf{K}\right)\mathbf{x} \tag{5.3}$$

5.1.2 Coupled model

The same approach can be applied to the coupled model on (4.34). Firstly the equation is linearised around the states $\boldsymbol{\xi}^*$ and the inputs $\boldsymbol{\omega}^*$ which gives the linearised model:

$$\dot{\boldsymbol{\xi}} = \left(\boldsymbol{\mathcal{F}} + \mathbf{H}\Big(\mathbf{g}\left(\boldsymbol{\omega}^*\right)\Big)\right)(\boldsymbol{\xi} - \boldsymbol{\xi}^*) + \left(\left(\mathbf{H}(\boldsymbol{\xi}^*) + \boldsymbol{\mathcal{G}}\right)\frac{\partial \mathbf{g}(\boldsymbol{\omega}^*)}{\partial \boldsymbol{\omega}}\right)(\boldsymbol{\omega} - \boldsymbol{\omega}^*) \tag{5.4}$$

Note that $\frac{\partial \mathbf{g}(\boldsymbol{\omega}^*)}{\partial \boldsymbol{\omega}}$ is the inverse of the derivative of the function $\mathbf{f}(\mathbf{q})$, which means $\frac{\partial \mathbf{g}(\boldsymbol{\omega}^*)}{\partial \boldsymbol{\omega}} = \left(\frac{\partial \mathbf{f}(\mathbf{q}^*)}{\partial \mathbf{q}}\right)^{-1}$, where $\mathbf{q}^*$ is the operating point for the hydraulic flows. Applying the state feedback from (5.1) and defining $\mathbf{x} = (\boldsymbol{\xi} - \boldsymbol{\xi}^*)$ results in the linear state space model:

$$\dot{\mathbf{x}} = \left(\underbrace{\boldsymbol{\mathcal{F}} + \mathbf{H}\Big(\mathbf{g}\left(\boldsymbol{\omega}^*\right)\Big)}_{\mathbf{A}} + \underbrace{\left(\mathbf{H}(\boldsymbol{\xi}^*) + \boldsymbol{\mathcal{G}}\right)\frac{\partial \mathbf{g}(\boldsymbol{\omega}^*)}{\partial \boldsymbol{\omega}}}_{\mathbf{B}}\mathbf{K}\right)\mathbf{x} \tag{5.5}$$

5.1.3 Comparison

By comparing (5.3) and (5.5), it can be seen the that the system matrix $\bar{\mathbf{A}}$ and $\mathbf{A}$ are identical since $\bar{\boldsymbol{\Lambda}}^{-1}\bar{\boldsymbol{\omega}}^* = \mathbf{q}^* = \mathbf{g}\left(\boldsymbol{\omega}^*\right)$. This was expected as these matrices describes the systems dynamics without input, which is the linearised thermodynamics, and therefore $\mathbf{A}$ is used to describe both models. As the difference between the two system originates in the hydraulic network, these are tied to the inputs of the system, which are described by $\bar{\mathbf{B}}$ and $\mathbf{B}$. Indeed, by investigating these two matrices it can be seen that these differ by the decoupled model having the term $\bar{\boldsymbol{\Lambda}}^{-1}$, while the coupled system has $\frac{\partial \mathbf{g}(\boldsymbol{\omega}^*)}{\partial \boldsymbol{\omega}}$. By simulating a open-loop step response of the two linearised system, shown on figure 5.1, the impact of the hydraulic becomes apparent.

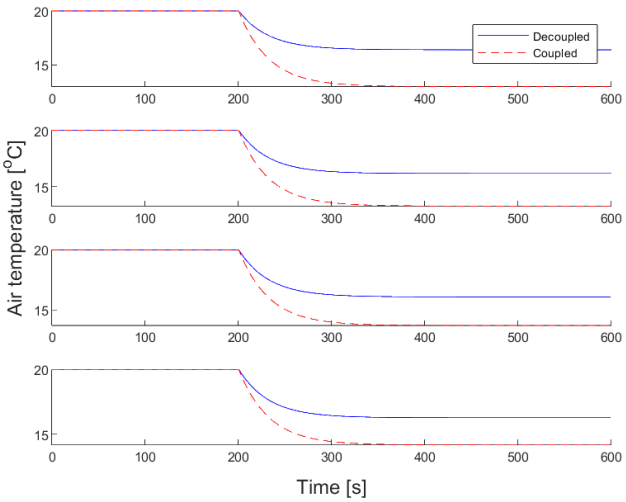

Figure 5.1: Open-loop step response of the linearised decoupled and coupled system.

From the difference between it is clear that the designed controller should be able to stabilize both system. Additionally the coupled model introduces connections from the hydraulics, which has been simplified. Therefore, the designed controller should be robust towards these uncertainties.

5.2 Uncertainties in models

When designing a controller, the model is supposed to describe the dynamics of the physical system which is to be controlled. However, when deriving a model, it is well known that the mathematical model is different from the physical model [4]. These differences in the model are known as model uncertainties, and originates from inaccuracies and assumptions in the modeling process. As such, there are many different sources of uncertainties, but these can be categorized into either dynamic or parametric uncertainties [4].

When these uncertain models are used to design a controller, this controller is guaranteed to perform differently than designed, since the system it controls is different from the one it was designed on [4]. Due to this, the notion of robust control was introduced to formulate analysis and design tools which guarantee stability and performance despite these uncertainties. The dynamics in robust control theory is represented in terms of a set of possible models which describes the systems and its uncertainties. This set, often denoted $\tilde{\mathbf{G}}$, is defined by the nominal, or average, model $\mathbf{G}_0$ and a set of bounded uncertainties $\mathbf{\Delta}$.

As previously stated, these uncertainties are categorised into parametric and dynamic uncertainties. Parametric uncertainties are the ones describing an uncertainty with respect to a parameter. With these types of uncertainties the dynamic equation is known, however the parametric values are uncertain [4]. These types of uncertainties are typical when systems are linearised or determined through identification techniques. Given these uncertainties only describe parameters, it is assumed the uncertainty of a given parameter is in the interval $[\rho_{\min}, \rho_{\max}]$, from which a general form can be expressed as [4]:

$$\rho = \rho_0 + \rho_{\mathrm{d}}\delta \tag{5.6}$$

Where:

ρ	$\in \mathbb{R}$	is the uncertain parameter
ρ_0	$\in \mathbb{R}$	is the nominal parameter value
ρ_{d}	$\in \mathbb{R}$	is the difference $\frac{\rho_{\max}-\rho_{\min}}{2}$
δ	$\in \mathbb{R}$	is the bounded uncertainty given by: $\lvert\delta\rvert < 1$

Dynamic uncertainties describe dynamics which are unaccounted for in the mathematical model. These are often higher frequency dynamics, which are deliberately ignored so a lower order model is obtained, it can however also be dynamics due to physical phenomenons which are unknown [4]. As these uncertainties are more complex, no single way of representing them exists. Instead, different representations exist depending on the suspected type of uncertainty. Commonly used LTI representations are input multiplicative uncertainty, output multiplicative uncertainty, and additive uncertainty, which influence can be seen from the illustrations on figure 5.2.

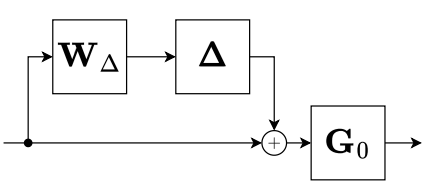

(a) Input multiplicative uncertainty.

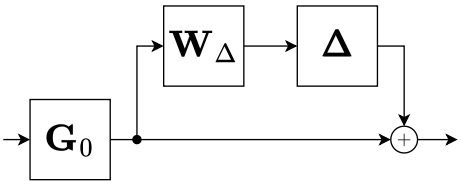

(b) Output multiplicative uncertainty.

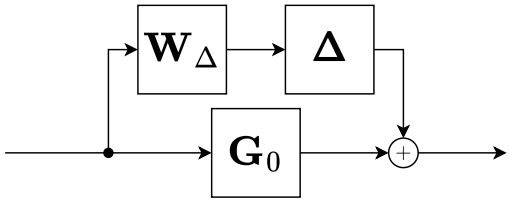

(c) Additive uncertainty.

Figure 5.2: Commonly used types of uncertainties [5, p.293].

In the case of input multiplicative uncertainties, these can be expressed by the model [4]:

$$\tilde{\mathbf{G}} = \left\{ \mathbf{G}(s) \quad | \quad \mathbf{G}(s) = \mathbf{G}_0(s)(\mathbf{I}_4 + \mathbf{\Delta}\mathbf{W}_\Delta(s)), \quad \mathbf{\Delta} \in ||\Delta||_\infty \leq 1 \right\} \tag{5.7}$$

Where:

$\tilde{\mathbf{G}}$	is the set of transfer functions for the uncertain system
$\mathbf{G}_0(s)$	is the nominal model
$\mathbf{W}_\Delta(s)$	is the maximal multiplicative model deviation
$\mathbf{\Delta}$	is the set of uncertainties defined by all stable transfer function Δ fulfilling $\|\|\Delta\|\|_\infty \leq 1$

While these two categories of uncertainties describe different aspects, both are often present when modeling [4]. This might not be intuitive, but when modelling low frequencies, the dynamics are often known, but the specific parameters are uncertain, while the higher frequency dynamics are often assumed insignificant. Given both types of uncertainties are present, a representation of both is desired. Such a representation can be expressed as an extended general control configuration shown on figure 5.3a [5, p.289]. The general control configuration provides a useful structure during analysis and synthesis of a controller. Furthermore, figure 5.3a can be transformed into the NΔ-structure on figure 5.3b. In this structure, the controller has been used to close the interconnection of **y** and **u** loop, and as such the new structure is useful for analysis of the system with a controller [5, p.289].

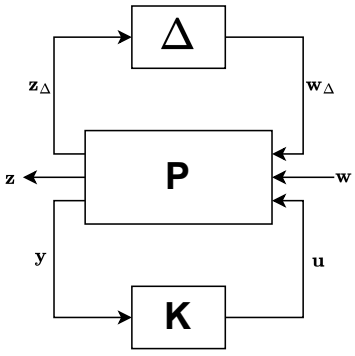

(a) The general control configuration, where P is the model of the interconnections between the inputs and outputs, K is the controller, and Δ is the uncertainties [5, p.290].

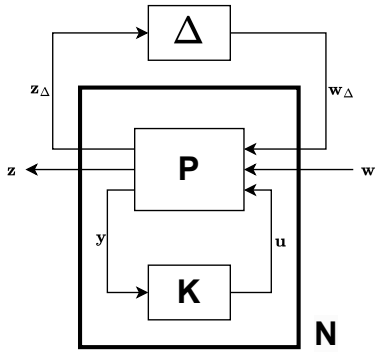

(b) The NΔ-structure where the interconnection with the controller has been incorporated into the N block [5, p.290].

Figure 5.3: General control configurations, where (a) is used for synthesis while (b) is used for analysis.

Until now $\mathbf{\Delta} \in \mathbb{C}^{p \times q}$ has been assumed to be any uncertainty fulfilling $||\mathbf{\Delta}||_\infty < 1$, which is also known as unstructured uncertainties. This assumption implied that no structural information of the uncertainties are considered, hence the naming. Instead, in cases where knowledge of the structure of the uncertainties are available, $\mathbf{\Delta}$ can be redefined to be a block diagonal matrix whose diagonal entries encapsulate the given structure of the uncertainty. Following this, the uncertainty can be formulated as:

$$\text{Unstructured: } \mathbf{\Delta}_\text{U} = \{\mathbf{\Delta} \in \mathbb{C}^{p \times q} \mid ||\mathbf{\Delta}||_\infty < 1\} \tag{5.8}$$

$$\text{Structured: } \mathbf{\Delta}_\text{S} = \begin{bmatrix} \mathbf{\Delta}_1 & \mathbf{0} & \mathbf{0} \\ \mathbf{0} & \ddots & \mathbf{0} \\ \mathbf{0} & \mathbf{0} & \mathbf{\Delta}_\text{n} \end{bmatrix} = \{\mathbf{\Delta}_\text{i} \in \mathbb{C}^{p_\text{i} \times q_\text{i}} \mid ||\mathbf{\Delta}_\text{i}||_\infty < 1\} \tag{5.9}$$

From the two definitions, it can be seen that the structured uncertainties is a subset of unstructured uncertainties.

5.3 Robust stability

As previously stated, every model has uncertainties, and as such it is necessary to find a condition which guarantees the designed system be stable for all these uncertainties [4]. If the system is stable for every uncertainty, then the system is said to be robust stable. More specific robust stability is defined for a given controller $\mathbf{K}$ as [6, p.97]:

Robust stability: *$\boldsymbol{K}$ robustly stabilizes figure 5.3b against the uncertainties $\mathbf{\Delta}_\text{i} \in \mathbf{\Delta}$ if $\boldsymbol{K}$ stabilizes the system figure 5.3b for any uncertainty $\mathbf{\Delta}_\text{i}$ taken out of the underlying set $\mathbf{\Delta}$.*

This definition requires validating if the system is stable for every uncertainty in the set, which is inefficient, and as such the definition is of little use given it cannot be tested efficiently [5, p.300]. If instead, the interconnection between $\mathbf{w}_\Delta$ and $\mathbf{z}_\Delta$, as illustrated on figure 5.4, is investigated, a condition for robust stability can be defined by the small gain theorem [7, p.66]:

Theorem 1 (Small gain theorem) *Assume that $||\boldsymbol{M}||_\infty < 1$ and $||\mathbf{\Delta}||_\infty \leq 1$, then the interconnection on figure 5.4 is asymptotically stable, meaning any initial condition close to an equilibrium will be driven to the equilibrium, for every uncertainty in the set $\mathbf{\Delta}$.*

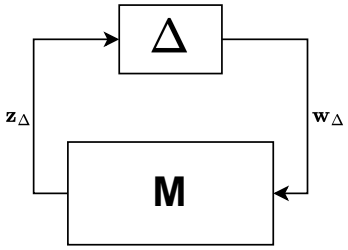

Figure 5.4: The MΔ-structure, where $\mathbf{M}$, derived from $\mathbf{N}$, describers the interconnection between $\mathbf{w}_\Delta$ and $\mathbf{z}_\Delta$.

This implies that by verifying the H_∞-norm of $\mathbf{M}(s)$ is less than 1, then the system is robust stable towards the uncertainties bounded by $||\mathbf{\Delta}||_\infty \leq 1$. This gives a simple condition, which can efficiently be calculated, to verify robust stability. The H_∞-norm has two definitions depending on the type of system. For SISO systems the H_∞ describes the largest gain $\|G(s)\|_\infty = \max_s |G(s)|$, while for MIMO systems H_∞ describes the largest singular value $\|\mathbf{G}(s)\|_\infty = \max_s \sigma(|\mathbf{G}(s)|)$ [5, p.60,80]. Unfortunately both definitions are only applicable for transfer functions, however, a bound on the H_∞-norm can be determined for a state space representation by the bounded real lemma [7, p.64]:

Lemma 1.1 (Bounded real lemma) *Let us consider an LTI system with transfer function:*

$$\widehat{\boldsymbol{G}}(s) = \boldsymbol{C}(s\boldsymbol{I} + \boldsymbol{A})^{-1}\boldsymbol{B} + \boldsymbol{D}$$

Then, the following statements are equivalent:

1. *The H_∞-norm of $\widehat{\boldsymbol{G}}$ is smaller than $\gamma > 0$.*
2. *There exists a $\boldsymbol{P} > 0$ such that the LMI*

$$\begin{bmatrix} \boldsymbol{A}^T\boldsymbol{P} + \boldsymbol{P}\boldsymbol{A} & \boldsymbol{P}\boldsymbol{B} & \boldsymbol{C}^T \\ \star & -\gamma\boldsymbol{I} & \boldsymbol{D}^T \\ \star & \star & -\gamma\boldsymbol{I} \end{bmatrix} < 0 \tag{5.10}$$

holds.

Combining theorem 1 and lemma 1.1, robust stability for a state space model can be guaranteed if the LMI in (5.10) is feasible for a $\gamma \leq 1$. The small gain theorem disregard structure in the uncertainty, and as such is only applicable for unstructured uncertainties. Due to this, the theorem yields conservative results in cases where the uncertainty is structured or parametric [4].

Since the uncertainty itself is not present in $\mathbf{M}$, and therefore not part of the calculation of the norm, simply structuring $\mathbf{\Delta}$ will not influence the calculation. Instead, the structure of the uncertainties can be introduced by using scaling matrices, which is structured in accordance with the uncertainty [5, p.306]. The scaling matrix $\mathbf{D}$ must be structured as a block-diagonal matrix, with dimensions corresponding to the respective dimensions of the uncertainty. To achieve the desired structure in $\mathbf{\Delta}$, the block-diagonals in $\mathbf{D}$, must be constructed following the relation in (5.11) [5, p.310]:

$$\begin{aligned} \mathbf{\Delta} &= \delta\mathbf{I}, & \mathbf{D} &= \text{Full matrix} \\ \mathbf{\Delta} &= \text{Full matrix}, & \mathbf{D} &= \delta\mathbf{I} \\ \mathbf{\Delta} &= \begin{bmatrix} \Delta_1 & 0 \\ 0 & \Delta_2 \end{bmatrix}, \Delta_1 \text{ and } \Delta_2 \text{ Full matrix}, & \mathbf{D} &= \begin{bmatrix} \delta_1\mathbf{I} & 0 \\ 0 & \delta_2\mathbf{I} \end{bmatrix}, \end{aligned} \tag{5.11}$$

In theory, any non-singular matrix which commute with the uncertainty, that is $\mathbf{\Delta D} = \mathbf{D\Delta}$, can be applied, which leads to the set of possible $\mathbf{D}$ as:

$$\boldsymbol{\mathcal{D}} = \left\{ \mathbf{D} \quad | \quad \mathbf{\Delta D} = \mathbf{D\Delta}, \right\} \tag{5.12}$$

The scaling matrix can be applied to the MΔ-structure as:

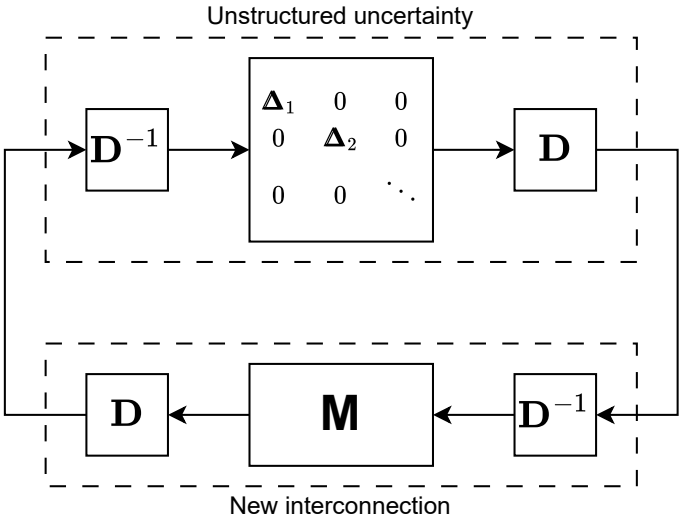

Figure 5.5: Interconnection of the MΔ-structure where the scaling matrices $\mathbf{D}$ is included to introduce structure [5, p.305].

By calculating the uncertainty in the upper box on figure 5.5, it can be seen that if $\mathbf{D}$ is structured in accordance with $\mathbf{\Delta D} = \mathbf{D\Delta}$, then the unstructured uncertainty reemerges [5, p.306]. Since $\mathbf{DD}^{-1} = \mathbf{I}$, the scaling matrices does not influence the closed loop

stability, however the new system, for which the stability is to be determined, is now given by $\mathbf{DMD}^{-1}$, which means the structure is included and will influence the norm. Using this structure, a new condition for robust stability can be formulated as [5, p.306]:

$$\min_{\mathbf{D}(\omega)\in\boldsymbol{\mathcal{D}}} ||\mathbf{D}(\omega)\mathbf{M}(j\omega)\mathbf{D}(\omega)^{-1}||_\infty < 1, \quad \forall\omega \tag{5.13}$$

While this condition can be used to determine a scaled H_∞-norm, it requires solving the minimisation for every frequency, meaning an infinite number of calculations. A better condition can be formulated in terms of the structured singular value, which uses this minimisation problem as a bound.

5.3.1 Structured Singular Value

The Structured Singular Value (SSV) is a function which generalizes the singular value and spectral radius [5, p.306]. More specifically, it provides a value for the H_∞-norm given any structure of the uncertainties. The SSV of $\mathbf{M}$ wrt. the set $\boldsymbol{\Delta}$ is defined as [6, p.113]:

$$\mu_\Delta(\mathbf{M}) = \frac{1}{\sup\{r|\det(\mathbf{I}-\mathbf{M}\Delta)\neq 0 \quad \forall\Delta\in r\boldsymbol{\Delta}\}} \tag{5.14}$$

This definition of the SSV states, that one should find the maximum value r, for which $\mathbf{I}-\mathbf{M}\Delta$ is non-singular in the set $r\boldsymbol{\Delta}$, which is essentially a scaling of the set of uncertainties [6, p.113]. The SSV is unfortunately difficult to calculate directly, however, efficient methods exists for determining an upper bound. By using the scaling matrix $\mathbf{D}$, the smallest upper bound can be found as [5, p.310]:

$$\mu_{\boldsymbol{\Delta}}(\mathbf{M}(j\omega)) \leq \min_{\mathbf{D}(\omega)\in\boldsymbol{\mathcal{D}}} ||\mathbf{D}(\omega)\mathbf{M}(j\omega)\mathbf{D}(\omega)^{-1}||_\infty, \quad \forall\omega \tag{5.15}$$

This minimization problem is convex and can be formulated as a Linear Matrix Inequality (LMI) [6, p.126]. From (5.13) and using (5.15), a condition for robust stability for structured uncertainty can be formulated as a generalization of the small-gain theorem [5, p.306]:

Theorem 2 (Generalized small gain theorem) *Assume that $\mu_{\boldsymbol{\Delta}}(\boldsymbol{M}(s)) < 1$ and $||\boldsymbol{\Delta}||_\infty \leq 1$, then the interconnection on figure 5.4 is asymptotically stable toward any structured uncertainty $\boldsymbol{\Delta}$.*

This condition requires the SSV must be below 1 for every frequency, however in practice the SSV is calculated for a finite number of frequencies an interpolated. The worst SSV can then be found and used to determine the bounds, and hence stability. This method gives an acceptable estimate, as the SSV is a continuous function when the uncertainties

are complex [6, p.124]. Another property of the SSV, is that it is monotonic in the set $\mathbf{\Delta}$. i.e. assume two sets of matrices satisfy:

$$\mathbf{\Delta}_1 \subset \mathbf{\Delta}_2 \tag{5.16a}$$

then

$$\mu_{\mathbf{\Delta}_1}(\mathbf{M}) \leq \mu_{\mathbf{\Delta}_2}(\mathbf{M}) \tag{5.16b}$$

Furthermore the SSV can be calculated explicitly for the following structures:

$$\begin{aligned} \mu_{\mathbf{\Delta}_1}(\mathbf{M}(s)) &= \rho\big(\mathbf{M}(s)\big), \qquad \mathbf{\Delta}_1 = \{\delta\mathbf{I} \in \mathbb{C}^{p\times q} \quad | \quad ||\delta||_\infty < 1\} \\ \mu_{\mathbf{\Delta}_2}(\mathbf{M}(s)) &= ||\mathbf{M}(s)||_\infty, \qquad \mathbf{\Delta}_2 = \{\mathbf{\Delta} \in \mathbb{C}^{p\times q} \quad | \quad ||\mathbf{\Delta}||_\infty < 1\} \end{aligned} \tag{5.17}$$

where $\rho(\cdot)$ is the spectral radius. These structures, given the monotonicity, has the property:

$$\mathbf{\Delta}_1 \subset \mathbf{\Delta} \subset \mathbf{\Delta}_2 \tag{5.18}$$

Which implies SSV must be bound by the H_∞-norm and the spectral radius:

$$\rho(\mathbf{M}(s)) \leq \mu_{\mathbf{\Delta}}(\mathbf{M}(s)) \leq ||\mathbf{M}(s)||_\infty \tag{5.19}$$

From this, it can be concluded that the SSV is bounded by the spectral radius and H_∞-norm, which implies that every possible structure of the uncertainties must be within these bounds. Addition, since the spectral radius gives the lowest possible value of the SSV, if this is larger than 1, then no structure can guarantee robust stability.

5.4 LMI Framework

The previously mentioned upper bound on the SSV can be found by solving an LMI, in addition, the bounded real lemma is defined as an LMI, and robust stability also requires that the system, with controller, is stable, which can also be defined as an LMI. Therefore, a brief introduction to LMIs are made. An LMI is an affine linear inequality defined over some variable called a matrix variable. This simply means that LMIs are convex constraints, which can be applied to an optimisation problem and solved with numerical methods [5, p.473]. More specifically, LMIs are a part of SemiDefinite Programming (SDP), which is a subfield of convex optimisation, where a linear objective function is constrained by LMIs and/or linear equality constraints, as such SDP problems are structured as:

$$\begin{aligned} \underset{\mathbf{x}}{\text{minimize}} \quad & \mathbf{c}^{\mathrm{T}}\mathbf{x} \\ \text{subject to} \quad & \mathbf{F}(\mathbf{x}) = \mathbf{F}_0 + \sum_{\mathrm{i}=1}^{m} x_{\mathrm{i}}\mathbf{F}_{\mathrm{i}} \geq 0 \\ & \mathbf{A}\mathbf{x} = \mathbf{b} \end{aligned} \tag{5.20}$$

Where:

m	$\in \mathbb{W}$	is the number of variables, which for the worst case is $\mathbf{F}_\mathrm{i} \in \mathbb{R}^{q_\mathrm{i} \times p_\mathrm{i}}$ is given by: $\sum_{\mathrm{i}=1}^{n}(q_\mathrm{i} \cdot p_\mathrm{i})$

Since these problems are convex, a solution can efficiently be found and the solution is guaranteed to be a global minimum. In this project YALMIP with the MOSEK solver is used to solve these problems, for more information the reader is referred to appendix II.

Due to LMIs being a part of SDP, many different problems, often categorised as LMI problems, can be formulated [5, p.476-479]. Most notable are *Linear objective minimization problem* (LOMP), *Generalized Eigenvalue Problem* (GEVP), and *LMI feasibility problem* (LMIFP). In LOMP and GEVP some linear function is minimized or maximized, where the difference between the two is that for LOMP, the objective must be convex, while in GEVP the objective can be quashi convex. On the other hand, the LMIFP is not attempting to find an optimal solution, instead it attempts to find a feasible solution, and as such the solution is not guaranteed to be unique. This essentially means the objective function on (5.20) is 0, which implies the problem is solved only subject to the LMI constraints.

The application of LMIs in control theory is not apparent from the formulation of the LMI problems, however their use emerges from Lyapunovs theory of Stability, which states that a continuous autonomous linear system $\dot{\mathbf{x}} = \mathbf{A}\mathbf{x}$ is stable iff there exists a [5, p.476]:

$$\mathbf{P} > 0 \tag{5.21}$$

such that

$$\mathbf{A}^{\mathrm{T}}\mathbf{P} + \mathbf{P}\mathbf{A} < 0 \tag{5.21a}$$

Where:

$\mathbf{A}$	$\in \mathbb{R}^{n \times n}$	State matrix
$\mathbf{P}$	$\in \mathbb{R}^{n \times n}$	Is the symmetric matrix variable for the LMI problem

If this LMI is feasible, then it is equivalent to the more traditional definition that, all states must go to $\mathbf{0}$ as time goes to infinity, or stability of the system is guaranteed iff. $\mathrm{Re}\{\lambda_\mathrm{i}(\mathbf{A})\} < 0, \forall i$. This definition allows for the validation of stability for a given continuous system. However, if the system is extended to contain an input, that is $\dot{\mathbf{x}} = \mathbf{A}\mathbf{x} + \mathbf{B}\mathbf{u}$, and apply a control law for state feedback $\mathbf{u} = \mathbf{K}\mathbf{x}$, then the dynamics of

the system becomes:

$$\dot{\mathbf{x}} = (\mathbf{A} + \mathbf{BK})\mathbf{x} \tag{5.22}$$

Where:

$\mathbf{B}$	$\in \mathbb{R}^{n \times p}$	input matrix
$\mathbf{K}$	$\in \mathbb{R}^{p \times n}$	state feedback

From the definition of stability in (5.21), it can be seen that the stability is now dependent on the feedback matrix $\mathbf{K}$. This implies that if $\mathbf{K}$ is set as a variable in the optimisation problem, then the LMI can be used to find a feedback $\mathbf{K}$ guaranteeing the system is stable. Writing Lyapunovs stability (5.21) for the system with feedback results in the inequality:

$$\begin{aligned} (\mathbf{A} + \mathbf{BK})^{\mathrm{T}} \mathbf{P} + \mathbf{P} (\mathbf{A} + \mathbf{BK}) < 0 \Rightarrow \\ \mathbf{A}^{\mathrm{T}}\mathbf{P} + \mathbf{PA} + \mathbf{K}^{\mathrm{T}}\mathbf{B}^{\mathrm{T}}\mathbf{P} + \mathbf{PBK} < 0 \end{aligned} \tag{5.23}$$

As (5.23) contains a nonlinearity it is no longer a LMI, but a bilinear matrix inequality. This can be rectified by changing the definition of the variables. This however, requires the variables to be next to each other in the terms, therefore a congruence transform with $\mathbf{P}^{-1}$ is applied resulting in:

$$\mathbf{P}^{-1}\mathbf{A}^{\mathrm{T}} + \mathbf{AP}^{-1} + \mathbf{P}^{-1}\mathbf{K}^{\mathrm{T}}\mathbf{B}^{\mathrm{T}} + \mathbf{BKP}^{-1} < 0 \tag{5.24}$$

Now with the variables causing the nonlinearities being next to each other, two new variables are defined as $\mathbf{Q} = \mathbf{P}^{-1}$ and $\mathbf{Y} = \mathbf{KQ}$, resulting in the LMI:

$$\mathbf{QA}^{\mathrm{T}} + \mathbf{AQ} + \mathbf{Y}^{\mathrm{T}}\mathbf{B}^{\mathrm{T}} + \mathbf{YB} < 0 \tag{5.25}$$

If the LMI is feasible for $\mathbf{Q} > 0$ and $\mathbf{Y}$, then $\mathbf{K}$ can be recovered as $\mathbf{K} = \mathbf{YQ}^{-1}$.

Application 6

This chapter aims to apply the methods described in chapter 5 to obtain a robustly stable controller for the system described in chapter 4. Initially parameters of the system will be given, afterwards the different methods will be applied.

6.1 System Parameters

The parameters of the systems is obtained from the paper [3].

Table 6.1: System parameters

Parameter	**Sym**	**i = 1**	**i = 2**	**i = 3**	**i = 4**	**Unit**
Heat transfer constant between water and air in AHU	B	$24.00 \cdot 10^3$	$14.00 \cdot 10^3$	$12.00 \cdot 10^3$	$20.00 \cdot 10^3$	$[\mathrm{W} \cdot \mathrm{K}^{-1}]$
Specific heat coefficient for water	C_{w}	4183				$[\mathrm{J} \cdot \mathrm{m}^{-3} \cdot \mathrm{K}^{-1}]$
Specific heat coefficient for air	C_{a}	728				$[\mathrm{J} \cdot \mathrm{m}^{-3} \cdot \mathrm{K}^{-1}]$
Density of water	ρ_w	997				$[\mathrm{Kg} \cdot \mathrm{m}^{-3}]$
Density of air	ρ_a	1.225				$[\mathrm{Kg} \cdot \mathrm{m}^{-3}]$
Nominal air temperature reference	$T^*_{\mathrm{a,ref}}$	293.15				[K]
Nominal ambient temperature	$T_{\mathrm{a,amb}}$	308.15				[K]

Nominal supply water temperature	$T_{\mathrm{w,c}}$	283.15				[K]
Water volume in AHU	V_W	$230.00 \cdot 10^{-3}$	$134.00 \cdot 10^{-3}$	$115.00 \cdot 10^{-3}$	$192.00 \cdot 10^{-3}$	$\left[\mathrm{m}^3\right]$
Air volume in AHU	V_a	9.00	5.20	4.50	7.50	$\left[\mathrm{m}^3\right]$
Nominal water flow through AHU	q	$5.75 \cdot 10^{-3}$	$3.336 \cdot 10^{-3}$	$2.89 \cdot 10^{-3}$	$4.81 \cdot 10^{-3}$	$\left[\frac{\mathrm{m}^3}{\mathrm{s}}\right]$
Nominal air flow through AHU	Q	5.98	3.49	2.99	4.98	$\left[\frac{\mathrm{m}^3}{\mathrm{s}}\right]$
Hydraulic resistance of the chilled water source	R_c	$8.85 \cdot 10^3$				$\left[\frac{\mathrm{Pa \cdot s}}{\mathrm{m}^3}\right]$
Hydraulic resistance of supply/return pipe to branch	R	$8.85 \cdot 10^3$	$20.45 \cdot 10^3$	$42.23 \cdot 10^3$	$108.26 \cdot 10^3$	$\left[\frac{\mathrm{Pa \cdot s}}{\mathrm{m}^3}\right]$
Hydraulic resistance of branch	r	$151.23 \cdot 10^3$	$442.59 \cdot 10^3$	$599.11 \cdot 10^3$	$216.51 \cdot 10^3$	$\left[\frac{\mathrm{Pa \cdot s}}{\mathrm{m}^3}\right]$
Pump constant	a	$453.69 \cdot 10^3$	$2212.96 \cdot 10^3$	$4193.79 \cdot 10^3$	$1948.61 \cdot 10^3$	$[\cdot]$
Pump constant	b	30	50	70	90	$[\cdot]$

6.2 Obtaining the general configuration

The methods for determining the robustness of a system, as described in section 5.3 is based on the general control configuration presented in section 5.2. As such, the configuration must be derived before robustness can be analyzed. The configuration describes the open loop system, where $\mathbf{P}$ describes the interconnection of all the inputs and outputs, and the controller $\mathbf{K}$ and uncertainty $\mathbf{\Delta}$, describes its own IO relation. This means that the model can be derived from the block diagram for the system shown on figure 6.1a. Note the block diagram uses the notation $\mathbf{B}_{\mathrm{u}}$ and $\mathbf{B}_{\mathrm{w}}$ for the input matrices, and $\mathbf{C}_{\mathrm{y}}$ and $\mathbf{C}_{\mathrm{z}}$ for the output matrices. These matrices relate to the models linearised in (5.3) and (5.5) as that $\mathbf{B}_{\mathrm{u}}$ can be substituted by either $\bar{\mathbf{B}}$ or $\mathbf{B}$ and $\mathbf{C}_{\mathrm{y}}$ is the output matrix from (4.25). The last matrices $\mathbf{B}_{\mathrm{w}}$ and $\mathbf{C}_{\mathrm{z}}$ are virtual matrices, which are used

in the synthesis process to specify the performance of the system, and are described in later examinations.

In this project, disturbances ($\mathbf{d}$) and sensor noise ($\mathbf{n}$) has been ignored, to simplify the calculations and deviations. The signals could be introduced to the synthesis by appending them to the reference $\mathbf{r}$ which expands $\mathbf{w}$ to $\begin{bmatrix}\mathbf{r} & \mathbf{d} & \mathbf{n}\end{bmatrix}^{\mathrm{T}}$. These exogenous inputs can then be applied to the methods in the chapter by introducing the signals at their respective locations on figure 6.1a.

Both figure 6.1a and 6.1b has some redundant signals, e.g. $\mathbf{u} = \mathbf{z}_\Delta$ and $\mathbf{y} = \mathbf{u}_\mathrm{k}$, these are used in later derivations and additions to the model and for consistency are also in this model.

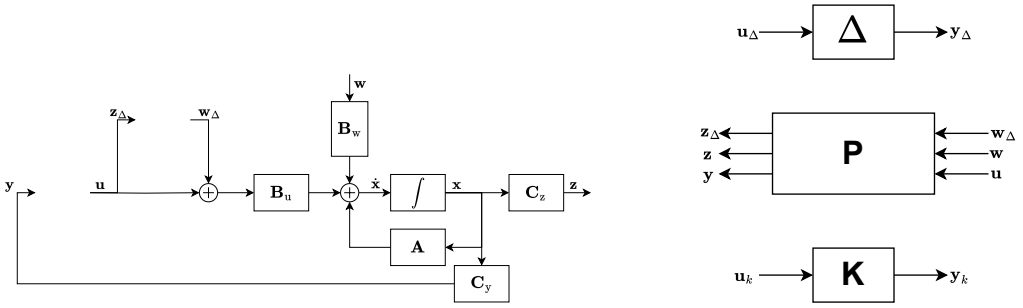

(a) Block diagram of the input uncertain system, where the controller $\mathbf{K}$ and uncertainty $\mathbf{\Delta}$ has been removed to illustrate the diagram is open-loop.

(b) The general control configuration without connections between the blocks, where $\mathbf{P}$ describes the interconnections.

Figure 6.1: Illustration of the block diagram for input uncertainty, and its equivalent open loop general control configuration, where $\mathbf{K}$ is the controller, and $\mathbf{\Delta}$ is the uncertainties.

From figure 6.1a, the equivalent $\mathbf{P}$, shown on figure 6.1b can be derived as:

$$\begin{bmatrix}\dot{\mathbf{x}}\\ \mathbf{z}_\Delta\\ \mathbf{z}\\ \mathbf{y}\end{bmatrix} = \begin{bmatrix}\mathbf{A} & \mathbf{B}_\mathrm{u} & \mathbf{B}_\mathrm{w} & \mathbf{B}_\mathrm{u}\\ \mathbf{0}_{4\times12} & \mathbf{0}_{4\times4} & \mathbf{0}_{4\times4} & \mathbf{I}_4\\ \mathbf{C}_\mathrm{z} & \mathbf{0}_{4\times4} & \mathbf{0}_{4\times4} & \mathbf{0}_{4\times4}\\ \mathbf{C}_\mathrm{y} & \mathbf{0}_{12\times4} & \mathbf{0}_{12\times4} & \mathbf{0}_{12\times4}\end{bmatrix}\begin{bmatrix}\mathbf{x}\\ \mathbf{w}_\Delta\\ \mathbf{w}\\ \mathbf{u}\end{bmatrix} \tag{6.1}$$

This representation is extended to include the IO relations of the controller and uncertainty shown on figure 6.1b. The new relations are applied to the system in a manner that simplifies later derivation.

$$\begin{bmatrix} \dot{\mathbf{x}} \\ \mathbf{z}_\Delta \\ \mathbf{y}_\Delta \\ \mathbf{z} \\ \mathbf{y} \\ \mathbf{y}_\mathrm{k} \end{bmatrix} = \begin{bmatrix} \mathbf{A} & \mathbf{0}_{12\times4} & \mathbf{B}_\mathrm{u} & \mathbf{B}_\mathrm{w} & \mathbf{0}_{12\times12} & \mathbf{B}_\mathrm{u} \\ \mathbf{0}_{4\times12} & \mathbf{0}_{4\times4} & \mathbf{0}_{4\times4} & \mathbf{0}_{4\times4} & \mathbf{0}_{4\times12} & \mathbf{I}_4 \\ \mathbf{0}_{4\times12} & \mathbf{\Delta} & \mathbf{0}_{4\times4} & \mathbf{0}_{4\times4} & \mathbf{0}_{4\times12} & \mathbf{0}_{4\times4} \\ \mathbf{C}_\mathrm{z} & \mathbf{0}_{4\times4} & \mathbf{0}_{4\times4} & \mathbf{0}_{4\times4} & \mathbf{0}_{4\times12} & \mathbf{0}_{4\times4} \\ \mathbf{C}_\mathrm{y} & \mathbf{0}_{12\times4} & \mathbf{0}_{12\times4} & \mathbf{0}_{12\times4} & \mathbf{0}_{12\times12} & \mathbf{0}_{12\times4} \\ \mathbf{0}_{4\times12} & \mathbf{0}_{4\times4} & \mathbf{0}_{4\times4} & \mathbf{0}_{4\times4} & \mathbf{K} & \mathbf{0}_{4\times4} \end{bmatrix} \begin{bmatrix} \mathbf{x} \\ \mathbf{u}_\Delta \\ \mathbf{w}_\Delta \\ \mathbf{w} \\ \mathbf{u}_\mathrm{k} \\ \mathbf{u} \end{bmatrix} \tag{6.2}$$

This representation can be used to derive the $\mathbf{N\Delta}$-structure, shown on figure 5.3b, where the loop around the controller is closed. Firstly the outputs regarding the loop $(\mathbf{y}, \mathbf{y}_\mathrm{k})$, is extracted from (6.2) and expressed in terms of the inputs to the remaining loops $(\mathbf{x}, \mathbf{u}_\Delta, \mathbf{w}_\Delta, \mathbf{w})$ and the inputs for the controller loop $(\mathbf{u}_\mathrm{k}, \mathbf{u})$ as:

$$\begin{bmatrix} \mathbf{y} \\ \mathbf{y}_\mathrm{k} \end{bmatrix} = \begin{bmatrix} \mathbf{C}_\mathrm{y} & \mathbf{0}_{12\times4} & \mathbf{0}_{12\times4} & \mathbf{0}_{12\times4} \\ \mathbf{0}_{4\times12} & \mathbf{0}_{4\times4} & \mathbf{0}_{4\times4} & \mathbf{0}_{4\times4} \end{bmatrix} \begin{bmatrix} \mathbf{x} \\ \mathbf{u}_\Delta \\ \mathbf{w}_\Delta \\ \mathbf{w} \end{bmatrix} + \begin{bmatrix} \mathbf{0}_{12\times12} & \mathbf{0}_{12\times4} \\ \mathbf{K} & \mathbf{0}_{4\times4} \end{bmatrix} \begin{bmatrix} \mathbf{u}_\mathrm{k} \\ \mathbf{u} \end{bmatrix} \tag{6.3}$$

From the blockdiagram on figure 6.1b, it can be seen that closing the connection gives $\mathbf{y} = \mathbf{u}_\mathrm{k}$ and $\mathbf{y}_\mathrm{k} = \mathbf{u}$, which means (6.3) can be expressed as:

$$\begin{bmatrix} \mathbf{y} \\ \mathbf{y}_\mathrm{k} \end{bmatrix} = \begin{bmatrix} \mathbf{I}_{12} & \mathbf{0}_{12\times4} \\ \mathbf{-K} & \mathbf{I}_4 \end{bmatrix}^{-1} \begin{bmatrix} \mathbf{C}_\mathrm{y} & \mathbf{0}_{12\times4} & \mathbf{0}_{12\times4} & \mathbf{0}_{12\times4} \\ \mathbf{0}_{4\times12} & \mathbf{0}_{4\times4} & \mathbf{0}_{4\times4} & \mathbf{0}_{4\times4} \end{bmatrix} \begin{bmatrix} \mathbf{x} \\ \mathbf{u}_\Delta \\ \mathbf{w}_\Delta \\ \mathbf{w} \end{bmatrix} \tag{6.4}$$

As (6.4) is expressed only in terms of the inputs from the remaining loops $(\mathbf{x}, \mathbf{u}_\Delta, \mathbf{w}_\Delta, \mathbf{w})$, it can be used to eliminate the outputs $(\mathbf{y}, \mathbf{y}_\mathrm{k})$ on (6.2), which results in the $\mathbf{N\Delta}$-structure represented as:

$$\begin{bmatrix} \dot{\mathbf{x}} \\ \mathbf{z}_\Delta \\ \mathbf{y}_\Delta \\ \mathbf{z} \end{bmatrix} = \begin{bmatrix} \mathbf{A} & \mathbf{0}_{12\times4} & \mathbf{B}_\mathrm{u} & \mathbf{B}_\mathrm{w} \\ \mathbf{0}_{4\times12} & \mathbf{0}_{4\times4} & \mathbf{0}_{4\times4} & \mathbf{0}_{4\times4} \\ \mathbf{0}_{4\times12} & \boldsymbol{\Delta} & \mathbf{0}_{4\times4} & \mathbf{0}_{4\times4} \\ \mathbf{C}_\mathrm{z} & \mathbf{0}_{4\times4} & \mathbf{0}_{4\times4} & \mathbf{0}_{4\times4} \end{bmatrix} \begin{bmatrix} \mathbf{x} \\ \mathbf{u}_\Delta \\ \mathbf{w}_\Delta \\ \mathbf{w} \end{bmatrix} +$$

$$\begin{bmatrix} \mathbf{0}_{12\times12} & \mathbf{B}_\mathrm{u} \\ \mathbf{0}_{4\times12} & \mathbf{I}_4 \\ \mathbf{0}_{4\times12} & \mathbf{0}_{4\times4} \\ \mathbf{0}_{4\times12} & \mathbf{0}_{4\times4} \end{bmatrix} \begin{bmatrix} \mathbf{I}_{12} & \mathbf{0}_{12\times4} \\ \mathbf{-K} & \mathbf{I}_4 \end{bmatrix}^{-1} \begin{bmatrix} \mathbf{C}_\mathrm{y} & \mathbf{0}_{12\times4} & \mathbf{0}_{12\times4} & \mathbf{0}_{12\times4} \\ \mathbf{0}_{4\times12} & \mathbf{0}_{4\times4} & \mathbf{0}_{4\times4} & \mathbf{0}_{4\times4} \end{bmatrix} \begin{bmatrix} \mathbf{x} \\ \mathbf{u}_\Delta \\ \mathbf{w}_\Delta \\ \mathbf{w} \end{bmatrix} \tag{6.5}$$

$$= \begin{bmatrix} \mathbf{A}+\mathbf{B}_\mathrm{u}\mathbf{K}\mathbf{C}_\mathrm{y} & \mathbf{0}_{12\times4} & \mathbf{B}_\mathrm{u} & \mathbf{B}_\mathrm{w} \\ \mathbf{K}\mathbf{C}_\mathrm{y} & \mathbf{0}_{4\times4} & \mathbf{0}_{4\times4} & \mathbf{0}_{4\times4} \\ \mathbf{0}_{4\times4} & \boldsymbol{\Delta} & \mathbf{0}_{4\times4} & \mathbf{0}_{4\times4} \\ \mathbf{C}_\mathrm{z} & \mathbf{0}_{4\times4} & \mathbf{0}_{4\times4} & \mathbf{0}_{4\times4} \end{bmatrix} \begin{bmatrix} \mathbf{x} \\ \mathbf{u}_\Delta \\ \mathbf{w}_\Delta \\ \mathbf{w} \end{bmatrix}$$

From this structure, the interconnection between $\mathbf{z}_\Delta$ and $\mathbf{w}_\Delta$, called $\mathbf{N}_{11}$ or $\mathbf{M}$, can be used to determine robust stability. Furthermore, since $\mathbf{C}_\mathrm{y} = \mathbf{I}_{12}$ it can be neglected as $\mathbf{K}\mathbf{C}_\mathrm{y} = \mathbf{K}$. From this, the interconnection can be expressed as:

$$\mathbf{N}_{11}(s) = \mathbf{M}(s) = \mathbf{K}\Big(s\mathbf{I}_{12} - (\mathbf{A}+\mathbf{B}_\mathrm{u}\mathbf{K})\Big)^{-1}\mathbf{B}_\mathrm{u} \tag{6.6}$$

or as the state space model:

$$\begin{aligned} \dot{\mathbf{x}} &= \mathbf{A}_\mathrm{m}\mathbf{x} + \mathbf{B}_\mathrm{m}\mathbf{w}_\Delta \\ \mathbf{z}_\Delta &= \mathbf{C}_\mathrm{m}\mathbf{x} \end{aligned} \tag{6.7}$$

with:

$$\mathbf{A}_\mathrm{m} = \mathbf{A}+\mathbf{B}_\mathrm{u}\mathbf{K}, \qquad \mathbf{B}_\mathrm{m} = \mathbf{B}_\mathrm{u}, \qquad \mathbf{C}_\mathrm{m} = \mathbf{K} \tag{6.7a}$$

This description of $\mathbf{M}$ can now be used in the bounded real lemma to find an upper bound on the H_∞-norm.

6.3 Synthesis of robust controller

To synthesise a robust controller, this project builds on the already established design procedures in [3]. The idea behind the procedures are the same, however to validate

robust stability, this project utilizes the bounded real lemma expressed in lemma 1.1. This implies the design procedures can be formulated as:

Design procedure 1 synthesises a controller which stabilizes the decoupled system (5.3) by solving Lyapunovs stability defined by the LMI derived in (5.25). With the parameters for the decoupled system, this LMI can be written as:

$$\mathbf{AQ} + \mathbf{QA}^{\mathrm{T}} + \bar{\mathbf{B}}\mathbf{Y} + \mathbf{Y}^{\mathrm{T}}\bar{\mathbf{B}}^{\mathrm{T}} < 0 \tag{6.8}$$

with $\mathbf{Q} = \mathrm{diag}(\mathbf{Q}_1, \ldots, \mathbf{Q}_\mathrm{n}) > 0$, $\mathbf{Q}_\mathrm{i} \in \mathbb{R}^{3\times3}$, $\mathbf{Y} \in \mathbb{R}^{4\times12}$. From this LMI, the synthesised controller can be recovered by solving $\mathbf{K} = \mathbf{YQ}^{-1}$. Following this, the robustness is analysed by computing a bound on the H_∞-norm, using the bounded real lemma on the interconnection expressed in (6.7).

$$\begin{bmatrix} \mathbf{R}(\mathbf{A}+\mathbf{BK}) + (\mathbf{A}+\mathbf{BK})^{\mathrm{T}}\mathbf{R} & \mathbf{RB} & \mathbf{K}^{\mathrm{T}} \\ \star & -\gamma\mathbf{I}_4 & \mathbf{0}_{4\times4} \\ \star & \star & -\gamma\mathbf{I}_4 \end{bmatrix} < 0 \tag{6.9}$$

with $\gamma > 0$, $\mathbf{R} = \mathrm{diag}(\mathbf{R}_1, \ldots, \mathbf{R}_\mathrm{n}) > 0$, $\mathbf{R}_\mathrm{i} \in \mathbb{R}^{3\times3}$. If this LMI is feasible with a $\gamma < 1$, then the H_∞-norm is less than 1, which implies the coupled system (5.5) is robust stable.

Design procedure 2 synthesises a controller, by simultaneously solving for stability of the decoupled system (5.3) and robust stability of the coupled system (5.5). This requires a transformation of (6.9), similar to the one described in section 5.4. This simplifies the design procedure to simultaneously solve (6.8) and:

$$\begin{bmatrix} \mathbf{AQ} + \mathbf{QA}^{\mathrm{T}} + \mathbf{BY} + \mathbf{Y}^{\mathrm{T}}\mathbf{B}^{\mathrm{T}} & \mathbf{B} & \mathbf{Y}^{\mathrm{T}} \\ \star & -\gamma\mathbf{I}_4 & \mathbf{0}_{4\times4} \\ \star & \star & -\gamma\mathbf{I}_4 \end{bmatrix} < 0 \tag{6.10}$$

with $\mathbf{Q} = \mathrm{diag}(\mathbf{Q}_1, \ldots, \mathbf{Q}_\mathrm{n}) > 0$, $\mathbf{Q}_\mathrm{i} \in \mathbb{R}^{3\times3}$ and $\gamma > 0$, while minimizing wrt. γ. This procedure also uses the bounded real lemma to bound γ, which means the synthesised controller will find the lowest value of γ which still stabilizes both systems. This implies that if γ is used as a parameter equal to one, this procedure will find a controller which is guaranteed to be robustly stable. The default option using this design procedure is $\gamma = 1$.

To test the performance of the controller, two different simulations, both simulating a step response, are run on the system with the designed controller. The first simulates the decoupled linear system and the other simulates the coupled linear system. These simulations are useful for validating the performance of the controller.

6.4 Investigation

Using design procedure 1, a controller is synthesised which shows satisfactory response in both simulations as shown on figure 6.2a. However, the procedure yields a $\gamma = 119.16$, which means robust stability is not guaranteed. On the other hand, using design procedure 2, the synthesised controller is robust stable, however when simulated, the system showed undesirable performance, to the degree that the controller failed to step as shown on figure 6.2b.

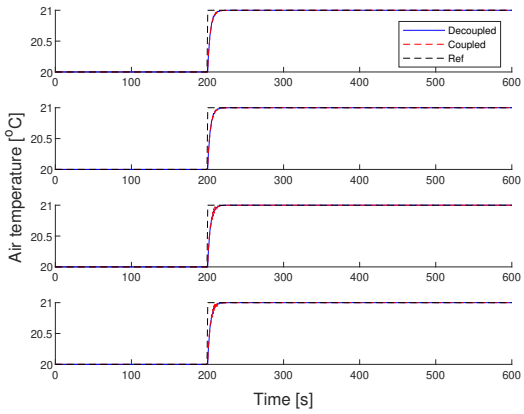

(a) Simulated response of the system with a controller synthesised by design procedure 1.

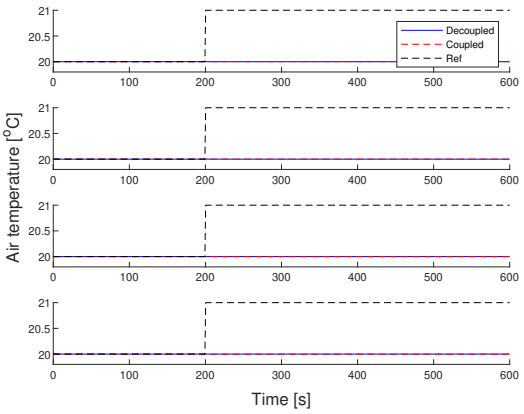

(b) Simulated response of the system with a controller synthesised by design procedure 2.

Figure 6.2: Simulated step response of the system with the synthesised controllers.

The response from system with the controller synthesised by the two procedures showed contradicting results, i.e. if good performance is desired robust stability cannot be guaranteed, and inversely if robust stability is desired, the controller has poor performance.

6.4.1 Examination of stability from state matrix

As the uncertainty impacts the inputs and could potentially cause undesirable inputs, it was examined if a better stability of the state dynamics would yield better results. Calculating the eigenvalues of the state matrix, showed that $\mathbf{A}$ is only marginal stable, i.e. it has eigenvalues on the imaginary axis. As such, the eigenvalues of $\mathbf{A}$ was moved into the left half plane by altering $\mathbf{A}$, defined in (4.22), to:

$$\mathbf{A}_{\text{modified}} = \begin{bmatrix} -\left(\frac{q_{\text{i}}^*}{V_{\text{w,i}}} + \frac{B_{\text{i}}}{C_{\text{w}}\rho_{\text{w}}V_{\text{w,i}}}\right) & \frac{B_{\text{i}}}{C_{\text{w}}\rho_{\text{w}}V_{\text{w,i}}} & 0 \\ \frac{B_{\text{i}}}{C_{\text{a}}\rho_{\text{a}}V_{\text{a,i}}} & -\left(\frac{Q_{\text{i}}}{V_{\text{a,i}}} + \frac{B_{\text{i}}}{C_{\text{a}}\rho_{\text{a}}V_{\text{a,i}}}\right) & 0 \\ 0 & 1 & -1 \end{bmatrix} \tag{6.11}$$

Synthesising new controllers using the modified **A** slightly reduced γ in design procedure 1, however, the value was found to be 85.54, meaning it is still not robust stable. By investigating the step response, shown on figure 6.3, it can be seen that neither controller achieves satisfactory results, as neither controller manages to perform the step.

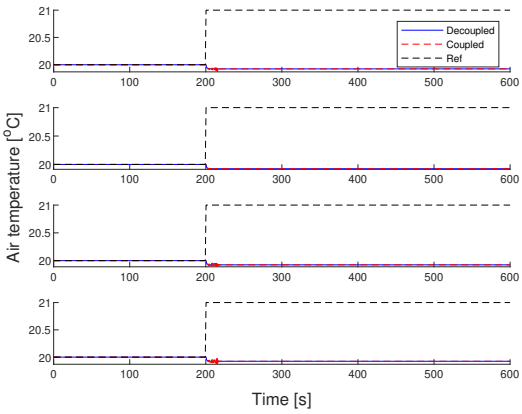

(a) Simulated response of the system with a controller synthesised by design procedure 1.

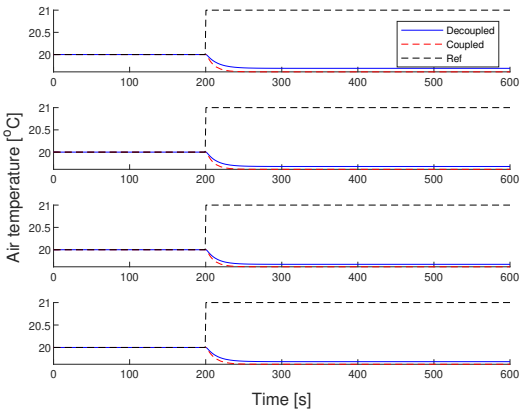

(b) Simulated response of the system with a controller synthesised by design procedure 2.

Figure 6.3: Simulated step response of the system with the synthesised controllers with **A** modified.

6.4.2 Examination of structured uncertainties

Given the response with the modified **A** proved undesirable, attention was moved back towards the baseline on figure 6.2. Particularly, the controller synthesised by design procedure 2 indicates robust stability is obtained if the controller is numerically small relative to **A**. In fact, the controller values are close to 0, meaning there is no control of the system, but it relies on the stability of the plant to remain stable.

It is known that, if a robust controller is conservative, it is likely due to the uncertainty being assumed to be unstructured, as described in section 5.3. Therefore, the possibility of structure in the uncertainty is examined. As described in section 5.3, robust stability under structured uncertainty is quantified by the $\mu_\Delta(\mathbf{M}(s))$, which is a quantity bounded between the unstructured uncertainty, given by $||\mathbf{M}(s)||_\infty$ and the structure with only a single variable $\delta\mathbf{I}$, which is given by the spectral radius $\rho(\mathbf{M}(s))$. In (5.17), it was shown that given a specific structured, the SSV becomes $\mu_\Delta(\mathbf{M}(s)) = ||\mathbf{M}(s)||_\infty$ or $\mu_\Delta(\mathbf{M}(s)) = \rho(\mathbf{M}(s))$. Using this relation and the generalized small gain theorem from theorem 2, robust stability can be guaranteed if these bounds yield a value less than one.

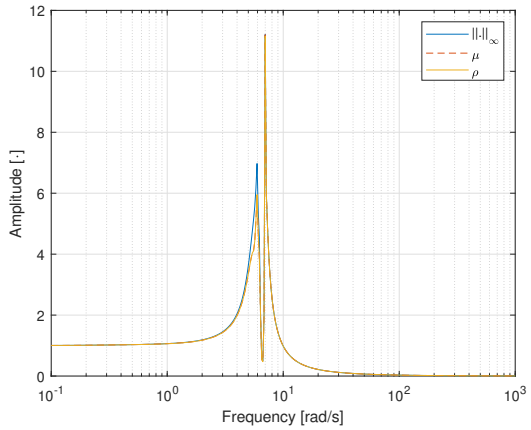

(a) The H_∞-norm, SSV and spectral radius plotted over frequency with the controller synthesised from design procedure 1.

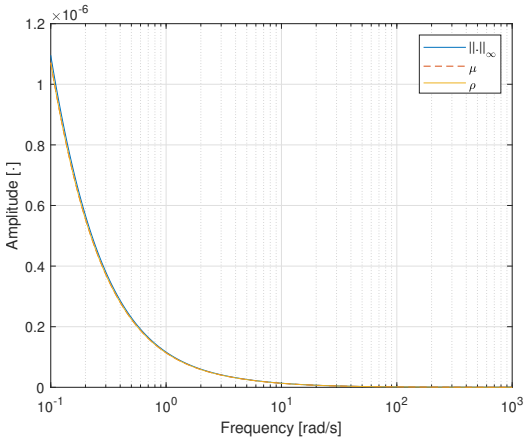

(b) The H_∞-norm, SSV and spectral radius plotted over frequency with the controller synthesised from design procedure 2.

Figure 6.4: The impact of structure in the uncertainty.

Figure 6.4a illustrates that the largest spectral radius of $\mathbf{M}(s)$ is larger than one, which implies no possible structure of the uncertainty can guarantee stability for the controller using design procedure 1. Furthermore, in both figure 6.4a and figure 6.4b, the two bounds are almost the same, which suggest the structure only has a small impact on robust stability.

As noted in the description of the design procedure 2, γ can be selected as a variable which can be minimized, to find a stable controller with the best robustness, however not guaranteed to be robust stable. Using this procedure unfortunately results in a controller, which cannot guarantee robust stability. However, from figure 6.5a the largest spectral radius is found to be 1.0023, which implies the system is close to being robust stable.

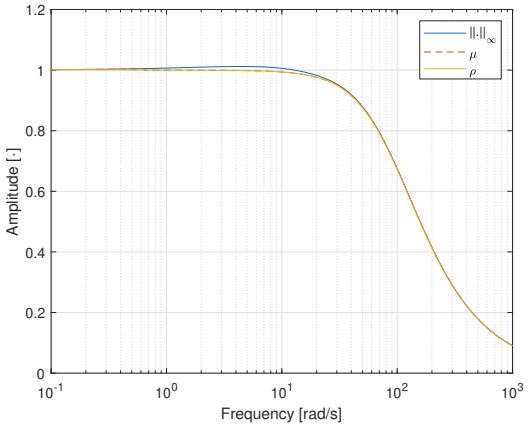

(a) The H_∞-norm, SSV and spectral radius plotted over frequency.

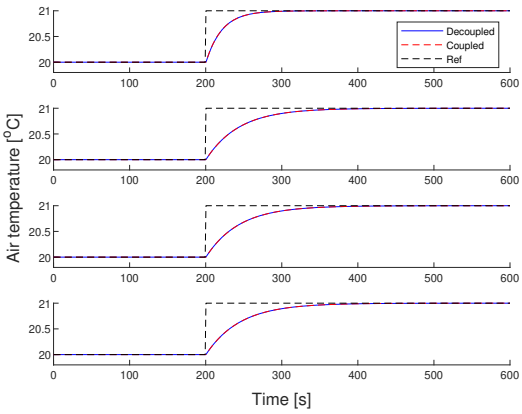

(b) Step response of the coupled and decoupled system.

Figure 6.5: The impact of structure in the uncertainty and step response of system with the controller synthesised using design procedure 2 with γ as a variable found to be 1.0023.

Furthermore, the step response of the system shown on figure 6.5b, show that the controller is able to perform the step in a desirable manner and remain stable, but not fulfilling the condition for robust stability.

6.4.3 Examination of real structured uncertainties

In the previous examination it was found that no structure could guarantee robust stability when the uncertainties where complex. This examination attempts to determine if real uncertainties can guarantee robust stability. Real uncertainties imply the uncertainty can vary between ± 1 of its nominal value, and as such are a realistic uncertainty. Unfortunately, the SSV is less reliable and difficult to compute when real uncertainties are present [6]. However, if a different interpretation of robust stability is used, Linear Parameter Varying (LPV) system can be used to determine robust stability.

In LPV systems, some or all of the system matrices are dependent on a parameter $\rho(t) \in \mathcal{P}$, where $\mathcal{P} = \left\{\rho : \mathbb{R}_{\geq 0} \to \Delta_\rho \subseteq \mathbb{R}^N\right\}$ and N is the number of parameters [7, p.3-4]. The variable ρ can vary, which for a simple dynamic system means $\dot{\mathbf{x}} = \mathbf{A}(\rho)\mathbf{x}$. For such an LPV system, stability can be determined through the use of a parameter varying Lyapunov function $\mathbf{P}(\rho)$. This type of stability is called Parameter-Dependent Quadratic (PDQ) stability [4, p.163] or robust stability [7, p.46], and is determined by solving the LMI:

$$\mathbf{A}(\rho)^{\mathrm{T}}\mathbf{P}(\rho) + \mathbf{P}(\rho)\mathbf{A}(\rho) + \sum_{\mathrm{i}=1}^{N} \dot{\rho}_{\mathrm{i}} \frac{\partial \mathbf{P}(\rho)}{\partial \rho_{\mathrm{i}}} < 0, \qquad \forall (\rho, \dot{\rho}) \in \mathcal{P} \times \mathcal{V} \tag{6.12}$$

with $\mathbf{P}(\rho) > 0$, $\mathcal{P}$ being a compact set and $\mathcal{V}$ a hypercube. This stability condition includes the rate of which the parameter can change $\dot{\rho} \in \mathcal{V}$, however, if there is no bound on the rate, this condition reduces to quadratic stability, in which the Lyapunov parameter is constant [4, p.163]:

$$\mathbf{A}(\rho)^{\mathrm{T}}\mathbf{P} + \mathbf{P}\mathbf{A}(\rho) < 0, \qquad \forall \rho \in \mathcal{P} \tag{6.13}$$

with $\mathbf{P} > 0$. In the case that the parameter is time-invariant, condition (6.13) is sufficient for robust stability. This condition requires validation for an infinite number of ρ, however, if $\mathcal{P}$ is a convex polytope and $\mathbf{A}(\rho)$ is affine in ρ, then by the Vertex property(Theorem) it is necessary and sufficient to validate the stability at the vertices [7, p.52][4, p.156]. (6.13) determines stability of the open-loop system, if the loop is closed using a controller $\mathbf{K}$ and using the procedure described in (5.23), (6.13) becomes:

$$\mathbf{A}(\rho)\mathbf{Q} + \mathbf{Q}\mathbf{A}(\rho)^{\mathrm{T}} + \mathbf{B}(\rho)\mathbf{Y} + \mathbf{Y}^{\mathrm{T}}\mathbf{B}(\rho)^{\mathrm{T}} < 0, \qquad \forall \rho \in \mathcal{P} \tag{6.14}$$

with $\mathbf{Q} > 0$. As this examination is into real uncertainties of the system, these are time-invariant, furthermore, the uncertainties are given by $\delta\mathbf{I}_4, \delta \in [-1; 1]$, this means the set becomes $\bar{\mathcal{P}} = \left\{\rho \in \mathcal{P} \mid \Delta_\rho = [-1,1]\right\}$. This means, by the vertex property(Theorem), that robust stability is achieved by solving (6.14) at the two vertices -1 and 1. Additionally, the uncertainties only affect the inputs of the system, which means $\mathbf{A}(\rho) = \mathbf{A}$ and $\mathbf{B}(\rho) = (1 + \rho)\mathbf{B}$. From this, a controller can be synthesized by simultaneously solving stability of the decoupled system (6.8) and:

$$\mathbf{A}\mathbf{Q} + \mathbf{Q}\mathbf{A}^{\mathrm{T}} + (1 + v)\mathbf{B}\mathbf{Y} + (1 + v)\mathbf{Y}^{\mathrm{T}}\mathbf{B}^{\mathrm{T}} < 0, \quad \forall \quad v \in \mathbf{vert}(\bar{\mathcal{P}}) \tag{6.15}$$

with $\mathbf{Q} = \mathrm{diag}(\mathbf{Q}_1, \ldots, \mathbf{Q}_{\mathrm{n}}) > 0$, $\mathbf{Q}_{\mathrm{i}} \in \mathbb{R}^{3\times3}$. This procedure synthesised a controller which could stabilize the system and be robust stable towards the uncertainties. By performing a step response, shown on figure 6.6, it can be seen the system shows desirable performance.

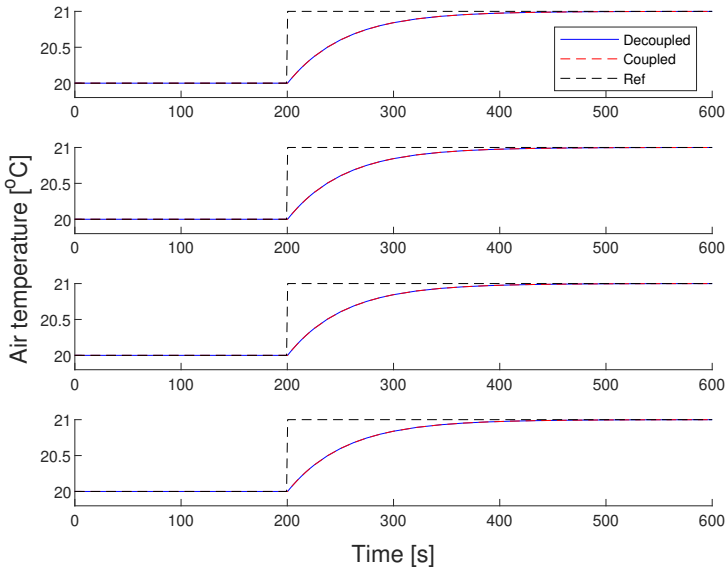

Figure 6.6: Step response of the coupled and decoupled system with a controller designed for identical real uncertainties on the inputs.

This shows that given real uncertainties robust stability can be achieved. The case shown in figure 6.6 only showed the simple case of every input being affected identically by the uncertainty. To investigate a broader robustness, the structure of the uncertainty is change to a diagonal matrix with different uncertainties for each input:

$$\Delta = \begin{bmatrix} \delta_1 & 0 & 0 & 0 \\ 0 & \delta_2 & 0 & 0 \\ 0 & 0 & \delta_3 & 0 \\ 0 & 0 & 0 & \delta_4 \end{bmatrix}, \qquad \delta_{\mathrm{i}} \in [-1,1] \tag{6.16}$$

With four uncertainties, the set $\bar{\mathcal{P}}$ becomes $\bar{\mathcal{P}} = \left\{\rho \in \mathcal{P} \mid \Delta_\rho = [-1,1]^4\right\}$. Additionally, with the uncertainties being a matrix instead of a scalar, (6.15) is rewritten to formulate the uncertainties as a matrix.

$$\mathbf{AQ} + \mathbf{QA}^{\mathrm{T}} + \mathbf{B}(\mathbf{I}_4 + \mathrm{diag}(\mathbf{v}))\mathbf{Y} + \mathbf{Y}^{\mathrm{T}}(\mathbf{I}_4 + \mathrm{diag}(\mathbf{v}))^{\mathrm{T}}\mathbf{B}^{\mathrm{T}} < 0, \quad \forall \quad \mathbf{v} \in \mathbf{vert}(\bar{\mathcal{P}}) \tag{6.17}$$

with $\mathbf{Q} = \mathrm{diag}(\mathbf{Q}_1, \ldots, \mathbf{Q}_{\mathrm{n}}) > 0$, $\mathbf{Q}_{\mathrm{i}} \in \mathbb{R}^{3\times 3}$. Solving this LMI yields a feasible solution, however the models become marginally stable. Indeed by simulating a step response, shown on figure 6.7, it can be seen the controller is incapable of adjusting to the new reference.

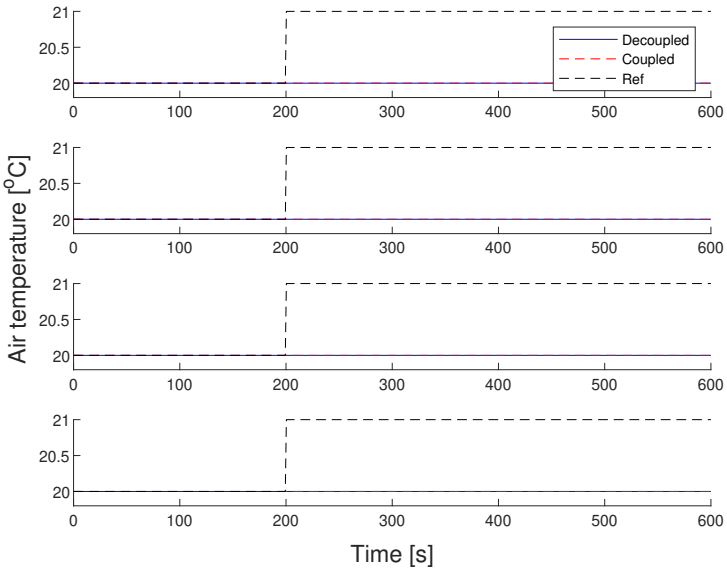

Figure 6.7: Step response of the coupled and decoupled system with a controller designed for different real uncertainties on the inputs.

This result was not surprising when considering the case presented. When determining stability at the vertices, some uncertainties are 1 while others are -1, this corresponds to some AHU being able to adjust, while others are unable to. This case will never be stable due to the coupling in the hydraulics, and as such the best option is to synthesise a controller of zeroes.

6.4.4 Examination of weighted uncertainties

The previous investigations showed robust stability could only be achieved in the case of a single real uncertainty affecting all the inputs. This case is limited, therefore, this section examines utilizing the weight function $\mathbf{W}_\Delta(s)$ from figure 5.2 on the input of $\mathbf{\Delta}$, to affect the uncertainties and thereby achieve robust stability. As illustrated on the block diagram on figure 6.8, the weighting function can be used to inject restrictions onto $\mathbf{\Delta}$, such as mitigating the effect of the uncertainties at given frequencies. To analyse the effect of $\mathbf{W}_\Delta(s)$ a new description of $\mathbf{P}$ is required.

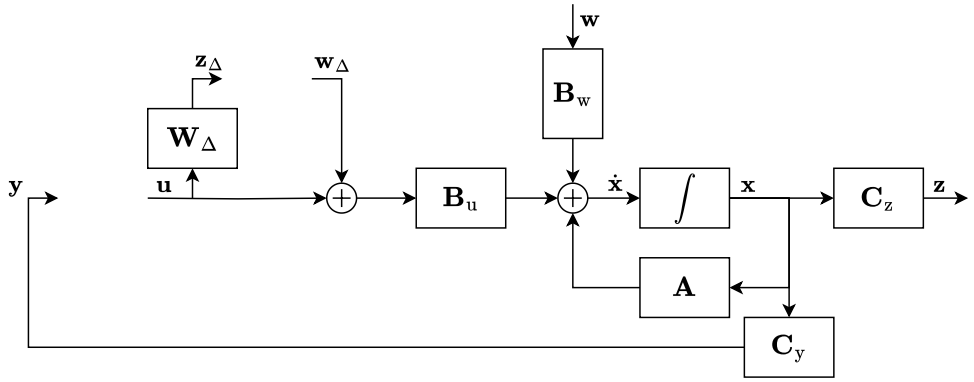

Figure 6.8: Block diagram of the input uncertain system with the weighting function $\mathbf{W}_\Delta$, where the controller $\mathbf{K}$ and uncertainty $\mathbf{\Delta}$ has been removed to illustrate the diagram is open-loop.

$\mathbf{W}_\Delta(s)$ can be expressed in state space as:

$$\mathbf{W}_\Delta(s) \stackrel{ss}{=} \left[\begin{array}{c|c} \mathbf{A}_{\mathrm{w}\Delta} & \mathbf{B}_{\mathrm{w}\Delta} \\ \hline \mathbf{C}_{\mathrm{w}\Delta} & \mathbf{D}_{\mathrm{w}\Delta} \end{array}\right] \tag{6.18}$$

Using the same procedure as described in section 6.2, an expression for $\mathbf{P}$ in the general control configuration, which incorporates the weighting $\mathbf{W}_\Delta$, can be expressed as:

$$\begin{bmatrix} \dot{\mathbf{x}} \\ \dot{\mathbf{x}}_{\mathrm{w}\Delta} \\ \mathbf{z}_\Delta \\ \mathbf{z} \\ \mathbf{y} \\ \mathbf{y}_\Delta \\ \mathbf{y}_\mathrm{K} \end{bmatrix} = \begin{bmatrix} \mathbf{A} & \mathbf{0}_{12\times4} & \mathbf{B}_\mathrm{u} & \mathbf{B}_\mathrm{w} & \mathbf{0}_{12\times12} & \mathbf{0}_{12\times4} & \mathbf{B}_\mathrm{u} \\ \mathbf{0}_{4\times12} & \mathbf{A}_{\mathrm{w}\Delta} & \mathbf{0}_{4\times4} & \mathbf{0}_{4\times4} & \mathbf{0}_{4\times12} & \mathbf{0}_{4\times4} & \mathbf{B}_{\mathrm{w}\Delta} \\ \mathbf{0}_{4\times12} & \mathbf{C}_{\mathrm{w}\Delta} & \mathbf{0}_{4\times4} & \mathbf{0}_{4\times4} & \mathbf{0}_{4\times12} & \mathbf{0}_{4\times4} & \mathbf{D}_{\mathrm{w}\Delta} \\ \mathbf{C}_\mathrm{z} & \mathbf{0}_{4\times4} & \mathbf{0}_{4\times4} & \mathbf{0}_{4\times4} & \mathbf{0}_{4\times12} & \mathbf{0}_{4\times4} & \mathbf{0}_{4\times4} \\ \mathbf{C}_\mathrm{y} & \mathbf{0}_{12\times4} & \mathbf{0}_{12\times4} & \mathbf{0}_{12\times4} & \mathbf{0}_{12\times12} & \mathbf{0}_{12\times4} & \mathbf{0}_{12\times4} \\ \mathbf{0}_{4\times4} & \mathbf{0}_{4\times4} & \mathbf{0}_{4\times4} & \mathbf{0}_{4\times4} & \mathbf{0}_{4\times12} & \mathbf{\Delta} & \mathbf{0}_{4\times4} \\ \mathbf{0}_{12\times4} & \mathbf{0}_{12\times4} & \mathbf{0}_{12\times4} & \mathbf{0}_{12\times4} & \mathbf{K} & \mathbf{0}_{12\times4} & \mathbf{0}_{12\times4}3 \end{bmatrix} \begin{bmatrix} \mathbf{x} \\ \mathbf{x}_\mathrm{w} \\ \mathbf{w}_\Delta \\ \mathbf{w} \\ \mathbf{u}_\mathrm{k} \\ \mathbf{u}_\Delta \\ \mathbf{u} \end{bmatrix} \tag{6.19}$$

Similar to section 6.2, the controller can be incorporated into the model by closing the lower loop, resulting in the interconnections, described by $\mathbf{N}_\mathrm{w}$, becoming:

$$\begin{bmatrix} \dot{\mathbf{x}} \\ \dot{\mathbf{x}}_{\mathrm{w}\Delta} \\ \mathbf{z}_{\Delta} \\ \mathbf{z} \\ \mathbf{y}_{\Delta} \end{bmatrix} = \begin{bmatrix} \mathbf{A}+\mathbf{B}_{\mathrm{u}}\mathbf{K} & \mathbf{0}_{12\times4} & \mathbf{B}_{\mathrm{u}} & \mathbf{B}_{\mathrm{w}} & \mathbf{0}_{12\times4} \\ \mathbf{B}_{\mathrm{w}\Delta}\mathbf{K} & \mathbf{A}_{\mathrm{w}\Delta} & \mathbf{0}_{4\times4} & \mathbf{0}_{4\times4} & \mathbf{0}_{4\times4} \\ \mathbf{D}_{\mathrm{w}\Delta}\mathbf{K} & \mathbf{C}_{\mathrm{w}\Delta} & \mathbf{0}_{4\times4} & \mathbf{0}_{4\times4} & \mathbf{0}_{4\times4} \\ \mathbf{C}_{\mathrm{z}} & \mathbf{0}_{4\times4} & \mathbf{0}_{4\times4} & \mathbf{0}_{4\times4} & \mathbf{0}_{4\times4} \\ \mathbf{0}_{4\times12} & \mathbf{0}_{4\times4} & \mathbf{0}_{4\times4} & \mathbf{0}_{4\times4} & \Delta \end{bmatrix} \begin{bmatrix} \mathbf{x} \\ \mathbf{x}_{\mathrm{w}\Delta} \\ \mathbf{w}_{\Delta} \\ \mathbf{w} \\ \mathbf{u}_{\Delta} \end{bmatrix} \tag{6.20}$$

From this structure, the desired interconnection $\mathbf{w}_{\Delta}$ to $\mathbf{z}_{\Delta}$, can be expressed as:

$$\mathbf{M}_{\mathrm{w}} = \begin{bmatrix} \mathbf{D}_{\mathrm{w}\Delta}\mathbf{K} & \mathbf{C}_{\mathrm{w}\Delta} \end{bmatrix} \left(s\mathbf{I}_{16} - \begin{bmatrix} \mathbf{A}+\mathbf{B}_{\mathrm{u}}\mathbf{K} & \mathbf{0}_{12\times4} \\ \mathbf{B}_{\mathrm{w}\Delta}\mathbf{K} & \mathbf{A}_{\mathrm{w}\Delta} \end{bmatrix} \right)^{-1} \begin{bmatrix} \mathbf{B}_{\mathrm{u}} \\ \mathbf{0}_{4\times4} \end{bmatrix} \tag{6.21}$$

or as the state space model:

$$\begin{aligned} \dot{\mathbf{x}} &= \mathbf{A}_{\mathrm{mw}}\mathbf{x} + \mathbf{B}_{\mathrm{mw}}\mathbf{w}_{\Delta} \\ \mathbf{z}_{\Delta} &= \mathbf{C}_{\mathrm{mw}}\mathbf{x} \end{aligned} \tag{6.22}$$

with:

$$\mathbf{A}_{\mathrm{mw}} = \begin{bmatrix} \mathbf{A}+\mathbf{B}_{\mathrm{u}}\mathbf{K} & \mathbf{0}_{12\times4} \\ \mathbf{B}_{\mathrm{w}\Delta}\mathbf{K} & \mathbf{A}_{\mathrm{w}\Delta} \end{bmatrix}, \qquad \mathbf{B}_{\mathrm{mw}} = \begin{bmatrix} \mathbf{B}_{\mathrm{u}} \\ \mathbf{0}_{4\times4} \end{bmatrix}, \qquad \mathbf{C}_{\mathrm{mw}} = \begin{bmatrix} \mathbf{D}_{\mathrm{w}\Delta}\mathbf{K} & \mathbf{C}_{\mathrm{w}\Delta} \end{bmatrix} \tag{6.22a}$$

Before the effect can be analysed, a numeric value of the weight function must be derived. As the object is to verify stability towards uncertainties in the input, the weight function should describe the behaviour of the inputs. Given these uncertainties are caused by the hydraulics, the weight function is chosen to describe the influence of each individual pump on the remaining pumps, which is difference between the coupled and decoupled hydraulics $\mathbf{B}-\bar{\mathbf{B}}$. As seen on figure 6.8, the uncertainty is acting on the input signal, which is $\mathbf{u} \in \mathbb{R}^{4\times1}$, however $\mathbf{B}-\bar{\mathbf{B}} \in \mathbb{R}^{12\times4}$, which means it cannot be used. The figure also shows the uncertainty being added to the nominal input before entering the system, this implies $\mathbf{B}_{\mathrm{u}}$ affects the uncertainty twice, and hence if the inverse of $\mathbf{B}_{\mathrm{u}}$ is pre-multiplied to $(\mathbf{B}-\bar{\mathbf{B}})$, this both removes the additional multiplication of $\mathbf{B}_{\mathrm{u}}$ and changes the dimensions of the uncertainty to be in $\mathbb{R}^{4\times4}$. However, $\mathbf{B}$ is not square and therefore does not have an inverse, instead the pseudo inverse is used, resulting in the weight defined as:

$$\mathbf{B}^{\dagger}(\mathbf{B}-\bar{\mathbf{B}}) = \mathbf{B}^{\dagger}\left(\mathbf{H}(\boldsymbol{\xi}^{*}) + \boldsymbol{\mathcal{G}}\right)\left(\frac{\partial \mathbf{g}(\boldsymbol{\omega}^{\boldsymbol{*}})}{\partial \boldsymbol{\omega}} - \bar{\boldsymbol{\Lambda}}^{-1}\right) \tag{6.23}$$

Where:

$\mathbf{B}^\dagger \quad \in \mathbb{R}^{4\times 12}$ | is the pseudo-inverse of $\mathbf{B}$.

This definition of the uncertainties are based on the model derived from the hydraulics, which was assumed to be static. As such, (6.23) is only a scaling, which is a direct feedforward on the input, and can be expressed in terms of $\mathbf{W}_\Delta$ as:

$$\mathbf{W}_\Delta(s) \overset{ss}{=} \left[\begin{array}{c|c} \mathbf{0}_{4\times 4} & \mathbf{0}_{4\times 4} \\ \hline \mathbf{0}_{4\times 4} & \mathbf{B}^\dagger \left(\mathbf{H}(\boldsymbol{\xi}^*) + \boldsymbol{\mathcal{G}}\right)\left(\frac{\partial \mathbf{g}(\boldsymbol{\omega}^*)}{\partial \boldsymbol{\omega}} - \bar{\boldsymbol{\Lambda}}^{-1}\right) \end{array}\right] \tag{6.24}$$

With the weight function determined, the effect on the robustness can now be investigated. For this, a controller is synthesized using design procedure 2 with γ as a variable. The singular values of the controller with and without the weight function over frequency is shown on figure 6.9a and figure 6.9b respectively.

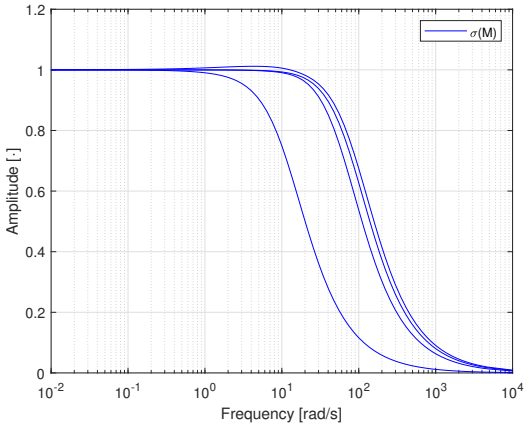

(a) Singular values of $\mathbf{M}$ with unity weight function plotted over the frequency range $[10^{-3}; 10^4]$.

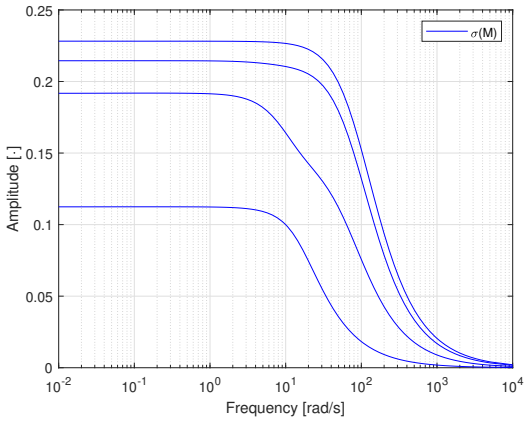

(b) Singular values of $\mathbf{M}$ with weight function defined in (6.24) plotted over the frequency range $[10^{-3}; 10^4]$.

Figure 6.9: Singular values of the uncertain interconnection $\mathbf{M}$, with and without a weight function, plotted over the frequency range $[10^{-3}; 10^4]$.

The unity gain, on figure 6.9a, shows the earlier established conclusion, that the synthesised $\mathbf{K}$, does not guarantee robust stability. When the weight is applied, the singular values are reduced such that the largest singular value is smaller than 1 over every frequency, thereby resulting in the system fulfilling the criteria for robust stability.

6.4.5 Synthesis using weighted uncertainties

In section 6.4.4 it was found that the synthesised feedback gain $\mathbf{K}$ from design procedure 2 could make the system robust stable, if the weighting function in (6.24) was applied. From figure 6.9b it can also be seen that the singular values are significantly lower than one, which means the synthesised $\mathbf{K}$ might be more conservative than necessary for achieving robust stability.

This section therefore focuses on deriving a method for synthesising a $\mathbf{K}$ with the knowledge of the weighting function $\mathbf{W}_\Delta$. This procedure follows from Design procedure 2, however, since the decoupled system, and the new coupled system with the weighting function has a different number of states, the Lyapunov variable $\mathbf{Q}$ cannot be applied to the new system. Nevertheless, from the definition of Lyapunov stability, the dynamic system is defined as $\dot{\mathbf{x}} = \mathbf{A}\mathbf{x}$, which by investigating the state of the new system $\mathbf{x}_{\text{mw}} = \begin{bmatrix} \mathbf{x} & \mathbf{x}_{\text{w}\Delta} \end{bmatrix}^{\text{T}}$ it can be seen the first states are the same as the decoupled, while the latter are new. This implies a Lyapunov variable can be structured as:

$$\bar{\mathbf{P}} = \begin{bmatrix} \mathbf{P} & \mathbf{P}_{1,2} \\ \star & \mathbf{P}_{2,2} \end{bmatrix} \tag{6.25}$$

with $\mathbf{P} = \text{diag}(\mathbf{P}_1, \ldots, \mathbf{P}_{\text{n}})$, $\mathbf{P}_{\text{i}} \in \mathbb{R}^{3\times 3}$ and $\mathbf{P}_{\text{i,j}}$ appropriate dimensions. Using this Lyapunov variable, robust stability of the coupled system can be determined by solving the bounded real lemma in (5.10) wrt. the derived $\mathbf{A}_{\text{mw}}$, $\mathbf{B}_{\text{mw}}$, $\mathbf{C}_{\text{mw}}$ and $\mathbf{D}_{\text{mw}}$ matrices from (6.22), i.e

$$\begin{bmatrix} \mathbf{A}_{\text{mw}}^{\text{T}}\bar{\mathbf{P}} + \bar{\mathbf{P}}\mathbf{A}_{\text{mw}} & \bar{\mathbf{P}}\mathbf{B}_{\text{mw}} & \mathbf{C}_{\text{mw}}^{\text{T}} \\ \star & -\gamma\mathbf{I}_4 & \mathbf{D}_{\text{mw}}^{\text{T}} \\ \star & \star & -\gamma\mathbf{I}_4 \end{bmatrix} < 0 \tag{6.26}$$

with $\bar{\mathbf{P}} > 0$. Before this inequality can be applied during synthesis, the expression must be rewritten such that $\mathbf{K}$ is pulled out from both $\mathbf{A}_{\text{mw}}$ and $\mathbf{C}_{\text{mw}}$. This can be achieved by rewriting $\mathbf{A}_{\text{mw}}$ and $\mathbf{C}_{\text{mw}}$ as:

$$\mathbf{A}_{\text{mw}} = \underbrace{\begin{bmatrix} \mathbf{A} & \mathbf{0}_{12\times 4} \\ \mathbf{0}_{4\times 12} & \mathbf{A}_{\text{w}\Delta} \end{bmatrix}}_{\bar{\mathbf{A}}_{\text{mw}}} + \underbrace{\begin{bmatrix} \mathbf{B}_{\text{u}} & \mathbf{0}_{12\times 4} \\ \mathbf{B}_{\text{w}\Delta} & \mathbf{0}_{4\times 4} \end{bmatrix}}_{\bar{\mathbf{B}}_{\text{mw}}} \underbrace{\begin{bmatrix} \mathbf{K} & \mathbf{0}_{4\times 4} \\ \mathbf{0}_{4\times 12} & \mathbf{I}_4 \end{bmatrix}}_{\bar{\mathbf{K}}_{\text{mw}}} \tag{6.27}$$

$$\mathbf{C}_{\text{mw}} = \underbrace{\begin{bmatrix} \mathbf{D}_{\text{w}\Delta} & \mathbf{C}_{\text{w}\Delta} \end{bmatrix}}_{\bar{\mathbf{C}}_{\text{mw}}} \underbrace{\begin{bmatrix} \mathbf{K} & \mathbf{0}_{4\times 4} \\ \mathbf{0}_{4\times 12} & \mathbf{I}_4 \end{bmatrix}}_{\bar{\mathbf{K}}_{\text{mw}}} \tag{6.28}$$

Using these definition (6.26) is rewritten as:

$$\begin{bmatrix} (\bar{\mathbf{A}}_{\text{mw}} + \bar{\mathbf{B}}_{\text{mw}}\bar{\mathbf{K}}_{\text{mw}})^{\text{T}}\bar{\mathbf{P}} + \bar{\mathbf{P}}(\bar{\mathbf{A}}_{\text{mw}} + \bar{\mathbf{B}}_{\text{mw}}\bar{\mathbf{K}}_{\text{mw}}) & \bar{\mathbf{P}}\mathbf{B}_{\text{mw}} & \bar{\mathbf{K}}_{\text{mw}}^{\text{T}}\bar{\mathbf{C}}_{\text{mw}}^{\text{T}} \\ \star & -\gamma\mathbf{I}_4 & \mathbf{D}_{\text{mw}}^{\text{T}} \\ \star & \star & -\gamma\mathbf{I}_4 \end{bmatrix} < 0 \tag{6.29}$$

This inequality is unfortunately bi-linear, however by using the same method described in section 6.3 an LMI can be formulated as:

$$\begin{bmatrix} \bar{\mathbf{A}}_{\text{mw}}\bar{\mathbf{Q}} + \bar{\mathbf{Q}}\bar{\mathbf{A}}_{\text{mw}}^{\text{T}} + \bar{\mathbf{B}}_{\text{mw}}\bar{\mathbf{Y}} + \bar{\mathbf{Y}}^{\text{T}}\bar{\mathbf{B}}_{\text{mw}}^{\text{T}} & \mathbf{B}_{\text{mw}} & \bar{\mathbf{Y}}^{\text{T}}\bar{\mathbf{C}}_{\text{mw}}^{\text{T}} \\ \star & -\gamma\mathbf{I}_4 & \mathbf{D}_{\text{mw}}^{\text{T}} \\ \star & \star & -\gamma\mathbf{I}_4 \end{bmatrix} < 0 \tag{6.30}$$

with:

$$\bar{\mathbf{Q}} = \bar{\mathbf{P}}^{-1}, \qquad \bar{\mathbf{Y}} = \bar{\mathbf{K}}_{\text{mw}}\bar{\mathbf{Q}} = \begin{bmatrix} \mathbf{K}\mathbf{Q} & \mathbf{K}\mathbf{Q}_{1,2} \\ \mathbf{Q}_{1,2}^{\text{T}} & \mathbf{Q}_{22} \end{bmatrix} \tag{6.30a}$$

By solving (6.8) and (6.30) with $\bar{\mathbf{Q}} > 0$ and $\gamma > 0$ simultaneously, a $\mathbf{K}$ can be synthesised. It is worth noting that due to the structure of $\mathbf{C}_{\text{mw}}$ in (6.28), $\mathbf{K}$ only influences the term if $\mathbf{D}_{\text{w}\Delta} \neq \mathbf{0}$. This means that if the weighing functions does not have a feedforward term, then γ in (6.30) becomes unbounded by $\mathbf{K}$, and has no influence on the controller synthesis.

Using the definition of the weight from (6.24) a $\mathbf{K}$ is synthesised for $\gamma = 1$ and another for γ as a variable found to be 0.2282. The resulting step response for the two cases can be seen on figure 6.10.

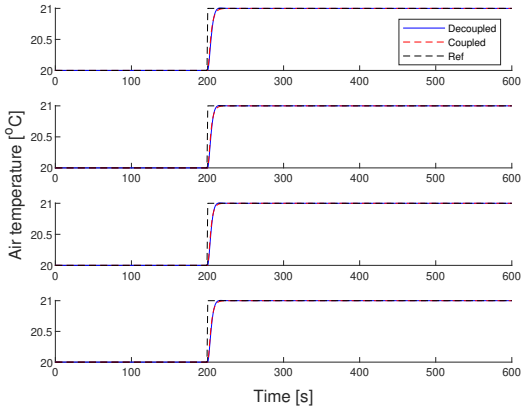

(a) Step response of the coupled and decoupled system with **K** synthesised using the weight function (6.24) and $\gamma = 1$.

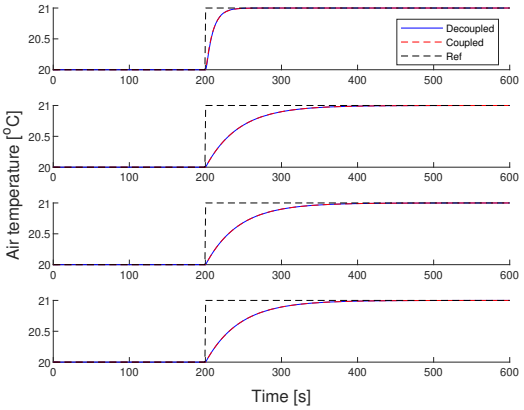

(b) Step response of the coupled and decoupled system with **K** synthesised using the weight function (6.24) and $\gamma = 0.2282$.

Figure 6.10: Step response of the coupled and decoupled system with **K** synthesised using the weight function (6.24).

For $\gamma = 1$ it can be seen that the controller results in a more aggressive controller while the controller for $\gamma = 0.2282$ results in a more conservative controller as it guarantees a stronger robustness. As two different controllers are obtained, it would suggest the possibility to move between the two controllers and try to enforce some performance on the closed loop from **w** to **z** by varying the amount of achieved robustness.

6.4.6 Examination of performance

In section 6.4.5 robustness was achieved for multiple controllers, therefore it is examined if a controller **K** can be synthesised, such that a specific performance of the system can be achieved. For a system with uncertainties, performance can be specified as nominal-and robust-performance. Nominal performance disregards the uncertainties and is determined by the interconnection from **w** to **z** being stable. Robust performance expands on this, and is determined by the interconnection from **w** to **z** to be stable for all uncertainties in $\mathbf{\Delta}$ [6, p.146].

To analyse performance, the general configuration, seen on figure 6.11, can be used. It should be noted that two additional weights have been added to the system $\mathbf{W}_z$ and $\mathbf{W}_w$ as in section 6.4.5, with the same objective of inferring a priori knowledge of the system into the performance analysis [6, p.138-140]. The choice of weights will be introduced later.

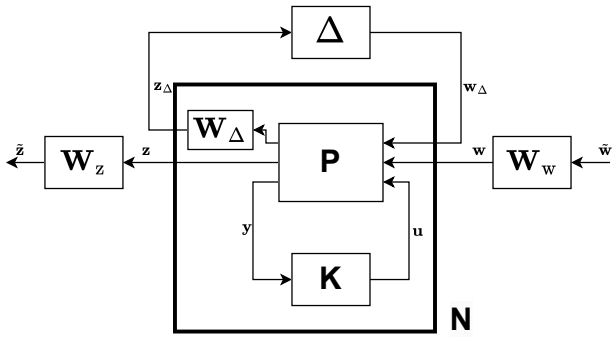

Figure 6.11: The general configuration with weights on the exogenous input and controlled output.

The configuration from figure 6.11 can be written as the system:

$$\begin{bmatrix} \mathbf{z}_\Delta \\ \mathbf{z} \end{bmatrix} = \begin{bmatrix} \mathbf{M} & \mathbf{N}_{1,2} \\ \mathbf{N}_{2,1} & \mathbf{N}_{2,2} \end{bmatrix} \begin{bmatrix} \mathbf{w}_\Delta \\ \mathbf{w} \end{bmatrix} \tag{6.31}$$

Where $\mathbf{M}$, $\mathbf{N}_{1,2}$, $\mathbf{N}_{2,1}$, and $\mathbf{N}_{2,2}$ describe the transfer function between the respective inputs to outputs. From this, nominal performance of the system on figure 6.11, is determined as the relation between $\mathbf{z}$ and $\mathbf{w}$, ie. how much the exogenous inputs affect the controlled outputs. From this, it is clear that this relation is desired to be small, as this infers that the disturbance has little influence on the controlled outputs. The nominal performance is quantified in terms of the H_∞-norm, and specifically if $||\mathbf{N}_{2,2}(s)||_\infty \leq 1$ then the system is said to have nominal performance [6, p.146]. From this definition, it is clear that for any system with nominal performance, no disturbance $\mathbf{w}$ can cause an unstable behavior in regards to the selected $\mathbf{z}$ [6]. When determining robust performance, the impact of the uncertainties must be considered. This requires $\mathbf{\Delta}$ to be included in the calculations, which is ineffective. This can fortunately be solved by using the main loop theorem, which defines a new set of uncertainties $\mathbf{\Delta}_\text{e} = \text{diag}(\mathbf{\Delta}, \hat{\mathbf{\Delta}})$ where $\hat{\mathbf{\Delta}}$ is a full block uncertainty, with the same dimensions as $\mathbf{N}_{2,2}$ [6, p.147-151]. Using the extended uncertainty, robust performance can be determined by calculating $\mu_{\mathbf{\Delta}_\text{e}}(\mathbf{N}(s)) \leq 1$. From this, conditions for robust stability, nominal performance and robust performance can be expressed as:

Robust stable	**Nominal performance**	**Robust performance**
$\mu_{\mathbf{\Delta}}(\mathbf{M}(s)) \leq 1$	$\|\|\mathbf{N}_{2,2}(s)\|\|_\infty \leq 1$	$\mu_{\mathbf{\Delta}_\text{e}}(\mathbf{N}(s)) \leq 1$

(6.32)

From these definitions, it can also be concluded that robust stability is guaranteed by robust performance [6, p.149]. These metrics are determined strictly from the systems transfer functions, which means impacts from the entire frequency domain is considered.

However, $\mathbf{w}$ and $\mathbf{z}$ are often frequency dependent, and therefore should not be considered over the entire frequency domain [6, p.138-140]. Instead, priori information can be applied in the analysis using the weight functions $\mathbf{W}_\mathrm{z}$ and $\mathbf{W}_\mathrm{w}$, as shown in figure 6.11, which result in two new signals:

$$\tilde{\mathbf{z}} = \mathbf{W}_\mathrm{z}(s)\mathbf{z} \qquad\qquad \mathbf{w} = \mathbf{W}_\mathrm{w}(s)\tilde{\mathbf{w}} \tag{6.33}$$

These new signals can be written into (6.31) as:

$$\begin{bmatrix} \mathbf{z}_\Delta \\ \tilde{\mathbf{z}} \end{bmatrix} = \underbrace{\begin{bmatrix} \mathbf{M} & \mathbf{N}_{1,2}\mathbf{W}_\mathrm{w} \\ \mathbf{W}_z\mathbf{N}_{2,1} & \mathbf{W}_\mathrm{z}\mathbf{N}_{2,2}\mathbf{W}_\mathrm{w} \end{bmatrix}}_{\mathbf{N}_\mathrm{w}} \begin{bmatrix} \mathbf{w}_\Delta \\ \tilde{\mathbf{w}} \end{bmatrix} \tag{6.34}$$

From (6.34), it can be seen that the weights does not effect the robust stability, as it relates to the signals $\mathbf{w}_\Delta$ and $\mathbf{z}_\Delta$. The weights does however change both nominal performance and robust performance, as these describes the response from $\mathbf{w}$ to $\mathbf{z}$, and the entire $\mathbf{N}_\mathrm{w}$ respectively. As such these can be written with the weights as:

Nominal performance	**Robust performance**	
$\|\|\mathbf{W}_\mathrm{z}\mathbf{N}_{2,2}\mathbf{W}_\mathrm{w}(s)\|\|_\infty \leq 1$	$\mu_{\mathbf{\Delta}_\mathrm{e}}(\mathbf{N}_\mathrm{w}(s)) \leq 1$	(6.35)

To validate the performance with the weights, the system (6.22) must be expanded to include the dynamics of the weights. This is achieved by augmenting the block diagram from figure 6.8 to contain the new wights $\mathbf{W}_\mathrm{w}$ and $\mathbf{W}_\mathrm{z}$, as depicted in figure 6.12. Furthermore, the weights are defined in state space as:

$$\mathbf{W}_\mathrm{z}(s) \overset{ss}{=} \left[\begin{array}{c|c} \mathbf{A}_\mathrm{wz} & \mathbf{B}_\mathrm{wz} \\ \hline \mathbf{C}_\mathrm{wz} & \mathbf{D}_\mathrm{wz} \end{array}\right] \qquad\qquad \mathbf{W}_\mathrm{w}(s) \overset{ss}{=} \left[\begin{array}{c|c} \mathbf{A}_\mathrm{ww} & \mathbf{B}_\mathrm{ww} \\ \hline \mathbf{C}_\mathrm{ww} & \mathbf{D}_\mathrm{ww} \end{array}\right] \tag{6.36}$$

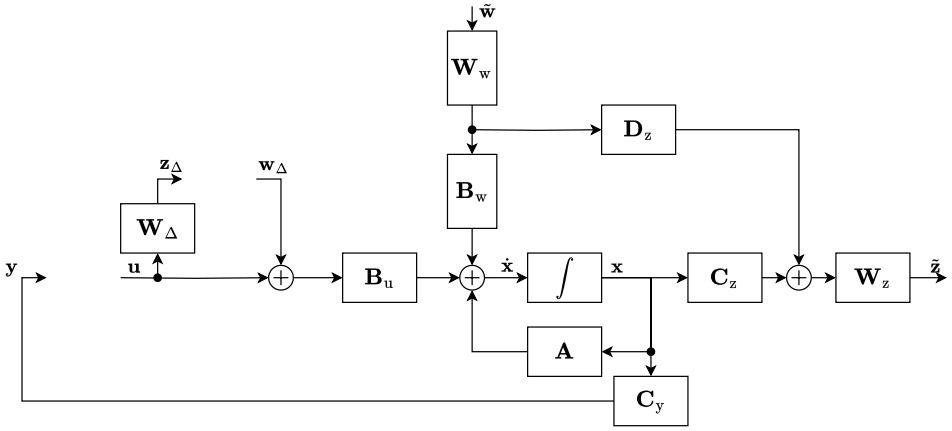

Figure 6.12: Block diagram of the input uncertain system with the weighting function $\mathbf{W}_\Delta$, where the controller $\mathbf{K}$ and uncertainty $\mathbf{\Delta}$ has been removed to illustrate the diagram is open-loop.

Based on figure 6.12 and (6.36) a state space model can be obtained as:

$$\begin{bmatrix} \dot{\mathbf{x}} \\ \dot{\mathbf{x}}_{\text{ww}} \\ \dot{\mathbf{x}}_{\text{wz}} \\ \mathbf{z}_\Delta \\ \tilde{\mathbf{z}} \\ \mathbf{z} \\ \mathbf{y}_\Delta \\ \mathbf{y}_{\text{w}} \\ \mathbf{y}_{\text{k}} \\ \mathbf{y} \end{bmatrix} = \begin{bmatrix} \mathbf{A} & \mathbf{0}_{12\times4} & \mathbf{0}_{12\times4} & \mathbf{B}_{\text{u}} & \mathbf{0}_{12\times4} & \mathbf{B}_{\text{w}} & \mathbf{0}_{12\times4} & \mathbf{0}_{12\times4} & \mathbf{B}_{\text{u}} & \mathbf{0}_{12\times12} \\ \mathbf{0}_{4\times12} & \mathbf{A}_{\text{ww}} & \mathbf{0}_{4\times4} & \mathbf{0}_{4\times4} & \mathbf{0}_{4\times4} & \mathbf{0}_{4\times4} & \mathbf{0}_{4\times4} & \mathbf{B}_{\text{w}} & \mathbf{0}_{4\times4} & \mathbf{0}_{4\times12} \\ \mathbf{0}_{4\times12} & \mathbf{0}_{4\times4} & \mathbf{A}_{\text{wz}} & \mathbf{0}_{4\times4} & \mathbf{B}_{\text{wz}} & \mathbf{0}_{4\times4} & \mathbf{0}_{4\times4} & \mathbf{0}_{4\times4} & \mathbf{0}_{4\times4} & \mathbf{0}_{4\times12} \\ \mathbf{0}_{4\times12} & \mathbf{0}_{4\times4} & \mathbf{0}_{4\times4} & \mathbf{0}_{4\times4} & \mathbf{0}_{4\times4} & \mathbf{0}_{4\times4} & \mathbf{0}_{4\times4} & \mathbf{0}_{4\times4} & \mathbf{D}_{\text{w}\Delta} & \mathbf{0}_{4\times12} \\ \mathbf{0}_{4\times12} & \mathbf{0}_{4\times4} & \mathbf{C}_{\text{wz}} & \mathbf{0}_{4\times4} & \mathbf{D}_{\text{wz}} & \mathbf{0}_{4\times4} & \mathbf{0}_{4\times4} & \mathbf{0}_{4\times4} & \mathbf{0}_{4\times4} & \mathbf{0}_{4\times12} \\ \mathbf{C}_{\text{z}} & \mathbf{0}_{4\times4} & \mathbf{0}_{4\times4} & \mathbf{0}_{4\times4} & \mathbf{0}_{4\times4} & \mathbf{D}_{\text{z}} & \mathbf{0}_{4\times4} & \mathbf{0}_{4\times4} & \mathbf{0}_{4\times4} & \mathbf{0}_{4\times12} \\ \mathbf{0}_{4\times12} & \mathbf{0}_{4\times4} & \mathbf{0}_{4\times4} & \mathbf{0}_{4\times4} & \mathbf{0}_{4\times4} & \mathbf{0}_{4\times4} & \mathbf{\Delta} & \mathbf{0}_{4\times4} & \mathbf{0}_{4\times4} & \mathbf{0}_{4\times12} \\ \mathbf{0}_{4\times12} & \mathbf{C}_{\text{ww}} & \mathbf{0}_{4\times4} & \mathbf{0}_{4\times4} & \mathbf{0}_{4\times4} & \mathbf{0}_{4\times4} & \mathbf{0}_{4\times4} & \mathbf{D}_{\text{ww}} & \mathbf{0}_{4\times4} & \mathbf{0}_{4\times12} \\ \mathbf{0}_{12\times12} & \mathbf{0}_{12\times4} & \mathbf{0}_{12\times4} & \mathbf{0}_{12\times4} & \mathbf{0}_{12\times4} & \mathbf{0}_{12\times4} & \mathbf{0}_{12\times4} & \mathbf{0}_{12\times4} & \mathbf{0}_{12\times4} & \mathbf{K} \\ \mathbf{C}_{\text{y}} & \mathbf{0}_{4\times4} & \mathbf{0}_{4\times4} & \mathbf{0}_{4\times4} & \mathbf{0}_{4\times4} & \mathbf{0}_{4\times4} & \mathbf{0}_{4\times4} & \mathbf{0}_{4\times4} & \mathbf{0}_{4\times4} & \mathbf{0}_{4\times12} \end{bmatrix} \begin{bmatrix} \mathbf{x} \\ \mathbf{x}_{\text{ww}} \\ \mathbf{x}_{\text{wz}} \\ \mathbf{w}_\Delta \\ \mathbf{u}_{\text{z}} \\ \mathbf{w} \\ \mathbf{u}_\Delta \\ \tilde{\mathbf{w}} \\ \mathbf{u} \\ \mathbf{u}_k \end{bmatrix} \tag{6.37}$$

Similar to in section 6.2, the loops are closed around the controller and the auxiliary signals $\mathbf{z} = \mathbf{u}_{\text{z}}$ and $\mathbf{y}_{\text{w}} = \mathbf{w}$, which results in:

$$\begin{bmatrix} \dot{\mathbf{x}} \\ \dot{\mathbf{x}}_{\mathrm{ww}} \\ \dot{\mathbf{x}}_{\mathrm{wz}} \\ \mathbf{z}_{\Delta} \\ \tilde{\mathbf{z}} \\ \mathbf{y}_{\Delta} \end{bmatrix} = \begin{bmatrix} \mathbf{A}+\mathbf{B}_{\mathrm{u}}\mathbf{K} & \mathbf{B}_{\mathrm{w}}\mathbf{C}_{\mathrm{ww}} & \mathbf{0}_{12\times4} & \mathbf{B}_{\mathrm{u}} & \mathbf{0}_{12\times4} & \mathbf{B}_{\mathrm{w}}\mathbf{D}_{\mathrm{ww}} \\ \mathbf{0}_{4\times12} & \mathbf{A}_{\mathrm{ww}} & \mathbf{0}_{4\times4} & \mathbf{0}_{4\times4} & \mathbf{0}_{4\times4} & \mathbf{B}_{\mathrm{ww}} \\ \mathbf{B}_{\mathrm{wz}}\mathbf{C}_{\mathrm{z}} & \mathbf{B}_{\mathrm{wz}}\mathbf{D}_{\mathrm{z}}\mathbf{C}_{\mathrm{ww}} & \mathbf{A}_{\mathrm{wz}} & \mathbf{0}_{4\times4} & \mathbf{0}_{4\times4} & \mathbf{B}_{\mathrm{wz}}\mathbf{D}_{\mathrm{z}}\mathbf{D}_{\mathrm{ww}} \\ \mathbf{D}_{\mathrm{w}\Delta}\mathbf{K} & \mathbf{0}_{4\times4} & \mathbf{0}_{4\times4} & \mathbf{0}_{4\times4} & \mathbf{0}_{4\times4} & \mathbf{0}_{4\times4} \\ \mathbf{D}_{\mathrm{wz}}\mathbf{C}_{\mathrm{z}} & \mathbf{D}_{\mathrm{wz}}\mathbf{D}_{\mathrm{z}}\mathbf{C}_{\mathrm{ww}} & \mathbf{C}_{\mathrm{wz}} & \mathbf{0}_{4\times4} & \mathbf{0}_{4\times4} & \mathbf{B}_{\mathrm{wz}}\mathbf{D}_{\mathrm{z}}\mathbf{D}_{\mathrm{ww}} \\ \mathbf{0}_{4\times12} & \mathbf{0}_{4\times4} & \mathbf{0}_{4\times4} & \mathbf{0}_{4\times4} & \boldsymbol{\Delta} & \mathbf{0}_{4\times4} \end{bmatrix} \begin{bmatrix} \mathbf{x} \\ \mathbf{x}_{\mathrm{ww}} \\ \mathbf{x}_{\mathrm{wz}} \\ \mathbf{w}_{\Delta} \\ \mathbf{u}_{\Delta} \\ \tilde{\mathbf{w}} \end{bmatrix} \tag{6.38}$$

From (6.38), $\mathbf{N}_{\mathrm{w}}$ can be expressed as the following state space representation.

$$\begin{aligned} \dot{\mathbf{x}}_{\mathrm{Nw}} &= \mathbf{A}_{\mathrm{Nw}}\mathbf{x}_{\mathrm{Nw}} + \mathbf{B}_{\mathrm{Nw}}\mathbf{w}_{\mathrm{Nw}} \\ \mathbf{z}_{\mathrm{Nw}} &= \mathbf{C}_{\mathrm{Nw}}\mathbf{x}_{\mathrm{Nw}} + \mathbf{D}_{\mathrm{Nw}}\mathbf{w}_{\mathrm{Nw}} \end{aligned} \tag{6.39}$$

with:

$$\mathbf{x}_{\mathrm{Nw}} = \begin{bmatrix} \mathbf{x} & \mathbf{x}_{\mathrm{ww}} & \mathbf{x}_{\mathrm{wz}} \end{bmatrix}^{\mathrm{T}}, \qquad \mathbf{w}_{\mathrm{Nw}} = \begin{bmatrix} \mathbf{w}_{\Delta} & \tilde{\mathbf{w}} \end{bmatrix}^{\mathrm{T}} \tag{6.39a}$$

$$\mathbf{A}_{\mathrm{Nw}} = \begin{bmatrix} \mathbf{A}+\mathbf{B}_{\mathrm{u}}\mathbf{K} & \mathbf{B}_{\mathrm{w}}\mathbf{C}_{\mathrm{ww}} & \mathbf{0}_{12\times4} \\ \mathbf{0}_{12\times4} & \mathbf{A}_{\mathrm{ww}} & \mathbf{0}_{4\times4} \\ \mathbf{B}_{\mathrm{wz}}\mathbf{C}_{\mathrm{z}} & \mathbf{B}_{\mathrm{wz}}\mathbf{D}_{\mathrm{z}}\mathbf{C}_{\mathrm{ww}} & \mathbf{A}_{\mathrm{wz}} \end{bmatrix}, \quad \mathbf{B}_{\mathrm{Nw}} = \begin{bmatrix} \mathbf{B}_{\mathrm{u}} & \mathbf{B}_{\mathrm{w}}\mathbf{D}_{\mathrm{ww}} \\ \mathbf{0}_{4\times4} & \mathbf{B}_{\mathrm{ww}} \\ \mathbf{0}_{4\times4} & \mathbf{B}_{\mathrm{wz}}\mathbf{D}_{\mathrm{z}}\mathbf{D}_{\mathrm{ww}} \end{bmatrix} \tag{6.39b}$$

$$\mathbf{C}_{\mathrm{Nw}} = \begin{bmatrix} \mathbf{D}_{\mathrm{w}\Delta}\mathbf{K} & \mathbf{0}_{4\times4} & \mathbf{0}_{4\times4} \\ \mathbf{D}_{\mathrm{wz}}\mathbf{C}_{\mathrm{z}} & \mathbf{D}_{\mathrm{wz}}\mathbf{D}_{\mathrm{z}}\mathbf{C}_{\mathrm{ww}} & \mathbf{C}_{\mathrm{wz}} \end{bmatrix}, \qquad \mathbf{D}_{\mathrm{Nw}} = \begin{bmatrix} \mathbf{0}_{4\times4} & \mathbf{0}_{4\times4} \\ \mathbf{0}_{4\times4} & \mathbf{B}_{\mathrm{wz}}\mathbf{D}_{\mathrm{z}}\mathbf{D}_{\mathrm{ww}} \end{bmatrix} \tag{6.39c}$$

Similar to when uncertainty weights were introduced in section 6.4.5, this requires the Lyapunov variable to be expanded as:

$$\hat{\mathbf{P}} = \begin{bmatrix} \mathbf{P} & \mathbf{P}_{1,2} & \mathbf{P}_{1,3} \\ \star & \mathbf{P}_{2,2} & \mathbf{P}_{2,3} \\ \star & \star & \mathbf{P}_{3,3} \end{bmatrix} \tag{6.40}$$

with $\mathbf{P} = \mathrm{diag}(\mathbf{P}_1, \ldots, \mathbf{P}_{\mathrm{n}})$, $\mathbf{P}_{\mathrm{i}} \in \mathbb{R}^{3\times3}$ and $\mathbf{P}_{\mathrm{i,j}}$ appropriate dimensions. With the model derived, the performance can be calculated using the bounded real lemma from (5.10). This however first requires the matrices $\mathbf{B}_{\mathrm{w}}$, $\mathbf{C}_{\mathrm{z}}$, $\mathbf{D}_{\mathrm{z}}$ and the weights to be expressed. The matrix $\mathbf{B}_{\mathrm{w}}$ describes how the exogenous inputs affect the system, which for the HVAC

system is the reference, as no disturbance or sensor noise is treated. As the objective is to control the air temperature, applying the reference to the air temperature state is obvious. However, as each AHU has an integral state on the air temperature, applying the reference to the integral state would drive the air to the desired temperature. Therefore, $\mathbf{B}_{\mathrm{w}}$ is designed to allow the unique air temperature reference for each AHU to enter independently as:

$$\mathbf{B}_{\mathrm{w}} = \begin{bmatrix} 0 & 0 & -1 & 0 & 0 & 0 & 0 & 0 & 0 & 0 & 0 & 0 \\ 0 & 0 & 0 & 0 & 0 & -1 & 0 & 0 & 0 & 0 & 0 & 0 \\ 0 & 0 & 0 & 0 & 0 & 0 & 0 & 0 & -1 & 0 & 0 & 0 \\ 0 & 0 & 0 & 0 & 0 & 0 & 0 & 0 & 0 & 0 & 0 & -1 \end{bmatrix}^{\mathrm{T}} \tag{6.41}$$

As $\mathbf{z}$ is the controlled outputs or errors which is minimised wrt., these are desired to be expressed as the difference between the reference and air temperature of the individual AHU. This can be achieved by defining the feedforward matrix $\mathbf{D}_{\mathrm{z}}$ as identity and $\mathbf{C}_{\mathrm{z}}$ such the the air temperature is selected from the states. This implies the two matrices can be defined as:

$$\mathbf{C}_{\mathrm{z}} = \begin{bmatrix} 0 & 1 & 0 & 0 & 0 & 0 & 0 & 0 & 0 & 0 & 0 & 0 \\ 0 & 0 & 0 & 0 & 1 & 0 & 0 & 0 & 0 & 0 & 0 & 0 \\ 0 & 0 & 0 & 0 & 0 & 0 & 0 & 1 & 0 & 0 & 0 & 0 \\ 0 & 0 & 0 & 0 & 0 & 0 & 0 & 0 & 0 & 0 & 1 & 0 \end{bmatrix}, \qquad \mathbf{D}_{\mathrm{z}} = -\mathbf{I}_4 \tag{6.42}$$

The weight $\mathbf{W}_{\mathrm{w}}$ describe the frequency content of $\mathbf{w}$ [5, p.363]. Without the weight $\mathbf{w}$ is a white signal, meaning it acts on every frequency. In practice, this is not the case and $\mathbf{w}$ has some dynamics. For this system, $\mathbf{w}$ describes the references, which are typically low frequency [6, p.138]. For the HVAC system, the reference would be set by a user, and would theoretically not be adjusted rapidly. As such $\mathbf{W}_{\mathrm{w}}$ is modelled as a first-order low-pass filter with a cutoff frequency at one hertz, which in state space can be defined as (6.43).

$\mathbf{W}_{\mathrm{z}}$ describes behaviour of $\mathbf{z}$, which is the error between the reference and output of the system. For this system, it is chosen to apply a constant scaling of one, which implies $\mathbf{W}_{\mathrm{z}}$ can be defined as (6.43).

$$\mathbf{W}_{\mathrm{w}}(s) \overset{ss}{=} \left[\begin{array}{c|c} -2\pi\mathbf{I}_4 & 2\mathbf{I}_4 \\ \hline \pi\mathbf{I}_4 & \mathbf{0}_{4\times4} \end{array}\right], \qquad \mathbf{W}_{\mathrm{z}}(s) \overset{ss}{=} \left[\begin{array}{c|c} \mathbf{0}_{4\times4} & \mathbf{0}_{4\times4} \\ \hline \mathbf{0}_{4\times4} & \mathbf{I}_4 \end{array}\right] \tag{6.43}$$

With these definitions, robust performance can be determined by calculating the bounded real lemma (5.10) on the system (6.39) and validating condition (6.35). While this allows for analysis, as mentioned it is of interest to synthesise a controller with desired performance. To synthesise with performance, the system (6.39) could be split so the controller is separated similar to section 6.4.5. Another option, called frequency weighted model matching, is explored, where the controller is synthesised so the system response best match a desired response.

Frequency Weighted Model Matching

As mentioned frequency weighted model matching (FWMM) is a method for synthesising a controller such that the systems matches a desired frequency response [5, p.363][6, p.142]. To achieve this, the desired response $\mathbf{W}_{\text{ref}}(s)$ can be introduced into the block diagram from figure 6.12 as shown on figure 6.13.

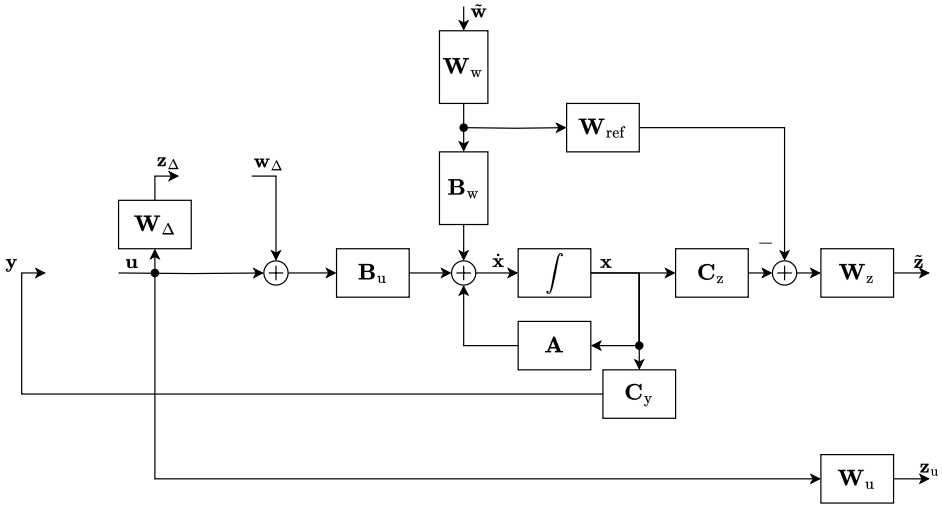

Figure 6.13: Block diagram for the synthesis using frequency weighted model matching, where the controller $\mathbf{K}$ and uncertainty $\mathbf{\Delta}$ has been removed to illustrate the diagram is open-loop.

By investigating the transfer function from $\tilde{\mathbf{w}}$ to $\tilde{\mathbf{z}}$, it can be seen how $\tilde{\mathbf{z}}$ describes the difference between the actual system output, and the output from the desired response. This implies that if the error $\tilde{\mathbf{z}}$ is zero, then the actual system is equal to the desired response, hence minimizing $\tilde{\mathbf{z}}$ will find a $\mathbf{K}$ that makes the system best match the desired response. Figure 6.13 also has the weighted output $\mathbf{z}_{\text{u}}$, which is the weighted input to the system. If this is appended to $\tilde{\mathbf{z}}$, then a controller will also minimize the actuation needed, since $\mathbf{W}_{\text{u}}\mathbf{u}$ becomes part of the output to be minimized [5, p.363].

Following the performance definitions (6.35), figure 6.13 can be used to express a robust

performance problem, for which a condition can be expressed as [5, p.364]:

$$\mu(\mathbf{N}_{\mathrm{DS}}(s)) \leq 1, \forall s \tag{6.44}$$

where $\mathbf{N}_{\mathrm{DS}}(s)$ describes the interconnection between

$$\begin{bmatrix} \tilde{\mathbf{w}} \\ \mathbf{w}_{\Delta} \end{bmatrix} \text{ and } \begin{bmatrix} \mathbf{z}_{\mathrm{ref}} \\ \mathbf{z}_{\mathrm{u}} \\ \mathbf{z}_{\Delta} \end{bmatrix} \tag{6.44a}$$

As mentioned in (5.17) for full uncertainty, the SSV is equivalent to the H_{∞}-norm, for which an upper bound can be found using (5.10). To apply the bounded real lemma, a description of the system is required. From figure 6.13 a state space description using the general control configuration can be expressed as:

$$
\begin{bmatrix} \dot{\mathbf{x}} \\ \dot{\mathbf{x}}_{\mathrm{ww}} \\ \dot{\mathbf{x}}_{\mathrm{wz}} \\ \dot{\mathbf{x}}_{\mathrm{wref}} \\ \dot{\mathbf{x}}_{\mathrm{wu}} \\ \tilde{\mathbf{z}} \\ \mathbf{z}_{\mathrm{u}} \\ \mathbf{z}_{\Delta} \\ \mathbf{y}_{\Delta} \\ \mathbf{y}_{\mathrm{w}} \\ \mathbf{y} \\ \mathbf{y}_{\mathrm{k}} \end{bmatrix} = \begin{bmatrix} \mathbf{A} & \mathbf{0}_{12\times4} & \mathbf{0}_{12\times4} & \mathbf{0}_{12\times4} & \mathbf{0}_{12\times4} & \mathbf{B}_{\mathrm{w}} & \mathbf{0}_{12\times4} & \mathbf{B}_{\mathrm{u}} \\ \mathbf{0}_{4\times12} & \mathbf{A}_{\mathrm{ww}} & \mathbf{0}_{4\times4} & \mathbf{0}_{4\times4} & \mathbf{0}_{4\times4} & \mathbf{0}_{4\times4} & \mathbf{B}_{\mathrm{ww}} & \mathbf{0}_{4\times4} \\ \mathbf{B}_{\mathrm{wz}}\mathbf{C}_{\mathrm{z}} & \mathbf{0}_{4\times4} & \mathbf{A}_{\mathrm{wz}} & -\mathbf{B}_{\mathrm{wz}}\mathbf{C}_{\mathrm{wref}} & \mathbf{0}_{4\times4} & -\mathbf{B}_{\mathrm{wz}}\mathbf{D}_{\mathrm{wref}} & \mathbf{0}_{4\times4} & \mathbf{0}_{4\times4} \\ \mathbf{0}_{4\times12} & \mathbf{0}_{4\times4} & \mathbf{0}_{4\times4} & \mathbf{A}_{\mathrm{wref}} & \mathbf{0}_{4\times4} & \mathbf{B}_{\mathrm{wref}} & \mathbf{0}_{4\times4} & \mathbf{0}_{4\times4} \\ \mathbf{0}_{4\times12} & \mathbf{0}_{4\times4} & \mathbf{0}_{4\times4} & \mathbf{0}_{4\times4} & \mathbf{A}_{\mathrm{wu}} & \mathbf{0}_{4\times4} & \mathbf{0}_{4\times4} & \mathbf{0}_{4\times4} \\ \mathbf{D}_{\mathrm{wz}}\mathbf{C}_{\mathrm{z}} & \mathbf{0}_{4\times4} & \mathbf{C}_{\mathrm{wz}} & -\mathbf{D}_{\mathrm{wz}}\mathbf{C}_{\mathrm{wref}} & \mathbf{0}_{4\times4} & -\mathbf{D}_{\mathrm{wz}}\mathbf{C}_{\mathrm{wref}} & \mathbf{0}_{4\times4} & \mathbf{0}_{4\times4} \\ \mathbf{0}_{4\times12} & \mathbf{0}_{4\times4} & \mathbf{0}_{4\times4} & \mathbf{0}_{4\times4} & \mathbf{C}_{\mathrm{wu}} & \mathbf{0}_{4\times4} & \mathbf{0}_{4\times4} & \mathbf{0}_{4\times4} \\ \mathbf{0}_{4\times12} & \mathbf{0}_{4\times4} & \mathbf{0}_{4\times4} & \mathbf{0}_{4\times4} & \mathbf{0}_{4\times4} & \mathbf{0}_{4\times4} & \mathbf{0}_{4\times4} & \mathbf{0}_{4\times4} \\ \mathbf{0}_{4\times12} & \mathbf{0}_{4\times4} & \mathbf{0}_{4\times4} & \mathbf{0}_{4\times4} & \mathbf{0}_{4\times4} & \mathbf{0}_{4\times4} & \mathbf{0}_{4\times4} & \mathbf{0}_{4\times4} \\ \mathbf{0}_{4\times12} & \mathbf{0}_{4\times4} & \mathbf{0}_{4\times4} & \mathbf{C}_{\mathrm{ref}} & \mathbf{0}_{4\times4} & \mathbf{D}_{\mathrm{ref}} & \mathbf{0}_{4\times4} & \mathbf{0}_{4\times4} \\ \mathbf{0}_{12\times12} & \mathbf{C}_{\mathrm{ww}} & \mathbf{0}_{12\times4} & \mathbf{0}_{12\times4} & \mathbf{0}_{12\times4} & \mathbf{0}_{12\times4} & \mathbf{D}_{\mathrm{ww}} & \mathbf{0}_{12\times4} \\ \mathbf{0}_{4\times12} & \mathbf{0}_{4\times4} & \mathbf{0}_{4\times4} & \mathbf{0}_{4\times4} & \mathbf{0}_{4\times4} & \mathbf{0}_{4\times4} & \mathbf{0}_{4\times4} & \mathbf{0}_{4\times4} \end{bmatrix}
$$

$$
\begin{bmatrix} \mathbf{0}_{12\times4} & \mathbf{B}_{\mathrm{u}} & \mathbf{0}_{12\times12} \\ \mathbf{0}_{4\times4} & \mathbf{0}_{4\times4} & \mathbf{0}_{4\times12} \\ \mathbf{0}_{4\times4} & \mathbf{0}_{4\times4} & \mathbf{0}_{4\times12} \\ \mathbf{0}_{4\times4} & \mathbf{0}_{4\times4} & \mathbf{0}_{4\times12} \\ \mathbf{0}_{4\times4} & \mathbf{B}_{\mathrm{wu}} & \mathbf{0}_{4\times12} \\ \mathbf{0}_{4\times4} & \mathbf{0}_{4\times4} & \mathbf{0}_{4\times12} \\ \mathbf{0}_{4\times4} & \mathbf{D}_{\mathrm{wu}} & \mathbf{0}_{4\times12} \\ \mathbf{0}_{4\times4} & \mathbf{D}_{\mathrm{w}\Delta} & \mathbf{0}_{4\times12} \\ \boldsymbol{\Delta} & \mathbf{0}_{4\times4} & \mathbf{0}_{4\times12} \\ \mathbf{0}_{4\times4} & \mathbf{0}_{4\times4} & \mathbf{0}_{4\times12} \\ \mathbf{0}_{12\times4} & \mathbf{0}_{12\times4} & \mathbf{0}_{12\times12} \\ \mathbf{0}_{4\times4} & \mathbf{0}_{4\times4} & \mathbf{K} \end{bmatrix} \begin{bmatrix} \mathbf{x} \\ \mathbf{x}_{\mathrm{ww}} \\ \mathbf{x}_{\mathrm{wz}} \\ \mathbf{x}_{\mathrm{wref}} \\ \mathbf{x}_{\mathrm{wu}} \\ \mathbf{w} \\ \tilde{\mathbf{w}} \\ \mathbf{w}_{\Delta} \\ \mathbf{u}_{\Delta} \\ \mathbf{u} \\ \mathbf{u}_{\mathrm{k}} \end{bmatrix} \tag{6.45}
$$

Using this expression, the auxiliary signal $\mathbf{y}_{\mathrm{w}} = \mathbf{w}$ and controller can be pulled into the expression similar to in section 6.3. This results in a system expressed by:

$$
\begin{bmatrix} \dot{\mathbf{x}} \\ \dot{\mathbf{x}}_{\mathrm{ww}} \\ \dot{\mathbf{x}}_{\mathrm{wz}} \\ \dot{\mathbf{x}}_{\mathrm{wref}} \\ \dot{\mathbf{x}}_{\mathrm{wu}} \\ \tilde{\mathbf{z}} \\ \mathbf{z}_{\mathrm{u}} \\ \mathbf{z}_{\Delta} \\ \mathbf{y}_{\Delta} \end{bmatrix} = \begin{bmatrix} \mathbf{A}+\mathbf{B}_{\mathrm{u}}\mathbf{K} & \mathbf{B}_{\mathrm{w}}\mathbf{C}_{\mathrm{ww}} & \mathbf{0}_{12\times4} & \mathbf{0}_{12\times4} & \mathbf{0}_{12\times4} \\ \mathbf{0}_{4\times12} & \mathbf{A}_{\mathrm{ww}} & \mathbf{0}_{4\times4} & \mathbf{0}_{4\times4} & \mathbf{0}_{4\times4} \\ \mathbf{B}_{\mathrm{wz}}\mathbf{C}_{\mathrm{z}} & -\mathbf{B}_{\mathrm{wz}}\mathbf{D}_{\mathrm{wref}}\mathbf{C}_{\mathrm{ww}} & \mathbf{A}_{\mathrm{wz}} & -\mathbf{B}_{\mathrm{wz}}\mathbf{C}_{\mathrm{wref}} & \mathbf{0}_{4\times4} \\ \mathbf{0}_{4\times12} & \mathbf{B}_{\mathrm{wref}}\mathbf{C}_{\mathrm{ww}} & \mathbf{0}_{4\times4} & \mathbf{A}_{\mathrm{wref}} & \mathbf{0}_{4\times4} \\ \mathbf{B}_{\mathrm{wu}}\mathbf{K} & \mathbf{0}_{4\times4} & \mathbf{0}_{4\times4} & \mathbf{0}_{4\times4} & \mathbf{A}_{\mathrm{wu}} \\ \mathbf{D}_{\mathrm{wz}}\mathbf{C}_{\mathrm{z}} & -\mathbf{D}_{\mathrm{wz}}\mathbf{D}_{\mathrm{ref}}\mathbf{C}_{\mathrm{ww}} & \mathbf{C}_{\mathrm{wz}} & -\mathbf{D}_{\mathrm{wz}}\mathbf{C}_{\mathrm{ref}} & \mathbf{0}_{4\times4} \\ \mathbf{D}_{\mathrm{wu}}\mathbf{K} & \mathbf{0}_{4\times4} & \mathbf{0}_{4\times4} & \mathbf{0}_{4\times4} & \mathbf{C}_{\mathrm{wu}} \\ \mathbf{D}_{\mathrm{w}\Delta}\mathbf{K} & \mathbf{0}_{4\times4} & \mathbf{0}_{4\times4} & \mathbf{0}_{4\times4} & \mathbf{0}_{4\times4} \\ \mathbf{0}_{4\times12} & \mathbf{0}_{4\times4} & \mathbf{0}_{4\times4} & \mathbf{0}_{4\times4} & \mathbf{0}_{4\times4} \end{bmatrix}
$$

$$
\begin{bmatrix} \mathbf{B}_{\mathrm{w}}\mathbf{D}_{\mathrm{ww}} & \mathbf{B}_{\mathrm{u}} & \mathbf{0}_{12\times4} \\ \mathbf{B}_{\mathrm{ww}} & \mathbf{0}_{4\times4} & \mathbf{0}_{4\times4} \\ -\mathbf{B}_{\mathrm{wz}}\mathbf{D}_{\mathrm{wref}}\mathbf{D}_{\mathrm{ww}} & \mathbf{0}_{4\times4} & \mathbf{0}_{4\times4} \\ \mathbf{B}_{\mathrm{wref}}\mathbf{D}_{\mathrm{ww}} & \mathbf{0}_{4\times4} & \mathbf{0}_{4\times4} \\ \mathbf{0}_{4\times4} & \mathbf{0}_{4\times4} & \mathbf{0}_{4\times4} \\ -\mathbf{D}_{\mathrm{wz}}\mathbf{D}_{\mathrm{wref}}\mathbf{D}_{\mathrm{ww}} & \mathbf{0}_{4\times4} & \mathbf{0}_{4\times4} \\ \mathbf{0}_{4\times4} & \mathbf{0}_{4\times4} & \mathbf{0}_{4\times4} \\ \mathbf{0}_{4\times4} & \mathbf{0}_{4\times4} & \mathbf{0}_{4\times4} \\ \mathbf{0}_{4\times4} & \mathbf{0}_{4\times4} & \boldsymbol{\Delta} \end{bmatrix} \begin{bmatrix} \mathbf{x} \\ \mathbf{x}_{\mathrm{ww}} \\ \mathbf{x}_{\mathrm{wz}} \\ \mathbf{x}_{\mathrm{wref}} \\ \mathbf{x}_{\mathrm{wu}} \\ \tilde{\mathbf{w}} \\ \mathbf{w}_{\Delta} \\ \mathbf{u}_{\Delta} \end{bmatrix} \tag{6.46}
$$

From this expression, the state space model from $\begin{bmatrix} \tilde{\mathbf{w}} & \mathbf{w}_{\Delta} \end{bmatrix}^{\mathrm{T}}$ to $\begin{bmatrix} \tilde{\mathbf{z}} & \mathbf{z}_{\mathrm{u}} & \mathbf{z}_{\Delta} \end{bmatrix}^{\mathrm{T}}$ can be written as:

$$
\begin{aligned} \dot{\mathbf{x}}_{\mathrm{DS}} &= \mathbf{A}_{\mathrm{DS}}\mathbf{x}_{\mathrm{DS}} + \mathbf{B}_{\mathrm{DS}}\mathbf{w}_{\mathrm{DS}} \\ \mathbf{z}_{\mathrm{DS}} &= \mathbf{C}_{\mathrm{DS}}\mathbf{x}_{\mathrm{DS}} + \mathbf{D}_{\mathrm{DS}}\mathbf{w}_{\mathrm{DS}} \end{aligned} \tag{6.47}
$$

where

$$
\mathbf{x}_{\mathrm{DS}} = \begin{bmatrix} \mathbf{x} & \mathbf{x}_{\mathrm{ww}} & \mathbf{x}_{\mathrm{wz}} & \mathbf{x}_{\mathrm{wref}} & \mathbf{x}_{\mathrm{wu}} \end{bmatrix}^{\mathrm{T}}, \qquad \mathbf{w}_{\mathrm{DS}} = \begin{bmatrix} \tilde{\mathbf{w}} & \mathbf{w}_{\Delta} \end{bmatrix}^{\mathrm{T}}, \qquad \mathbf{z}_{\mathrm{DS}} = \begin{bmatrix} \tilde{\mathbf{z}} & \mathbf{z}_{\mathrm{u}} & \mathbf{z}_{\Delta} \end{bmatrix}^{\mathrm{T}} \tag{6.47a}
$$

$$\mathbf{A}_{\mathrm{DS}} = \underbrace{\begin{bmatrix} \mathbf{A} & \mathbf{B}_{\mathrm{w}}\mathbf{C}_{\mathrm{ww}} & \mathbf{0}_{12\times4} & \mathbf{0}_{12\times4} & \mathbf{0}_{12\times4} \\ \mathbf{0}_{4\times12} & \mathbf{A}_{\mathrm{ww}} & \mathbf{0}_{4\times4} & \mathbf{0}_{4\times4} & \mathbf{0}_{4\times4} \\ \mathbf{B}_{\mathrm{wz}} & -\mathbf{B}_{\mathrm{wz}}\mathbf{D}_{\mathrm{wref}} & \mathbf{A}_{\mathrm{wz}} & -\mathbf{B}_{\mathrm{wz}}\mathbf{C}_{\mathrm{wref}} & \mathbf{0}_{4\times4} \\ \mathbf{0}_{4\times12} & \mathbf{B}_{\mathrm{wref}}\mathbf{C}_{\mathrm{ww}} & \mathbf{0}_{4\times4} & \mathbf{A}_{\mathrm{wref}} & \mathbf{0}_{4\times4} \\ \mathbf{0}_{4\times12} & \mathbf{0}_{4\times4} & \mathbf{0}_{4\times4} & \mathbf{0}_{4\times4} & \mathbf{A}_{\mathrm{wu}} \end{bmatrix}}_{\bar{\mathbf{A}}_{\mathrm{DS}}} + \underbrace{\begin{bmatrix} \mathbf{B}_{\mathrm{u}} \\ \mathbf{0}_{4\times4} \\ \mathbf{0}_{4\times4} \\ \mathbf{0}_{4\times4} \\ \mathbf{B}_{\mathrm{wu}} \end{bmatrix}}_{\bar{\mathbf{B}}_{\mathrm{DS}}} \underbrace{\begin{bmatrix} \mathbf{K} \\ \mathbf{0}_{4\times4} \\ \mathbf{0}_{4\times4} \\ \mathbf{0}_{4\times4} \\ \mathbf{0}_{4\times4} \end{bmatrix}^{\mathrm{T}}}_{\bar{\mathbf{K}}_{\mathrm{DS}}} \tag{6.47b}$$

$$\mathbf{C}_{\mathrm{DS}} = \underbrace{\begin{bmatrix} \mathbf{D}_{\mathrm{wz}}\mathbf{C}_{\mathrm{z}} & -\mathbf{D}_{\mathrm{wz}}\mathbf{D}_{\mathrm{ref}}\mathbf{C}_{\mathrm{ww}} & \mathbf{C}_{\mathrm{wz}} & -\mathbf{D}_{\mathrm{wz}}\mathbf{C}_{\mathrm{wref}} & \mathbf{0}_{4\times4} \\ \mathbf{0}_{4\times12} & \mathbf{0}_{4\times4} & \mathbf{0}_{4\times4} & \mathbf{0}_{4\times4} & \mathbf{C}_{\mathrm{wu}} \\ \mathbf{0}_{4\times12} & \mathbf{0}_{4\times4} & \mathbf{0}_{4\times4} & \mathbf{0}_{4\times4} & \mathbf{0}_{4\times4} \end{bmatrix}}_{\bar{\mathbf{C}}_{\mathrm{DS},1}} + \underbrace{\begin{bmatrix} \mathbf{0}_{4\times4} \\ \mathbf{D}_{\mathrm{wu}} \\ \mathbf{D}_{\mathrm{w}\Delta} \end{bmatrix}}_{\bar{\mathbf{C}}_{\mathrm{DS},2}} \underbrace{\begin{bmatrix} \mathbf{K} \\ \mathbf{0}_{4\times4} \\ \mathbf{0}_{4\times4} \\ \mathbf{0}_{4\times4} \\ \mathbf{0}_{4\times4} \end{bmatrix}^{\mathrm{T}}}_{\bar{\mathbf{K}}_{\mathrm{DS}}} \tag{6.47c}$$

$$\mathbf{B}_{\mathrm{DS}} = \begin{bmatrix} \mathbf{B}_{\mathrm{w}}\mathbf{D}_{\mathrm{ww}} & \mathbf{B}_{\mathrm{u}} \\ \mathbf{B}_{\mathrm{ww}} & \mathbf{0}_{4\times4} \\ -\mathbf{B}_{\mathrm{wz}}\mathbf{D}_{\mathrm{wref}}\mathbf{D}_{\mathrm{ww}} & \mathbf{0}_{4\times4} \\ \mathbf{B}_{\mathrm{wref}}\mathbf{D}_{\mathrm{ww}} & \mathbf{0}_{4\times4} \\ \mathbf{0}_{4\times4} & \mathbf{0}_{4\times4} \end{bmatrix}, \qquad \mathbf{D}_{\mathrm{DS}} = \begin{bmatrix} -\mathbf{D}_{\mathrm{wz}}\mathbf{D}_{\mathrm{wref}}\mathbf{D}_{\mathrm{ww}} & \mathbf{0}_{4\times4} \\ \mathbf{0}_{4\times4} & \mathbf{0}_{4\times4} \\ \mathbf{0}_{4\times4} & \mathbf{0}_{4\times4} \end{bmatrix} \tag{6.47d}$$

Using these definitions a controller can be synthesised by solving the bounded real lemma with a change of variable. That is finding a $\mathbf{Q}_{\mathrm{DS}} > 0$ such that:

$$\begin{bmatrix} \mathbf{Q}_{\mathrm{DS}}\bar{\mathbf{A}}_{\mathrm{DS}}^{\mathrm{T}} + \bar{\mathbf{A}}_{\mathrm{DS}}\mathbf{Q}_{\mathrm{DS}} + \hat{\mathbf{Y}}_{\mathrm{DS}}^{\mathrm{T}}\bar{\mathbf{B}}_{\mathrm{DS}}^{\mathrm{T}} + \bar{\mathbf{B}}_{\mathrm{DS}}\hat{\mathbf{Y}}_{\mathrm{DS}} & \mathbf{B}_{\mathrm{DS}} & \mathbf{Q}_{\mathrm{DS}}\bar{\mathbf{C}}_{\mathrm{DS},1}^{\mathrm{T}} + \hat{\mathbf{Y}}_{\mathrm{DS}}^{\mathrm{T}}\bar{\mathbf{C}}_{\mathrm{DS},2}^{\mathrm{T}} \\ \star & -\gamma\mathbf{I}_8 & \mathbf{D}_{\mathrm{DS}}^{\mathrm{T}} \\ \star & \star & -\gamma\mathbf{I}_{12} \end{bmatrix} < 0 \tag{6.48}$$

where:

$$\mathbf{Q}_{\mathrm{DS}} = \mathbf{P}_{\mathrm{DS}}^{-1} = \begin{bmatrix} \mathbf{Q} & \mathbf{Q}_{1,2} & \mathbf{Q}_{1,3} & \mathbf{Q}_{1,4} & \mathbf{Q}_{1,5} \\ \star & \mathbf{Q}_{2,2} & \mathbf{Q}_{2,3} & \mathbf{Q}_{2,4} & \mathbf{Q}_{2,5} \\ \star & \star & \mathbf{Q}_{3,3} & \mathbf{Q}_{3,4} & \mathbf{Q}_{3,5} \\ \star & \star & \star & \mathbf{Q}_{4,4} & \mathbf{Q}_{4,5} \\ \star & \star & \star & \star & \mathbf{Q}_{5,5} \end{bmatrix}, \qquad \hat{\mathbf{Y}}_{\mathrm{DS}} = \bar{\mathbf{K}}_{\mathrm{DS}}\mathbf{Q}_{\mathrm{DS}} = \begin{bmatrix} \mathbf{KQ} \\ \mathbf{KQ}_{1,2} \\ \mathbf{KQ}_{1,3} \\ \mathbf{KQ}_{4,1} \\ \mathbf{KQ}_{5,1} \end{bmatrix}^{\mathrm{T}} \tag{6.48a}$$

$\mathbf{Q} = \mathrm{diag}(\mathbf{Q}_1, \ldots, \mathbf{Q}_n)$, $\mathbf{Q}_i \in \mathbb{R}^{3\times 3}$ and $\mathbf{Q}_{i,j}$ appropriate dimensions. Before $\mathbf{K}$ can be synthesised, the desired response must be defined. For this project it is chosen to have a step response resulting in a settling time of ten minutes. Furthermore, it is desirable to limit the output of the controller such that the actuator does not saturate. To guarantee this, the actuation range of the pump must be known. As an example, this project will use the pump *MAGNA3 100-120F 97924315*, which is a pump that could be installed in the system [8]. For this type of pump, the amount of flow, which can be generated by the pump, is dependent on the height the water needs to be lifted, as shown in figure 6.14. For this project, it is assumed that the system can be installed in a configuration such that the height of the water is between 3 and 5 meters, which results in a maximum flowrate between 66 and 58$\frac{m^3}{h}$.

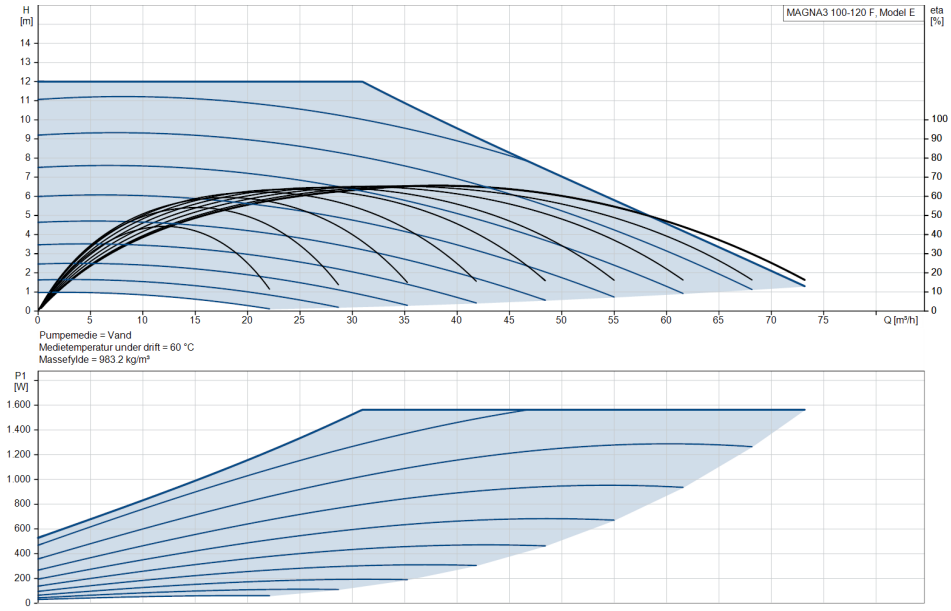

Figure 6.14: Pump characteristics of MAGNA3 [8].

With the actuation range found, the desired response must be realised. As the desired response only requires a settling time of ten minutes, this can be realised as a first order lowpass filter, for which it is known that after approximately five times the time-constant, the transient period is finished. This corresponds to defining the settling time threshold to be within 0.7% of the target value. From this, the desired response is defined as the state space realization:

$$\mathbf{W}_{\text{ref}}(s) \overset{ss}{=} \left[\begin{array}{c|c} -\frac{1}{120}\mathbf{I}_4 & \frac{1}{8}\mathbf{I}_4 \\ \hline \frac{1}{15}\mathbf{I}_4 & \mathbf{0}_{4\times 4} \end{array}\right] \tag{6.49}$$

Since $\mathbf{W}_{\text{ref}}$ is a first order lowpass filter, the maximal actuation required, will be the actuation needed to maintain steady-state. As the pump is assumed to be sufficient to achieve steady state at every reference, this implies $\mathbf{W}_{\text{u}}$ can be chosen as $\mathbf{0}_{4\times 4}$.

Applying $\mathbf{W}_{\text{ref}}$ with $\mathbf{W}_{\text{u}} = \mathbf{0}_{4\times 4}$ a $\mathbf{K}$ can be synthesised, resulting in the system response seen on figure 6.15a. From figure 6.15a it can be seen, that the controller does not meet the specified requirement of having a settling time of ten minutes, as it uses 6.667 minutes. As the synthesis tries to minimize the H_∞-norm of the error, to improve the response, the penalty on the error $\tilde{\mathbf{z}}$ was increase, which resulted in the response on figure 6.15b. The penalty was increased by adjusting the weight $\mathbf{W}_{\text{z}}$ to:

$$\mathbf{W}_{\text{z}}(s) \overset{ss}{=} \left[\begin{array}{c|c} \mathbf{0}_{4\times 4} & \mathbf{0}_{4\times 4} \\ \hline \mathbf{0}_{4\times 4} & 5\mathbf{I}_4 \end{array}\right] \tag{6.50}$$

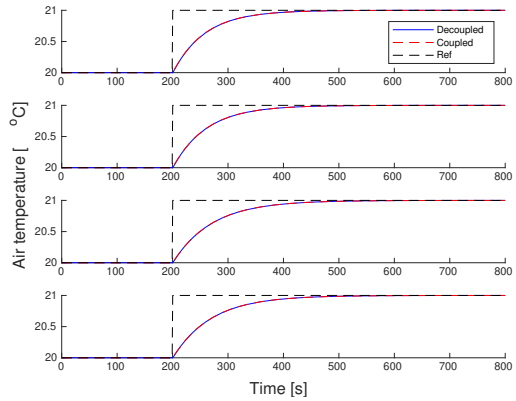

(a) Linear simulated response of the decoupled and coupled system with a controller synthesised to match $\mathbf{W}_{\text{ref}}$, resulting in a settling time of 290s.

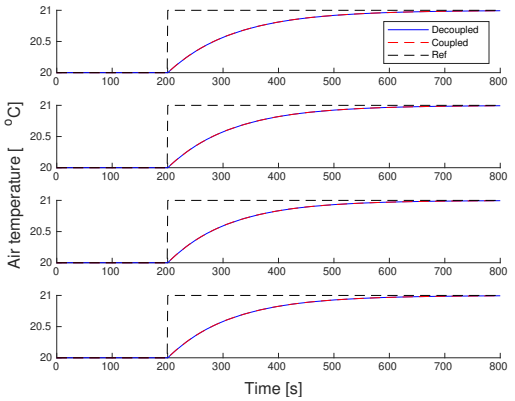

(b) Linear simulated response of the decoupled and coupled system with a controller synthesised to match $\mathbf{W}_{\text{ref}}$ with the adjusted weight $\mathbf{W}_{\text{z}}$ from (6.50), resulting in a settling time of 594s.

Figure 6.15: Step response of the coupled and decoupled system with a synthesised $\mathbf{K}$ based on $\mathbf{W}_{\text{ref}}$ and $\mathbf{W}_{\text{z}}$

As figure 6.15b shows a desired response using the synthesised controller, the worst case generated flow for each AHU can then be checked to see if the required flow exceed the amount which can be delivered from the pumps. The largest flow can be found by setting the reference to 10° as this is equal to matching the output of the chiller. The response of the AHU's can be seen on figure 6.16a, with the corresponding flow on figure 6.16b. From the flow, it can be seen that the maximum flow is $50\frac{m^3}{h}$, which is smaller then the specified limit of 66 and $58\frac{m^3}{h}$ for water heights between 3 and 5 meters specified. It can therefore be concluded, that the method can synthesise a controller guaranteeing robust performance, while matching the desired response, and not exceeding the flow limit of the pump.

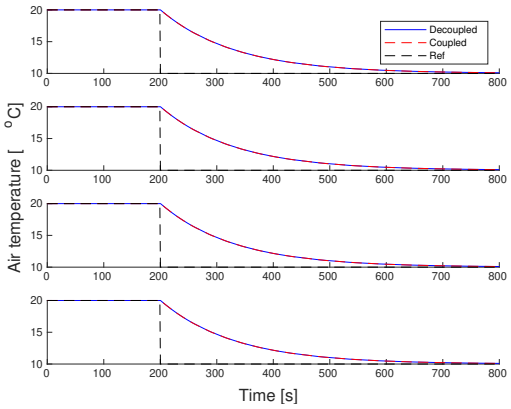

(a) Linear simulated response of the decoupled and coupled system, with a controller specified to match $\mathbf{W}_{\text{ref,fitted}}$ with a reference of 10°

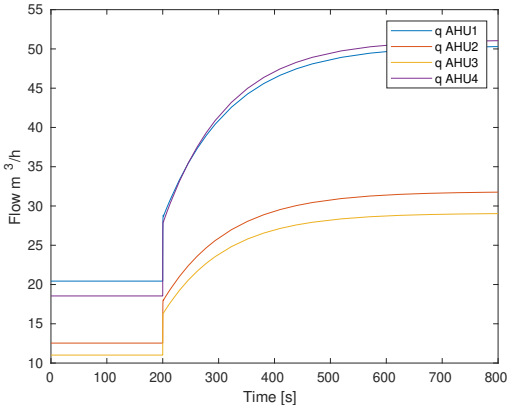

(b) Required flow to bring the system to 10° for a controller synthesised with operating point in 20°

Figure 6.16: Step- and controller- response for the synthesised controller $\mathbf{K}$

6.4.7 Examination of static output feedback

The previous examinations determined that a state feedback(SF) controller could be synthesised to be robust stable and achieve a desirable performance. However, the HVAC system investigated is in practice controlled by a PI-controller, which, for this system, implies only the air temperature T_a and integral state δ are available. As such, the following will examine if a static output feedback(SOF) controller exists. As the SOF controller only has access to T_a and δ, the output matrix $\mathbf{C}_y$ from (6.5) becomes:

$$\mathbf{C}_{\text{y,SOF}} = \begin{bmatrix} 0 & 1 & 0 & 0 & 0 & 0 & 0 & 0 & 0 & 0 & 0 & 0 \\ 0 & 0 & 1 & 0 & 0 & 0 & 0 & 0 & 0 & 0 & 0 & 0 \\ 0 & 0 & 0 & 0 & 1 & 0 & 0 & 0 & 0 & 0 & 0 & 0 \\ 0 & 0 & 0 & 0 & 0 & 1 & 0 & 0 & 0 & 0 & 0 & 0 \\ 0 & 0 & 0 & 0 & 0 & 0 & 0 & 1 & 0 & 0 & 0 & 0 \\ 0 & 0 & 0 & 0 & 0 & 0 & 0 & 0 & 1 & 0 & 0 & 0 \\ 0 & 0 & 0 & 0 & 0 & 0 & 0 & 0 & 0 & 0 & 1 & 0 \\ 0 & 0 & 0 & 0 & 0 & 0 & 0 & 0 & 0 & 0 & 0 & 1 \end{bmatrix} \tag{6.51}$$

This change of output matrix has significant impact on the design procedures previously developed. The previous methods utilized that $\mathbf{C}_{\text{y}} = \mathbf{I}_{12}$ to reduce $\mathbf{BKC}_{\text{y}}\mathbf{Q}$ to $\mathbf{BKQ}$. This allowed for the change of variable $\mathbf{Y} = \mathbf{KQ}$, and recovery of the controller as $\mathbf{K} = \mathbf{YQ}^{-1}$. Attempting this method for $\mathbf{C}_{\text{y,SOF}}$ yields the variable $\mathbf{Y} = \mathbf{KC}_{\text{y,SOF}}\mathbf{Q}$, from which the controller is recovered as $\mathbf{K} = \mathbf{Y}(\mathbf{C}_{\text{y,SOF}}\mathbf{Q})^{-1}$. This requires $\mathbf{C}_{\text{y,SOF}}\mathbf{Q}$ to be non-singular, however, given $\mathbf{C}_{\text{y,SOF}} \in \mathbb{R}^{8\times 12}$ and $\mathbf{Q} \in \mathbb{R}^{12\times 12}$, the product of the two would yield a non-square matrix, which would be non-invertible. Furthermore, no known alternative change of variable is known to exist for SOF [9]. Without the change of variable, the problem of stabilizing the system becomes the Bilinear Matrix Inequality (BMI):

$$(\mathbf{A} + \mathbf{BK}_{\text{SOF}}\mathbf{C}_{\text{y,SOF}})^{\text{T}}\mathbf{P} + \mathbf{P}(\mathbf{A} + \mathbf{BK}_{\text{SOF}}\mathbf{C}_{\text{y,SOF}}) < 0 \tag{6.52}$$

with $\mathbf{P} > 0$. To solve this problem, alternative methods are necessary for SOF synthesis. There exists several methods using iterative algorithms to solve the problem [10]. These methods has the property that they have monotonic non-decreasing criteria through iterations, which means the methods converge to a criteria, unfortunately there is no characterization of dead points, and the cost function often rapidly converges to a local plateau or minimum [10]. An alternative non-iterative method proposed in [9], firstly calculates a SF, and then uses that to calculate a SOF. To investigate which, if any, method performs best, both types are implemented and tested.

When considering the uncertainties, these are assumed to be polytopic similar to the ones introduced in the *examination of real uncertainties*. This implies the uncertainties on the matrices become $\mathbf{A}(\rho) = \mathbf{A}$, $\mathbf{B}(\rho) = \mathbf{B}(\mathbf{I}_4 + \text{diag}(\rho)\mathbf{W}_\Delta)$, and $\mathbf{C}_{\text{y,SOF}}(\rho) = \mathbf{C}_{\text{y,SOF}}$. Additionally, robust stability can be verified by guaranteeing stability at each vertex, which means the BMI on (6.52) can be expressed as:

$$\Big(\mathbf{A}+\mathbf{B}(\mathbf{I}_4+\mathrm{diag}(\mathbf{v})\mathbf{W}_\Delta)\mathbf{K}_{\mathrm{SOF}}\mathbf{C}_{\mathrm{y,SOF}}\Big)^{\mathrm{T}}\mathbf{P} + \mathbf{P}\Big(\mathbf{A}+\mathbf{B}(\mathbf{I}_4+\mathrm{diag}(\mathbf{v})\mathbf{W}_\Delta)\mathbf{K}_{\mathrm{SOF}}\mathbf{C}_{\mathrm{y,SOF}}\Big) < 0, \quad \forall \quad \mathbf{v}\in\mathbf{vert}(\mathcal{P}) \tag{6.53}$$

with $\mathbf{P} > 0$. However, for generalization of the methods and for cleaner notation, $\mathbf{A}(\rho)$, $\mathbf{B}(\rho)$, and $\mathbf{C}_{\mathrm{y,SOF}}(\rho)$ is used in the following derivations.

The methods also use the notion of a prescribed degree of stability or α-stability, which moves the closed loop poles to the left side of the line define by $\mathrm{Re}(s) = -\alpha$ for $\alpha > 0$ [11]. To implement α-stability, the $\mathbf{A}(\rho)$ matrix is perturbed as:

$$\mathbf{A}_\alpha(\rho) = \mathbf{A}(\rho) + \alpha\mathbf{I} \tag{6.54}$$

Applying the perturbation (6.54) to the Lyapunov stability from (5.25) results in an additional term:

$$\mathbf{Q}\mathbf{A}^{\mathrm{T}} + \mathbf{A}\mathbf{Q} + \mathbf{Y}^{\mathrm{T}}\mathbf{B}^{\mathrm{T}} + \mathbf{Y}\mathbf{B} + 2\alpha\mathbf{Q} < 0 \tag{6.55}$$

This additional term $\alpha\mathbf{Q}$ bounds the rate of convergence of the states by $e^{-\alpha t}$ [5, p.478].

Iterative method

The iterative method examined, called Iterative Linear Matrix Inequality (ILMI), iteratively solve a Quadratic Matrix Inequality (QMI), which guarantees the existence of a SOF controller [12]. The method has been expanded to include robust stability towards polytopic uncertainties. The method utilizes the following theorem, derived from (6.53):

Theorem 3 ([12]) *The realization* $(\boldsymbol{A}, \boldsymbol{B}, \boldsymbol{C}_{\mathrm{y,SOF}})$ *is robust stabilizable towards polytopic uncertainties* ρ *via static output feedback if and only if there exists matrices* $\boldsymbol{P} > 0$ *and* $\boldsymbol{K}_{\mathrm{SOF}}$ *satisfying the following matrix inequality:*

$$\boldsymbol{A}(\rho)^T\boldsymbol{P} + \boldsymbol{P}\boldsymbol{A}(\rho) - \boldsymbol{P}\boldsymbol{B}(\rho)\boldsymbol{B}(\rho)^T\boldsymbol{P} + \Big(\boldsymbol{B}(\rho)^T\boldsymbol{P} + \boldsymbol{K}_{\mathrm{SOF}}\boldsymbol{C}_{\mathrm{y,SOF}}(\rho)\Big)^T\Big(\boldsymbol{B}(\rho)^T\boldsymbol{P} + \boldsymbol{K}_{\mathrm{SOF}}\boldsymbol{C}_{\mathrm{y,SOF}}(\rho)\Big) < 0, \quad \forall\rho\in\mathcal{P} \tag{6.56}$$

This theorem guarantees the existence of a SOF controller, however similar to the BMI (6.53), this QMI cannot be solved efficiently. Some QMI can be transformed into LMI by using Schur complement, however due to the sign, the term $-\mathbf{P}\mathbf{B}(\rho)\mathbf{B}(\rho)^{\mathrm{T}}\mathbf{P}$ cannot be transformed using Schur complement. However, $\mathbf{P}\mathbf{B}(\rho)\mathbf{B}(\rho)^{\mathrm{T}}\mathbf{P}$ can be replaced by introducing a new variable $\mathbf{X}$ as [12]:

$$(\mathbf{X}-\mathbf{P})^{\mathrm{T}}\mathbf{B}(\rho)\mathbf{B}(\rho)^{\mathrm{T}}(\mathbf{X}-\mathbf{P}) \geq 0, \quad \forall\rho\in\mathcal{P} \tag{6.57}$$

This term is guaranteed to be positive semi definite [12]. Expanding the parentheses leads to an inequality:

$$\mathbf{X}^{\mathrm{T}}\mathbf{B}(\rho)\mathbf{B}(\rho)^{\mathrm{T}}\mathbf{P} + \mathbf{P}^{\mathrm{T}}\mathbf{B}(\rho)\mathbf{B}(\rho)^{\mathrm{T}}\mathbf{X} - \mathbf{X}^{\mathrm{T}}\mathbf{B}(\rho)\mathbf{B}(\rho)^{\mathrm{T}}\mathbf{X} \leq \mathbf{P}\mathbf{B}(\rho)\mathbf{B}(\rho)^{\mathrm{T}}\mathbf{P}, \quad \forall \rho \in \mathcal{P} \quad (6.58)$$

The left hand side of this inequality can replace $\mathbf{P}\mathbf{B}(\rho)\mathbf{B}(\rho)^{\mathrm{T}}\mathbf{P}$ in (6.56), which by applying Schur complement results in the matrix inequality (6.59). This replacement of variables results in (6.59) being a sufficient condition for (6.56) when $\mathbf{X}$ is fixed.

$$\begin{bmatrix} \mathbf{A}(\rho)^{\mathrm{T}}\mathbf{P} + \mathbf{P}\mathbf{A}(\rho) - \mathbf{X}^{\mathrm{T}}\mathbf{B}(\rho)\mathbf{B}(\rho)^{\mathrm{T}}\mathbf{P} - \mathbf{P}^{\mathrm{T}}\mathbf{B}(\rho)\mathbf{B}(\rho)^{\mathrm{T}}\mathbf{X} + \mathbf{X}^{\mathrm{T}}\mathbf{B}(\rho)\mathbf{B}(\rho)^{\mathrm{T}}\mathbf{X} & \left(\mathbf{B}(\rho)^{\mathrm{T}}\mathbf{P} + \mathbf{K}_{\mathrm{SOF}}\mathbf{C}_{\mathrm{y,SOF}}(\rho)\right)^{\mathrm{T}} \\ \left(\mathbf{B}(\rho)^{\mathrm{T}}\mathbf{P} + \mathbf{K}_{\mathrm{SOF}}\mathbf{C}_{\mathrm{y,SOF}}(\rho)\right) & -\mathbf{I} \end{bmatrix} < 0, \quad \forall \rho \in \mathcal{P} \quad (6.59)$$

with $\mathbf{P} > 0$, $\mathbf{X} > 0$ and $\mathbf{F}$. When $\mathbf{X}$ is fixed, the matrix inequality (6.59) has no quadratic terms and becomes an LMI. Fixing $\mathbf{X}$, changed (6.59) to only be a sufficient condition for the existence of a stabilizing SOF [12]. This is also apparent from (6.58), as this inequality becomes an equality when $\mathbf{P} = \mathbf{X}$, and hence (6.59) is a necessary and sufficient condition when $\mathbf{P} = \mathbf{X}$. The necessity of (6.59) can be recovered by perturbing $\mathbf{A}_\alpha(\rho) = \mathbf{A}(\rho) - (\alpha/2)\mathbf{I}_{12}$, $\alpha \geq 0$ [12]. Applying the perturbation to the (6.59) results in:

$$\begin{bmatrix} \mathbf{A}(\rho)^{\mathrm{T}}\mathbf{P} + \mathbf{P}\mathbf{A}(\rho) - \alpha\mathbf{P} - \mathbf{X}^{\mathrm{T}}\mathbf{B}(\rho)\mathbf{B}(\rho)^{\mathrm{T}}\mathbf{P} - \mathbf{P}^{\mathrm{T}}\mathbf{B}(\rho)\mathbf{B}(\rho)^{\mathrm{T}}\mathbf{X} + \mathbf{X}^{\mathrm{T}}\mathbf{B}(\rho)\mathbf{B}(\rho)^{\mathrm{T}}\mathbf{X} & \left(\mathbf{B}(\rho)^{\mathrm{T}}\mathbf{P} + \mathbf{K}_{\mathrm{SOF}}\mathbf{C}_{\mathrm{y,SOF}}(\rho)\right)^{\mathrm{T}} \\ \left(\mathbf{B}(\rho)^{\mathrm{T}}\mathbf{P} + \mathbf{K}_{\mathrm{SOF}}\mathbf{C}_{\mathrm{y,SOF}}(\rho)\right) & -\mathbf{I} \end{bmatrix} < 0, \quad \forall \rho \in \mathcal{P} \quad (6.60)$$

To illustrate the necessity, suppose that (6.56) holds, then (6.60) must also hold for some $\alpha > 0$ since:

$$\mathbf{X}^{\mathrm{T}}\mathbf{B}(\rho)\mathbf{B}(\rho)^{\mathrm{T}}\mathbf{P} + \mathbf{P}^{\mathrm{T}}\mathbf{B}(\rho)\mathbf{B}(\rho)^{\mathrm{T}}\mathbf{X} - \mathbf{X}^{\mathrm{T}}\mathbf{B}(\rho)\mathbf{B}(\rho)^{\mathrm{T}}\mathbf{X} + \alpha\mathbf{P} \geq \mathbf{P}\mathbf{B}(\rho)\mathbf{B}(\rho)^{\mathrm{T}}\mathbf{P}, \quad \forall \rho \in \mathcal{P} \quad (6.61)$$

This implies (6.56) is sufficient for (6.60) given (6.61) or in other words (6.60) and (6.61) is necessary for (6.56). Comparing this implementation of the perturbation to (6.54), it shows that this moves the closed loop poles to the left of $\mathrm{Re}(s) = \alpha$. This implies that by

reducing α the poles are moved towards the left half plane. As α becomes smaller, (6.60) closes in to the feasibility of (6.56) [12]. From this interpretation of α and from (6.60) and (6.59), if $\alpha = 0$, then (6.60) becomes sufficient for (6.56). As such, the sequence of α is desired to be non-increasing. To illustrate this is the case, note that (6.65a) is feasible for the optimal solution from the previous iterations $\mathbf{P}_\mathrm{i} = \mathbf{P}^*_{\mathrm{i\text{-}1}}$ and $\alpha_\mathrm{i} = \alpha^*_{\mathrm{i\text{-}1}}$ [12]. This implies (6.65a) for iteration i becomes:

$$\begin{bmatrix} \mathbf{A}(\rho)^\mathrm{T}\mathbf{P}_\mathrm{i} + \mathbf{P}_\mathrm{i}\mathbf{A}(\rho) - \alpha_\mathrm{i}\mathbf{P}_\mathrm{i} - \mathbf{P}_\mathrm{i}^\mathrm{T}\mathbf{B}(\rho)\mathbf{B}(\rho)^\mathrm{T}\mathbf{P}_\mathrm{i} & \Big(\mathbf{B}(\rho)^\mathrm{T}\mathbf{P}_\mathrm{i} + \mathbf{K}_\mathrm{SOF}\mathbf{C}_\mathrm{y,SOF}(\rho)\Big)^\mathrm{T} \\ \Big(\mathbf{B}(\rho)^\mathrm{T}\mathbf{P}_\mathrm{i} + \mathbf{K}_\mathrm{SOF}\mathbf{C}_\mathrm{y,SOF}(\rho)\Big) & -\mathbf{I} \end{bmatrix} < 0 \quad , \quad \forall \rho \in \mathcal{P} \tag{6.62}$$

However, since (6.65a) is sufficient for (6.62), then by solving step 2 in algorithm 1 the optimal α must fulfil $\alpha^*_\mathrm{i} \leq \alpha^*_{\mathrm{i\text{-}1}}$ [12]. Lastly, to guarantee the convergence of the algorithm, the sequence of $\mathbf{P}^*_\mathrm{i}$ must be decreasing, which is the case due to the minimisation of the trace($\mathbf{P}_\mathrm{i}$) in (6.66) [12].

Before the iterative steps of the algorithm can be performed, an initial $\mathbf{X}$ must be found. A suitable $\mathbf{X}$ can be derived from the Algebraic Riccati equation $\mathbf{A}^\mathrm{T}\mathbf{P} + \mathbf{P}\mathbf{A} - \mathbf{P}\mathbf{B}\mathbf{B}^\mathrm{T}\mathbf{P} + \mathbf{Q} = 0$ [12]. Expanding this to include stability at each vertex, the ARE can be solved from the optimisation problem:

$$\text{maximize trace}(\mathbf{P}) \tag{6.63}$$

subject to:

$$\begin{bmatrix} \mathbf{A}(\rho)^\mathrm{T}\mathbf{P} + \mathbf{P}\mathbf{A}(\rho) + \mathbf{Q} & \mathbf{P}\mathbf{B}(\rho) \\ \mathbf{B}(\rho)^\mathrm{T}\mathbf{P} & \mathbf{I} \end{bmatrix} > 0, \quad \forall \quad \rho \in \mathcal{P} \qquad \mathbf{P} > 0 \tag{6.63a}$$

Based on this, the ILMI algorithm is given as in algorithm 1. However, due to numerical errors when solving (6.65), (6.66) can become infeasible in which case, $\alpha_\mathrm{i} = \alpha^*_\mathrm{i} + \Delta_\alpha$, for $\Delta_\alpha > 0$ and (6.66) is solved again [12].

Algorithm 1: Iterative linear matrix inequality [12]

Input : $\mathbf{A}(\rho)$, $\mathbf{B}(\rho)$, $\mathbf{C}_{\text{y,SOF}}(\rho)$, $\mathbf{Q} > 0$

Output: $\mathbf{K}_{\text{SOF}}$

step 1: Solve the optimisation problem

$$\text{maximize } \text{trace}(\mathbf{P}) \tag{6.64}$$

subject to:

$$\begin{bmatrix} \mathbf{A}(\rho)^{\text{T}}\mathbf{P} + \mathbf{P}\mathbf{A}(\rho) + \mathbf{Q} & \mathbf{P}\mathbf{B}(\rho) \\ \mathbf{B}(\rho)^{\text{T}}\mathbf{P} & \mathbf{I} \end{bmatrix} > 0, \quad \forall \quad \rho \in \mathcal{P} \tag{6.64a}$$

$$\mathbf{P} > 0$$

Set $i = 1$ and $\mathbf{X}_{\text{i}} = \mathbf{P}$

step 2: Solve the LMI problem:

$$\text{minimize } \alpha_{\text{i}} \tag{6.65}$$

subject to:

$$\begin{bmatrix} \mathbf{A}(\rho)^{\text{T}}\mathbf{P}_{\text{i}} + \mathbf{P}_{\text{i}}\mathbf{A}(\rho) - \alpha\mathbf{P}_{\text{i}} - \mathbf{X}_{\text{i}}^{\text{T}}\mathbf{B}(\rho)\mathbf{B}(\rho)^{\text{T}}\mathbf{P}_{\text{i}} - \mathbf{P}_{\text{i}}^{\text{T}}\mathbf{B}(\rho)\mathbf{B}(\rho)^{\text{T}}\mathbf{X}_{\text{i}} \\ + \mathbf{X}_{\text{i}}^{\text{T}}\mathbf{B}(\rho)\mathbf{B}(\rho)^{\text{T}}\mathbf{X}_{\text{i}} \\ \Big(\mathbf{B}(\rho)^{\text{T}}\mathbf{P}_{\text{i}} + \mathbf{K}_{\text{SOF}}\mathbf{C}_{\text{y,SOF}}(\rho)\Big) \\ \Big(\mathbf{B}(\rho)^{\text{T}}\mathbf{P}_{\text{i}} + \mathbf{K}_{\text{SOF}}\mathbf{C}_{\text{y,SOF}}(\rho)\Big)^{\text{T}} \\ -\mathbf{I} \end{bmatrix} < 0, \quad \forall\rho \in \mathcal{P}$$

$$\mathbf{P} > 0 \tag{6.65a}$$

Set $\alpha_{\text{i}}^* = \alpha_{\text{i}}$

step 3: If $\alpha_{\text{i}}^* \leq 0$, $\mathbf{K}_{\text{SOF}}$ is a stabilizing SOF for the system, stop

step 4: If $\alpha_{\text{i}}^* > 0$ solve the LMI problem:

$$\text{minimize } \text{trace}(\mathbf{P}_{\text{i}}) \tag{6.66}$$

subject to: (6.65a) with $\alpha_{\text{i}} = \alpha_{\text{i}}^*$

Set $\mathbf{P}_{\text{i}}^* = \mathbf{P}_{\text{i}}$

step 5: If (6.66) is infeasible, set $\alpha_{\text{i}} = \alpha_{\text{i}}^* + \Delta_\alpha$, for $\Delta_\alpha > 0$ and go to step 4.

step 6: If $||\mathbf{X}_{\text{i}} - \mathbf{P}_{\text{i}}^*|| < \delta$, a prescribed tolerance, the system might not be SOF stabilizable, stop. Else set $i = i + 1$ and $\mathbf{X}_{\text{i}} = \mathbf{P}_{\text{i-1}}^*$ and go to step 2.

The termination criteria in step 3 terminates when a stabilizing controller has been found. From the implementation of α, whenever this value is lower than zero, every closed loop pole is in the left half plane, which means the system is stabilized by $\mathbf{K}_{\text{SOF}}$. The termination criteria in step 6, $||\mathbf{X}_\text{i} - \mathbf{P}_\text{i}^*|| < \delta$ terminates the algorithm because the system might not be stabilizable by a SOF. The condition originates from (6.58), where the inequality becomes an equality for $\mathbf{P} = \mathbf{X}$. This implies from theorem 3, that since the algorithm has not found a $\mathbf{K}_{\text{SOF}}$, then the system is not be stabilizable by SOF.

Applying the algorithm to the HVAC system with the uncertainty set $\bar{\mathcal{P}} = \left\{\rho \in \mathcal{P} \mid \Delta_\rho = [-1,1]\right\}$, yields a feasible solution with the step response shown on figure 6.17.

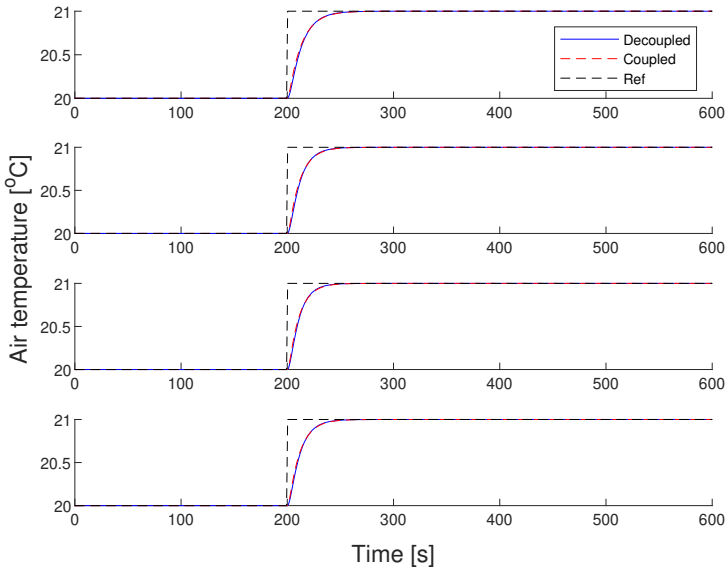

Figure 6.17: Step response of the coupled and decoupled system with $\mathbf{K}_{\text{SOF}}$ synthesised using algorithm 1.

From the response it can be seen the controller is able to reach the reference in a desirable manner, as it rises slowly and has no overshoot. The response is however much faster than the desired response investigated in section 6.4.6. As such it is of interest to investigate if a better response can be achieved. Before this is investigated, the three step method is examined.

Three step method

This method synthesises a stabilizing controller for (6.53) by transforming the problem to an LMI by using a $\mathbf{P}$ calculated from a previous equation. $\mathbf{P}$ has significant impact on which controllers can be synthesised from solving (6.53), and as such, $\mathbf{P}$ should be

found such that a stable controller exists. To find a $\mathbf{P}$ the method utilizes that [13]:

Theorem 4 ([13] [9]) *The realization* $(\boldsymbol{A}, \boldsymbol{B}, \boldsymbol{C}_{\text{y,SOF}})$ *is robust stabilizable towards polytopic uncertainties* ρ *via static output feedback if and only if the realization is simultaneously stabilizable and detectable (SSD).*

This means that SSD guarantees the existence of SOF controller which stabilizes the system. To determine if a realization is SSD the following must be feasible [13]:

$$\begin{aligned} \mathbf{A}(\rho)^{\mathrm{T}}\mathbf{P} + \mathbf{P}\mathbf{A}(\rho) - \mathbf{P}\mathbf{B}(\rho)\mathbf{B}(\rho)^{\mathrm{T}}\mathbf{P} < 0, \quad \forall \quad \rho \in \mathcal{P} \\ \mathbf{A}(\rho)^{\mathrm{T}}\mathbf{P} + \mathbf{P}\mathbf{A}(\rho) - \sigma\mathbf{C}_{\text{y,SOF}}(\rho)^{\mathrm{T}}\mathbf{C}_{\text{y,SOF}}(\rho) < 0, \quad \forall \quad \rho \in \mathcal{P} \end{aligned} \tag{6.67}$$

with $\mathbf{P} > 0$ and a scalar $\sigma > 0$. This condition guarantees the existence of a SOF controller, however (6.67) is a QMI, and it is therefore desirable to reformulate the stability condition. This can be achieved by implementing a SF controller $\mathbf{K}_{\text{SF}}$, which means (6.67) becomes:

$$\begin{aligned} \Big(\mathbf{A}(\rho) + \mathbf{B}(\rho)\mathbf{K}_{\text{SF}}\Big)^{\mathrm{T}}\mathbf{P} + \mathbf{P}\Big(\mathbf{A}(\rho) + \mathbf{B}(\rho)\mathbf{K}_{\text{SF}}\Big)^{\mathrm{T}} < 0, \quad \forall \quad \rho \in \mathcal{P} \\ \mathbf{A}(\rho)^{\mathrm{T}}\mathbf{P} + \mathbf{P}\mathbf{A}(\rho) - \sigma\mathbf{C}_{\text{y,SOF}}(\rho)^{\mathrm{T}}\mathbf{C}_{\text{y,SOF}}(\rho) < 0, \quad \forall \quad \rho \in \mathcal{P} \end{aligned} \tag{6.68}$$

with $\mathbf{P} > \mathbf{I}$ and a scalar $\sigma > 0$. If this LMI is feasible, then the realization is Simultaneously K-stable and detectable (SKSD), meaning the given $\mathbf{K}$ stabilizes the system while simultaneously the system is detectable. From the definition of SKSD, it is a sufficient condition for SSD [13]. This implies that if (6.68) is feasible, then the realization $(\mathbf{A}(\rho), \mathbf{B}(\rho), \mathbf{C}_{\text{y,SOF}}(\rho))$ is stabilizable by a static output feedback. Given this, the $\mathbf{P}$ found from (6.68) can be used in (6.53). It is worth noting that in (6.68) $\mathbf{P} - \mathbf{I} > 0$, this change is to improve numerical design in (6.53) [13]. Simply solving (6.53) using $\mathbf{P}$ will find any controller for which (6.53) is feasible. This could potentially lead to controllers with large values, which for most systems is undesirable. To rectify this, the feasibility problem (6.53) is turned into a minimisation problem, where the values of $\mathbf{K}_{\text{SOF}}$ is minimized [13]. This is achieved by minimising the vectorization $\mathbf{k} = \text{vec}(\mathbf{K}_{\text{SOF}})$ wrt. a scaled-2-norm defined by a positive definite $\mathbf{M}$ [13]. That is $||\mathbf{k}||_{\text{M2}} = \sqrt{\mathbf{k}^{\mathrm{T}}\mathbf{M}^{-1}\mathbf{k}}$. Introducing this minimisation to the feasibility problem (6.53) results in the minimisation problem:

$$\text{minimize } \gamma \tag{6.69}$$

subject to:

$$\begin{gathered}\begin{bmatrix}\gamma & \mathbf{k}^{\mathrm{T}} \\ \mathbf{k} & \mathbf{M}\end{bmatrix} > 0 \\ \Big(\mathbf{A}(\rho)+\mathbf{B}(\rho)\mathbf{K}_{\mathrm{SOF}}\mathbf{C}_{\mathrm{y,SOF}}(\rho)\Big)^{\mathrm{T}}\mathbf{P}+\mathbf{P}\Big(\mathbf{A}(\rho)+\mathbf{B}(\rho)\mathbf{K}_{\mathrm{SOF}}\mathbf{C}_{\mathrm{y,SOF}}(\rho)\Big) < 0, \\ \forall \quad \rho \in \mathcal{P}\end{gathered} \tag{6.69a}$$

where $\mathbf{k}$ is the vectorization of $\mathbf{K}_{\mathrm{SOF}}$, and $\mathbf{M}$ is a positive definite matrix describing the norm for which $\mathbf{k}$ is minimized. ($\mathbf{M} = \mathbf{I}$ corresponds to minimising $\mathbf{K}_{\mathrm{SOF}}$ wrt. the Frobenious norm).

From (6.69), it is clear that the $\mathbf{K}_{\mathrm{SOF}}$ found is dependent on the $\mathbf{P}$ used, this implies that there might be a smaller $\mathbf{K}_{\mathrm{SOF}}$ wrt. the chosen scaled-2-norm, however to find this, a corresponding $\mathbf{P}$ must be found first [13]. Furthermore, given $\mathbf{P}$ is dependent on $\mathbf{K}_{\mathrm{SF}}$, it is clear that the choice of SF impacts the SOF, which unfortunately means that there might exist some SSD systems where a $\mathbf{K}_{\mathrm{SF}}$ is found, but (6.68) is infeasible [13]. As this is the case, it is important that $\mathbf{K}_{\mathrm{SF}}$ is derived such that the system is SKSD [9]. A method for deriving a $\mathbf{K}_{\mathrm{SF}}$, which for LTI systems works in most cases, can be formulated in terms of minimising an invariant ellipsoid while solving for stability of the SF system (6.14) [9]. If the size of the ellipsoid is interpreted as the sum of its radii, then this can be achieved by the LMI minimisation problem [9]:

$$\text{minimize } \operatorname{trace}(\mathbf{Q}) \tag{6.70}$$

subject to:

$$\begin{gathered}\mathbf{Q}-\mathbf{I} > 0 \\ \mathbf{Q}\mathbf{A}(\rho)^{\mathrm{T}}+\mathbf{A}(\rho)\mathbf{Q}+\mathbf{Y}^{\mathrm{T}}\mathbf{B}(\rho)^{\mathrm{T}}+\mathbf{B}(\rho)\mathbf{Y} < 0, \quad \forall \quad \rho \in \mathcal{P}\end{gathered} \tag{6.70a}$$

Summarising the method, the algorithm for synthesising a controller is formulated as:

Algorithm 2: Synthesis of static output feedback controller [9]

Input : $\mathbf{A}(\rho)$, $\mathbf{B}(\rho)$, $\mathbf{C}_{\text{y,SOF}}(\rho)$ and α

Output: $\mathbf{K}_{\text{SOF}}$

step 1: Define $\mathbf{A}_\alpha(\rho) = \mathbf{A}(\rho) + \alpha\mathbf{I}$

step 2: Solve the LMI problem:

$$\text{minimize } \text{trace}(\mathbf{Q}) \tag{6.71}$$

subject to:

$$\begin{aligned} \mathbf{Q} - \mathbf{I} &> 0 \\ \mathbf{Q}\mathbf{A}_\alpha(\rho)^{\text{T}} + \mathbf{A}_\alpha(\rho)\mathbf{Q} + \mathbf{Y}^{\text{T}}\mathbf{B}(\rho)^{\text{T}} + \mathbf{B}(\rho)\mathbf{Y} &< 0, \quad \forall \quad \rho \in \mathcal{P} \end{aligned} \tag{6.71a}$$

step 3: Recover the SF controller

$$\mathbf{K}_{\text{SF}} = \mathbf{Y}\mathbf{Q}^{-1} \tag{6.72}$$

step 4: Solve the LMI feasibility problem

$$\text{find } \mathbf{P}, \sigma \tag{6.73}$$

such that:

$$\begin{aligned} \mathbf{P} &> \mathbf{I} \\ \Big(\mathbf{A}_\alpha(\rho) + \mathbf{B}(\rho)\mathbf{K}_{\text{SF}}\Big)^{\text{T}}\mathbf{P} + \mathbf{P}\Big(\mathbf{A}_\alpha(\rho) + \mathbf{B}(\rho)\mathbf{K}_{\text{SF}}\Big) &< 0, \quad \forall \quad \rho \in \mathcal{P} \\ \mathbf{A}_\alpha(\rho)^{\text{T}}\mathbf{P} + \mathbf{P}\mathbf{A}_\alpha(\rho) - \sigma\mathbf{C}_{\text{y,SOF}}(\rho)^{\text{T}}\mathbf{C}_{\text{y,SOF}}(\rho) &< 0, \quad \forall \quad \rho \in \mathcal{P} \\ \sigma &> 0 \end{aligned} \tag{6.73a}$$

step 5: Solve the LMI minimisation problem:

$$\text{minimize } \gamma \tag{6.74}$$

subject to:

$$\begin{aligned} \begin{bmatrix} \gamma & \mathbf{k}^{\text{T}} \\ \mathbf{k} & \mathbf{M} \end{bmatrix} &> 0 \\ \Big(\mathbf{A}_\alpha(\rho) + \mathbf{B}(\rho)\mathbf{K}_{\text{SOF}}\mathbf{C}_{\text{y,SOF}}(\rho)\Big)^{\text{T}}\mathbf{P} + \mathbf{P}\Big(\mathbf{A}_\alpha(\rho) & \\ + \mathbf{B}(\rho)\mathbf{K}_{\text{SOF}}\mathbf{C}_{\text{y,SOF}}(\rho)\Big) &< 0, \quad \forall \quad \rho \in \mathcal{P} \end{aligned} \tag{6.74a}$$

where $\mathbf{k}$ is the vectorization of $\mathbf{K}_{\text{SOF}}$, and $\mathbf{M}$ is a positive semidefinite matrix describing the norm for which $\mathbf{k}$ is minimized. ($\mathbf{M} = \mathbf{I}$ is the Frobenious norm).

Applying the algorithm to the HVAC system with $\alpha = 0$ the uncertainty set $\bar{\mathcal{P}} = \left\{\rho \in \mathcal{P} \mid \Delta_\rho = [-1,1]\right\}$, yields a feasible solution with the step response shown on figure 6.18a.

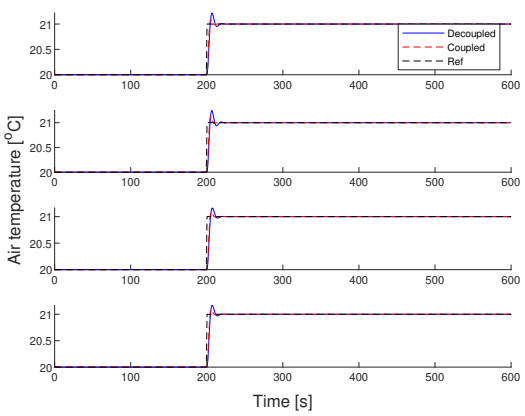

(a) Step response of the coupled and decoupled system with $\mathbf{K}_{\text{SOF}}$ synthesised using algorithm 2 with $\alpha = 0$.

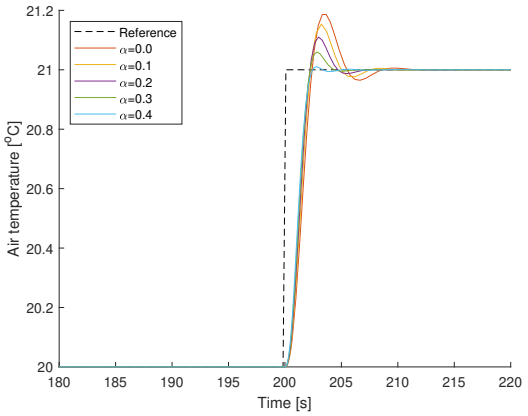

(b) Step response of the coupled system without uncertainties, with $\mathbf{K}_{\text{SOF}}$ synthesised using algorithm 2 with different values of α.

Figure 6.18: Step response of the coupled and decoupled system with $\mathbf{K}_{\text{SOF}}$ synthesised using algorithm 2.

From figure 6.18a it can be seen that the response of the system is aggressive and overshoots by a significant amount before quickly dropping and settling at the reference value. It is important to note that SKSD is dependent on the SF controller found in step 2 and 3 of algorithm 2. This implies that by adjusting the SF controller, the SOF controller will also be adjusted. As such, the algorithm is attempted with $\alpha = 0.5$, unfortunately this resulted in a conservative controller that was unable to adjust to the reference. This was assumed to be because the uncertainty requires the α-stability to be satisfied at each vertex. Nevertheless, to illustrate the influence of α, step responses for systems with controllers synthesised on the nominal plant for different values of α is shown on figure 6.18b. From figure 6.18b, it can be seen how adjusting α impacts the response by reducing the overshoot. This results illustrate how α affects the system, while not being applicable for the system investigated due to the uncertainties. Due to this, it is investigated if different methods for deriving the SF controller can yield a more desirable performing SOF controller.

Comparison

From figure 6.17 and figure 6.18 it can be seen that very different responses is achievable for SOF controllers. Particular the different synthesis methods resulted in very different

responses, as the three step method produced more aggressive controllers, while the ILMI is more relaxed.

6.4.8 Examination of SOF with performance

The previous examination showed two different methods for deriving a robust SOF controller for the HVAC system. This examination expands on this and introduces performance through FWMM as described in section 6.4.6. To introduce FWMM, the realization $(\mathbf{A}, \mathbf{B}, \mathbf{C}_{\text{y,SOF}})$ must be expanded to include the relation between $\tilde{\mathbf{w}}$ and $\begin{bmatrix} \tilde{\mathbf{z}} & \mathbf{z}_{\text{u}} \end{bmatrix}^{\text{T}}$. This relation can be expressed by the open loop system in (6.45). By removing the rows and columns relating to $\mathbf{w}_\Delta$ and $\mathbf{z}_\Delta$ and closing the control loop, the closed loop system becomes:

$$\begin{aligned} \dot{\mathbf{x}}_{\text{DS}} &= \mathbf{A}_{\text{DS}}\mathbf{x}_{\text{DS}} + \mathbf{B}_{\text{DS}}\tilde{\mathbf{w}} \\ \mathbf{z}_{\text{DS}} &= \mathbf{C}_{\text{DS}}\mathbf{x}_{\text{DS}} + \mathbf{D}_{\text{DS}}\tilde{\mathbf{w}} \end{aligned} \tag{6.75}$$

where

$$\mathbf{x}_{\text{DS}} = \begin{bmatrix} \mathbf{x} & \mathbf{x}_{\text{ww}} & \mathbf{x}_{\text{wz}} & \mathbf{x}_{\text{wref}} & \mathbf{x}_{\text{wu}} \end{bmatrix}^{\text{T}}, \qquad \mathbf{z}_{\text{DS}} = \begin{bmatrix} \tilde{\mathbf{z}} & \mathbf{z}_{\text{u}} \end{bmatrix}^{\text{T}} \tag{6.75a}$$

$$\mathbf{A}_{\text{DS}} = \underbrace{\begin{bmatrix} \mathbf{A} & \mathbf{B}_{\text{w}}\mathbf{C}_{\text{ww}} & \mathbf{0}_{12\times4} & \mathbf{0}_{12\times4} & \mathbf{0}_{12\times4} \\ \mathbf{0}_{4\times12} & \mathbf{A}_{\text{ww}} & \mathbf{0}_{4\times4} & \mathbf{0}_{4\times4} & \mathbf{0}_{4\times4} \\ \mathbf{B}_{\text{wz}} & -\mathbf{B}_{\text{wz}}\mathbf{D}_{\text{wref}} & \mathbf{A}_{\text{wz}} & -\mathbf{B}_{\text{wz}}\mathbf{C}_{\text{wref}} & \mathbf{0}_{4\times4} \\ \mathbf{0}_{4\times12} & \mathbf{B}_{\text{wref}}\mathbf{C}_{\text{ww}} & \mathbf{0}_{4\times4} & \mathbf{A}_{\text{wref}} & \mathbf{0}_{4\times4} \\ \mathbf{0}_{4\times12} & \mathbf{0}_{4\times4} & \mathbf{0}_{4\times4} & \mathbf{0}_{4\times4} & \mathbf{A}_{\text{wu}} \end{bmatrix}}_{\bar{\mathbf{A}}_{\text{DS}}} + \underbrace{\begin{bmatrix} \mathbf{B}_{\text{u}} \\ \mathbf{0}_{4\times4} \\ \mathbf{0}_{4\times4} \\ \mathbf{0}_{4\times4} \\ \mathbf{B}_{\text{wu}} \end{bmatrix}}_{\bar{\mathbf{B}}_{\text{DS}}} \mathbf{K}_{\text{SOF}} \underbrace{\begin{bmatrix} \mathbf{C}_{\text{y,SOF}} \\ \mathbf{0}_{8\times4} \\ \mathbf{0}_{8\times4} \\ \mathbf{0}_{8\times4} \\ \mathbf{0}_{8\times4} \end{bmatrix}^{\text{T}}}_{\bar{\mathbf{C}}_{\text{DS,2}}} \tag{6.75b}$$

$$\mathbf{C}_{\text{DS}} = \underbrace{\begin{bmatrix} \mathbf{D}_{\text{wz}}\mathbf{C}_{\text{z}} & -\mathbf{D}_{\text{wz}}\mathbf{D}_{\text{ref}}\mathbf{C}_{\text{ww}} & \mathbf{C}_{\text{wz}} & -\mathbf{D}_{\text{wz}}\mathbf{C}_{\text{wref}} & \mathbf{0}_{4\times4} \\ \mathbf{0}_{4\times12} & \mathbf{0}_{4\times4} & \mathbf{0}_{4\times4} & \mathbf{0}_{4\times4} & \mathbf{C}_{\text{wu}} \end{bmatrix}}_{\bar{\mathbf{C}}_{\text{DS,1}}} + \underbrace{\begin{bmatrix} \mathbf{0}_{4\times4} \\ \mathbf{D}_{\text{wu}} \end{bmatrix}}_{\bar{\mathbf{D}}_{\text{DS,1}}} \mathbf{K}_{\text{SOF}} \underbrace{\begin{bmatrix} \mathbf{C}_{\text{y,SOF}} \\ \mathbf{0}_{8\times4} \\ \mathbf{0}_{8\times4} \\ \mathbf{0}_{8\times4} \\ \mathbf{0}_{8\times4} \end{bmatrix}^{\text{T}}}_{\bar{\mathbf{C}}_{\text{DS,2}}} \tag{6.75c}$$

$$\mathbf{B}_{\mathrm{DS}} = \begin{bmatrix} \mathbf{B}_{\mathrm{w}}\mathbf{D}_{\mathrm{ww}} \\ \mathbf{B}_{\mathrm{ww}} \\ -\mathbf{B}_{\mathrm{wz}}\mathbf{D}_{\mathrm{wref}}\mathbf{D}_{\mathrm{ww}} \\ \mathbf{B}_{\mathrm{wref}}\mathbf{D}_{\mathrm{ww}} \\ \mathbf{0}_{4\times 4} \end{bmatrix}, \qquad \mathbf{D}_{\mathrm{DS}} = \begin{bmatrix} -\mathbf{D}_{\mathrm{wz}}\mathbf{D}_{\mathrm{wref}}\mathbf{D}_{\mathrm{ww}} \\ \mathbf{0}_{4\times 4} \end{bmatrix} \tag{6.75d}$$

The system (6.75) is missing the uncertainties from (6.47). This is due to the SOF investigation assuming the uncertainties are polytopic, and hence defined explicitly in $\mathbf{B}_{\mathrm{u}} = \mathbf{B}(\rho)$. That is $\mathbf{B}(\rho) = \mathbf{B}(\mathbf{I}_4 + \mathrm{diag}(\rho)\mathbf{W}_\Delta)$, $\forall \rho \in \mathcal{P}$. Using this description the two previous SOF algorithms are investigated to include the FWMM.

ILMI

The H_∞ bound used in FWMM can be introduced into the ILMI algorithm by redefining the variables of the realization $(\mathbf{A}, \mathbf{B}, \mathbf{C}_{\mathrm{y,SOF}})$ [12]. By writing the bounded real lemma for the closed loop system (6.75), it can be shown that it is equivalent to:

$$\bar{\mathbf{A}}^{\mathrm{T}}\bar{\mathbf{P}} + \bar{\mathbf{P}}\bar{\mathbf{A}} + \bar{\mathbf{P}}\bar{\mathbf{B}}\mathbf{K}_{\mathrm{SOF}}\bar{\mathbf{C}} + (\bar{\mathbf{P}}\bar{\mathbf{B}}\mathbf{K}_{\mathrm{SOF}}\bar{\mathbf{C}})^{\mathrm{T}} < 0 \tag{6.76}$$

where

$$\bar{\mathbf{P}} = \begin{bmatrix} \mathbf{P}_{\mathrm{DS}} & \mathbf{0}_{28\times 4} & \mathbf{0}_{28\times 8} \\ \mathbf{0}_{4\times 28} & \mathbf{I}_4 & \mathbf{0}_{4\times 8} \\ \mathbf{0}_{8\times 28} & \mathbf{0}_{8\times 4} & \mathbf{I}_8 \end{bmatrix}, \qquad \bar{\mathbf{A}} = \begin{bmatrix} \bar{\mathbf{A}}_{\mathrm{DS}} & \mathbf{B}_{\mathrm{DS}} & \mathbf{0}_{28\times 8} \\ \mathbf{0}_{4\times 28} & -\gamma/2\mathbf{I}_4 & \mathbf{0}_{4\times 8} \\ \bar{\mathbf{C}}_{\mathrm{DS},1} & \mathbf{D}_{\mathrm{DS}} & -\gamma/2\mathbf{I}_8 \end{bmatrix}, \tag{6.76a}$$

$$\bar{\mathbf{B}} = \begin{bmatrix} \bar{\mathbf{B}}_{\mathrm{DS}}(\rho) \\ \mathbf{0}_{4\times 4} \\ \bar{\mathbf{D}}_{\mathrm{DS},1} \end{bmatrix}, \qquad \bar{\mathbf{C}} = \begin{bmatrix} \bar{\mathbf{C}}_{\mathrm{DS},2} & \mathbf{0}_{8\times 4} & \mathbf{0}_{8\times 8} \end{bmatrix} \tag{6.76b}$$

with $\mathbf{P}_{\mathrm{DS}} > 0$. The inequality (6.76), is the static output stability problem (6.52) for the system defined by ($\bar{\mathbf{A}}$,$\bar{\mathbf{B}}$,$\bar{\mathbf{C}}$), and hence can be solved using the ILMI algorithm 1. Unlike the method from section 6.4.6, when implemented on the ILMI algorithm, γ cannot be minimised and is instead selected to a specific value before the algorithm is started. When γ is a constant, it becomes a tuning parameter, which is inversely related to $\mathbf{W}_{\mathrm{z}}$. Due to this, γ is selected to be one, and instead $\mathbf{W}_{\mathrm{z}}$ is used to tune the response in a manner similar to section 6.4.6.

This change of variable cause the optimisation problem for finding the initial $\mathbf{X}$ from (6.63) to become an unbounded problem. Instead, to find an initial $\mathbf{X}$, the SF with

FWMM from section 6.4.6 can be solved, and from that solution $\mathbf{X} = \mathbf{Q}_{\text{DS}}^{-1}$ can be used. Choosing $\mathbf{X}$ as this, guarantees the initial value is stable for state feedback, similar to how (6.63) found an initial stable $\mathbf{X}$ in the original algorithm.

Using the desired reference from (6.49) with $\mathbf{W}_{\text{u}} = \mathbf{0}_{4\times4}$ and the output weight $\mathbf{W}_{\text{z}}$ from (6.77) a controller was synthesised, with the system response shown on figure 6.19.

$$\mathbf{W}_{\text{z}}(s) \overset{ss}{=} \left[\begin{array}{c|c} \mathbf{0}_{4\times4} & \mathbf{0}_{4\times4} \\ \hline \mathbf{0}_{4\times4} & 6.5\mathbf{I}_4 \end{array}\right] \tag{6.77}$$

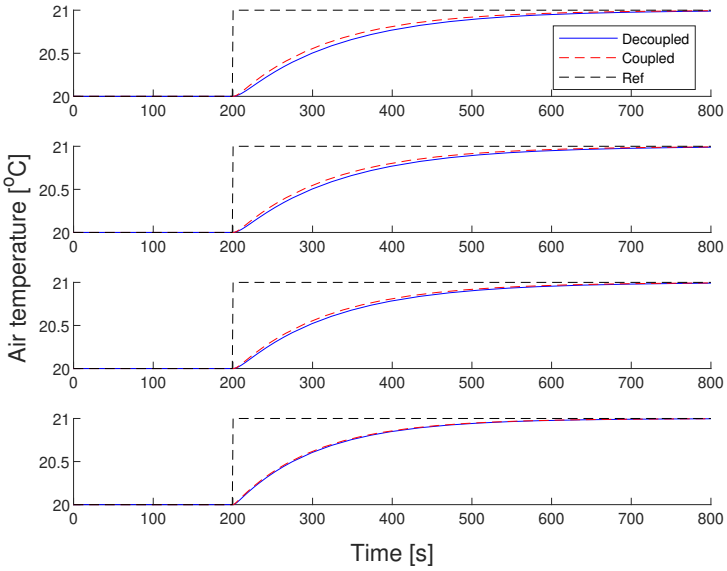

Figure 6.19: Step response of the coupled and decoupled system with a $\mathbf{K}_{\text{SOF}}$ synthesised from ILMI algorithm with FWMM.

From the step response on figure 6.19, it can be seen that the synthesised SOF controller yields a response similar to the desired $\mathbf{W}_{\text{ref}}$. It can therefore be concluded, that the procedure can synthesise a robust stable controller with a desired system response.

Three step method

FWMM can be included into the three step method by adjusting step 2, calculation of the SF controller, and step 4, finding the $\mathbf{P}$ that is used in the SOF calculation. This approach assumes that by adjusting these two steps to find a SF matching the desired response, and then applying that to find a $\mathbf{P}$, this $\mathbf{P}$ yields a SOF controller with a

similar response to the SF. The initial SF controller can be found by solving:

$$\text{minimize } \gamma \tag{6.78}$$

subject to:

$$\begin{bmatrix} \mathbf{Q}_{\mathrm{DS}}\bar{\mathbf{A}}_{\mathrm{DS}}^{\mathrm{T}} + \bar{\mathbf{A}}_{\mathrm{DS}}\mathbf{Q}_{\mathrm{DS}} + \hat{\mathbf{Y}}_{\mathrm{DS}}^{\mathrm{T}}\bar{\mathbf{B}}_{\mathrm{DS}}^{\mathrm{T}}(\rho) + \bar{\mathbf{B}}_{\mathrm{DS}}(\rho)\hat{\mathbf{Y}}_{\mathrm{DS}} & \mathbf{B}_{\mathrm{DS}} & \mathbf{Q}_{\mathrm{DS}}\bar{\mathbf{C}}_{\mathrm{DS},1}^{\mathrm{T}} + \hat{\mathbf{Y}}_{\mathrm{DS}}^{\mathrm{T}}\bar{\mathbf{C}}_{\mathrm{DS},2}^{\mathrm{T}} \\ \star & -\gamma\mathbf{I}_4 & \mathbf{D}_{\mathrm{DS}}^{\mathrm{T}} \\ \star & \star & -\gamma\mathbf{I}_8 \end{bmatrix} < 0, \quad \forall\rho \in \mathcal{P} \tag{6.78a}$$

$$\mathbf{Q}_{\mathrm{DS}} = \begin{bmatrix} \mathbf{Q} & \mathbf{Q}_{1,2} & \mathbf{Q}_{1,3} & \mathbf{Q}_{1,4} & \mathbf{Q}_{1,5} \\ \star & \mathbf{Q}_{2,2} & \mathbf{Q}_{2,3} & \mathbf{Q}_{2,4} & \mathbf{Q}_{2,5} \\ \star & \star & \mathbf{Q}_{3,3} & \mathbf{Q}_{3,4} & \mathbf{Q}_{3,5} \\ \star & \star & \star & \mathbf{Q}_{4,4} & \mathbf{Q}_{4,5} \\ \star & \star & \star & \star & \mathbf{Q}_{5,5} \end{bmatrix} > 0, \qquad \gamma > 0 \tag{6.78b}$$

with $\mathbf{Q} = \mathrm{diag}(\mathbf{Q}_1, \ldots, \mathbf{Q}_{\mathrm{n}})$, $\mathbf{Q}_{\mathrm{i}} \in \mathbb{R}^{3\times3}$, $\mathbf{Q}_{\mathrm{i,j}}$ appropriate dimensions, and the matrices given by (6.75). From this, the SF controller can be found as $\bar{\mathbf{K}}_{\mathrm{DS}} = \hat{\mathbf{Y}}_{\mathrm{DS}}\mathbf{Q}_{\mathrm{DS}}^{-1}$ and used to find a $\mathbf{P}$ by solving:

$$\text{minimize } \gamma \tag{6.79}$$

subject to:

$$\begin{bmatrix} \left(\bar{\mathbf{A}}_{\mathrm{DS}} + \bar{\mathbf{B}}_{\mathrm{DS}}(\rho)\bar{\mathbf{K}}_{\mathrm{DS}}\right)^{\mathrm{T}}\mathbf{P}_{\mathrm{DS}} + \mathbf{P}_{\mathrm{DS}}\left(\bar{\mathbf{A}}_{\mathrm{DS}} + \bar{\mathbf{B}}_{\mathrm{DS}}(\rho)\bar{\mathbf{K}}_{\mathrm{DS}}\right) & \mathbf{P}_{\mathrm{DS}}\mathbf{B}_{\mathrm{DS}} & \left(\bar{\mathbf{C}}_{\mathrm{DS},1} + \bar{\mathbf{D}}_{\mathrm{DS},1}\bar{\mathbf{K}}_{\mathrm{DS}}\right)^{\mathrm{T}} \\ \mathbf{P}_{\mathrm{DS}}\mathbf{B}_{\mathrm{DS}}^{\mathrm{T}} & -\gamma\mathbf{I}_4 & \mathbf{D}_{\mathrm{DS}}^{\mathrm{T}} \\ \left(\bar{\mathbf{C}}_{\mathrm{DS},1} + \bar{\mathbf{D}}_{\mathrm{DS},1}\bar{\mathbf{K}}_{\mathrm{DS}}\right) & \mathbf{D}_{\mathrm{DS}} & -\gamma\mathbf{I}_8 \end{bmatrix} < 0, \quad \forall\rho \in \mathcal{P} \tag{6.79a}$$

$$\mathbf{P}_{\mathrm{DS}} = \begin{bmatrix} \mathbf{P} & \mathbf{P}_{1,2} & \mathbf{P}_{1,3} & \mathbf{P}_{1,4} & \mathbf{P}_{1,5} \\ \star & \mathbf{P}_{2,2} & \mathbf{P}_{2,3} & \mathbf{P}_{2,4} & \mathbf{P}_{2,5} \\ \star & \star & \mathbf{P}_{3,3} & \mathbf{P}_{3,4} & \mathbf{P}_{3,5} \\ \star & \star & \star & \mathbf{P}_{4,4} & \mathbf{P}_{4,5} \\ \star & \star & \star & \star & \mathbf{P}_{5,5} \end{bmatrix} > 0, \qquad \gamma > 0 \tag{6.79b}$$

with $\mathbf{P} = \text{diag}(\mathbf{P}_1, \ldots, \mathbf{P}_n)$, $\mathbf{P}_i \in \mathbb{R}^{3\times3}$ and $\mathbf{P}_{i,j}$ appropriate dimensions. From this equation, $\mathbf{P}$ can be extracted from $\mathbf{P}_{DS}$ in (6.79b) and used to solve the minimisation problem (6.74) to find a SOF controller, with the desired performance.

When synthesising a controller to match the desired response, the algorithm fails to produce a SOF controller from the derived SF controller. This result shows the downside to this algorithm, while it is faster than the ILMI, it does not cover the entire SSD space, but only SKSD, which in this case results in it not being able to find a SOF controller, even though the ILMI algorithm can produce one.

Results 7

The previous chapter resulted in the development of two design procedures, one for a SF controller and one for a SOF controller, where their response could be matched to a desired response and fulfil the requirements from chapter 3. Controllers synthesised using these design procedures showed a satisfactory response based on a linear simulation of the system. These linear simulations does however not represent the real system accurately. As such, the controllers synthesised using the procedures are tested on a non-linear simulation of both the coupled and decoupled system, which gives a better understanding of the expected real world behaviour.

The controllers are synthesised to match the desired response of a first order system, with a settling time of ten minutes. To achieve the response the tuning parameters for the design procedures was chosen as:

$$\mathbf{W}_{\text{ref}}(s) \overset{ss}{=} \left[\begin{array}{c|c} -\frac{1}{120}\mathbf{I}_4 & \frac{1}{8}\mathbf{I}_4 \\ \hline \frac{1}{15}\mathbf{I}_4 & \mathbf{0}_{4\times4} \end{array}\right], \qquad \mathbf{W}_{\text{u}}(s) \overset{ss}{=} \left[\begin{array}{c|c} \mathbf{0}_{4\times4} & \mathbf{0}_{4\times4} \\ \hline \mathbf{0}_{4\times4} & \mathbf{0}_{4\times4} \end{array}\right] \tag{7.1}$$

$$\mathbf{W}_{\text{z,SF}}(s) \overset{ss}{=} \left[\begin{array}{c|c} \mathbf{0}_{4\times4} & \mathbf{0}_{4\times4} \\ \hline \mathbf{0}_{4\times4} & 5\mathbf{I}_4 \end{array}\right], \qquad \mathbf{W}_{\text{z,SOF}}(s) \overset{ss}{=} \left[\begin{array}{c|c} \mathbf{0}_{4\times4} & \mathbf{0}_{4\times4} \\ \hline \mathbf{0}_{4\times4} & 6.5\mathbf{I}_4 \end{array}\right] \tag{7.2}$$

The response of the two simulations can be seen on figure 7.1a and figure 7.1b.

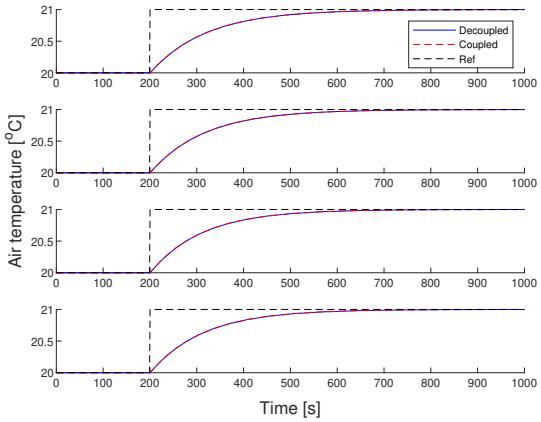

(a) Step response of the coupled and decoupled system, using the nonlinear simulation, with a SF controller.

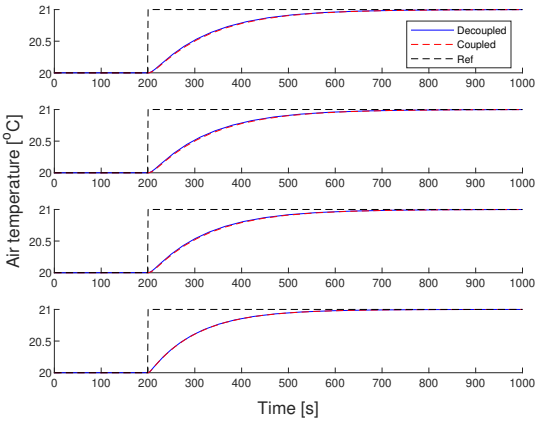

(b) Step response of the coupled and decoupled system, using the nonlinear simulation, with a SOF controller.

Figure 7.1: Step response using the nonlinear simulation.

From figure 7.1a, it can be seen the response, for both the coupled and decoupled system, matches the desired response as the response has a settling time of 594 s. Looking at figure 7.1b, these responses also follow the desired response, however they settle slightly slower. Specifically the settling time was found to be 608s. From this, it can be concluded that both design procedures synthesises a controller with a satisfactory performance, and even though the SF performs most similar to the desired response, the small lose in performance in SOF is acceptable considering the wider application for SOF controllers. To visualise how well the FWMM is, the desired response is shown on figure 7.2 with the response of AHU 1, from both the SF and SOF simulations.

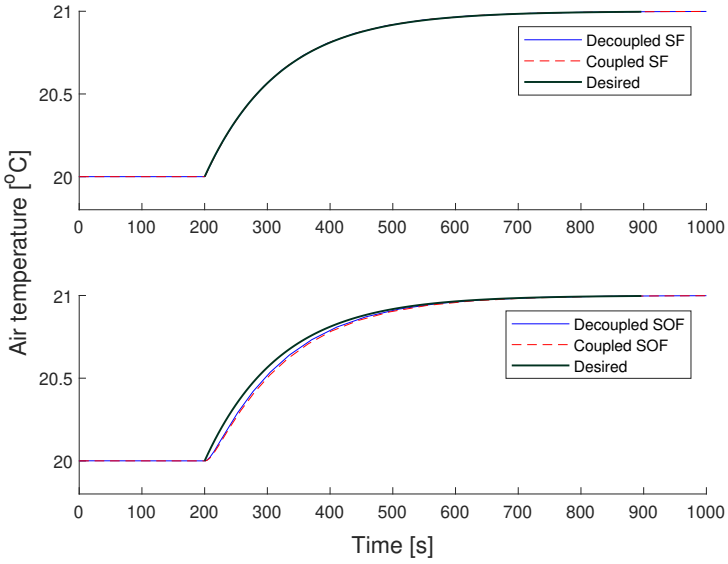

Figure 7.2: Step response of the desired and AHU 1 from both the SF and SOF simulations.

Figure 7.2 shows the responses follows almost identical to the desired response. To illustrate the design procedures are able to follow other responses, a new response with a settling time of two minutes is chosen for which controllers are synthesised. These responses can be seen on figure 7.3, and was found by adjusting the desired response to:

$$\mathbf{W}_{\text{ref}}(s) \stackrel{ss}{=} \left[\begin{array}{c|c} -\frac{1}{24}\mathbf{I}_4 & \frac{1}{4}\mathbf{I}_4 \\ \hline \frac{1}{6}\mathbf{I}_4 & \mathbf{0}_{4\times 4} \end{array}\right] \tag{7.3}$$

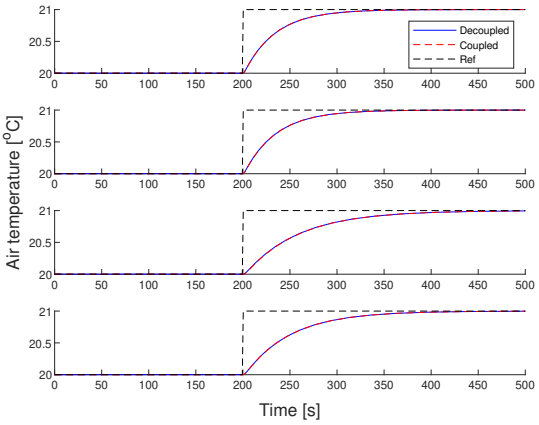

(a) Step response of the coupled and decoupled system, using the nonlinear simulation, with a SF controller.

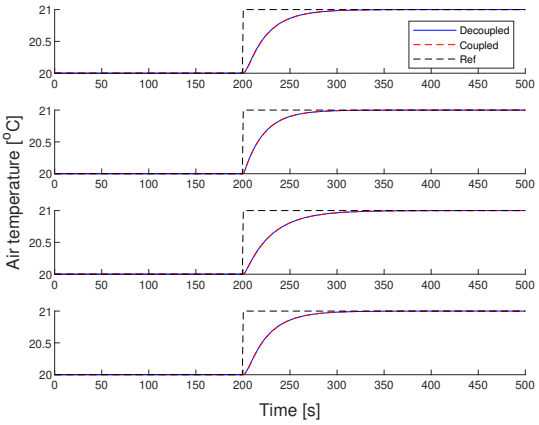

(b) Step response of the coupled and decoupled system, using the nonlinear simulation, with a SOF controller.

Figure 7.3: Step response using the nonlinear simulation with a two minute settling time as a desired response.

From figure 7.3a, it can be seen that the response adjusted to the change of $\mathbf{W}_{\text{ref}}$, however it has a slower settling time of 164 s. On the other hand the SOF controller with the system response on figure 7.3b, has a settling time of 121 s, which is close to the desired response of 120 s. This shows that both design procedures are able to adjust to a change in desired response.

Discussion 8

This chapter explore and analyse the outcome of the project, with particular focus on assumptions and design choices made in the preceding chapters, and how these correspond to real life scenarios. Furthermore, alternatives which might improve design or real world applicability is introduced and discussed.

The water to air heat exchanger model derived in section 4.1, was assumed to be homogeneous, meaning the entire water to air heat exchanger (WAHE) was discretized as a single control volume, which results in equal convection along the control volume. If instead, the WAHE was modelled using multiple control volumes cascaded, the temperature changes through the WAHE would be described, which would better describe the dynamics, at the cost of increasing the complexity. The increased complexity would greatly impact the design of the state feedback (SF) controller, as this requires a measurement or estimate for each state, hence more sensors or an observer would be required. On the other hand, the static output feedback (SOF) would properly not be affected, as it only requires the knowledge of the currently available outputs. This implies the method for SOF may be applied. Nevertheless, the exact impact on both SF and SOF could be of interest to investigate.

The hydraulic model derived in section 4.2, was modelled as static due to the assumption that the hydraulics is significantly faster then the thermodynamics. For the system model, this assumption is valid, however, for the weight of the uncertainty, the missing dynamics leaves out information, which could have been used to better describe the uncertainties. This in turn affects the determinations of robust stability, as the frequency content could be significant compared to the constant gain used. This could either open or limit the uncertainty range, for which the impact could be interesting to examine.

Noise and disturbances of the exogenous input were disregarded in the report to simplify the system derivation and testing of the design procedures, as stated in section 6.2. If these were modelled, it would better describe how these affect the system.

However, the disturbances would describe deviations in the model, which could potentially be included in uncertainties, and therefore be accounted for in the controller design. Furthermore, the controller design includes an integrator, which compensates for any low frequency disturbances, e.g. the airflow and inlet water temperature. The noise in the exogenous input consist of measurement noise of the system, and as such is usually high frequency. Given the lowpass frequency response of the system, these high frequency disturbances is attenuated, furthermore, since the system has feedback, the impact of the noise is reduced. Nevertheless, the noise and disturbances could be investigated for a more thorough analysis.

The weights used to tune the stability and performance of the synthesized controller, were all structured as either pass though or a first order low-pass filter. These simple structures were chosen, as their effect on the system is easy to understand. More complex filters, which might lead to a better stability and/or performance, could be used. These however, require more knowledge about the specific system and desired response, so specific parts can be targeted, whereas the simple filters aim at a more general part of the response. Nevertheless, investigating the impact of higher order weights could be of interest.

The three step method could not synthesise a SOF controller matching the desired response, which lead to the assumption that the system was not simultaneously k-stable and detectable (SKSD). However, the results of the previous steps in the algorithm was investigated. Here it was found that step 4 found a $\mathbf{P}$ and σ fulfilling the constraints (6.73), which implied the system should be SKSD, and as such a controller should exist for the given $\mathbf{P}$. Following this, the found $\mathbf{P}$ was used in the condition for simultaneously stabilizable and detectable (SSD) from (6.67), which found the condition was not meet. This discovery contradicts that SKSD is sufficient for SSD, furthermore, the same was validated for the robust stability case in section 6.4.7, which also found the system was not SSD for the given $\mathbf{P}$. This discovery implies that either the algorithm may be implemented wrong, or an error exists in the theory behind the algorithm.

The uncertainties was, in this project, interpreted as either norm-bounded by the ∞-norm or as polytopic. The different interpretations is due to difficulties in calculating real norm-bounded uncertainties with the structured singular value. Instead, the polytopic uncertainties where introduced, which are almost identical. The norm-bounded uncertainties are defined as $||\Delta||_\infty \leq 1$, which defines an n-dimensional solid hypercube. Similar, the polytopic uncertainties are defined as the convex hull of the vertices, and given the vertices are $\{-1,1\}^n$, these also define an n-dimensional solid hypercube. As

such, the difference between the uncertainties are that this project only allows real vertices in the polytopic case, while the norm-bounded also include complex uncertainties.

Conclusion 9

This report set out to derive a design procedure that could synthesise a robust controller for an heating ventilation and air condition (HVAC) system with a distributed pump design. The synthesised controller should stabilize the HVAC both with the coupling in the hydraulic network and without the coupling.

To that end, a model was derived for the HVAC with distributed pumping. Firstly, the thermodynamics in the water to air heat exchanger was expressed in terms of a one phase energy balance with the water and air temperature as states and using the flow as inputs. After this, the hydraulic network was described using a static expression, which gave a relation between the flow and angular velocity of the pumps. The hydraulics was modeled in two different ways, one where the coupling of the pumps were expressed, and one where these were ignore. Following this, the two models were used to replace the flow as inputs in the thermodynamics, which resulted in two nonlinear state space models. Lastly, the models where linearised resulting in two linear state space models.

Following this, different procedures was examined to determine if robust stability could be achieved. The initial method, based on [3], was not able to achieve robust stability. Building on the approach, it was found that a weight, describing the uncertainty, could be obtained from the difference between the coupled and decoupled model. Using this uncertainty, a method was found that could synthesis a state feedback (SF) controller which robustly stabilized the system and with a response that can be designed by model matching. Based on the achieved SF, it was then examined if a static output feedback (SOF) controller could be synthesised with similar results. Redefining the uncertainties as polytopic, a procedure, using linear parameter varying theory, was designed such that a robust stable SOF controller was obtained, which were also tuneable by frequency weighted model matching.

The SF and SOF controllers, which were synthesised from the linear system, was tested on the nonlinear simulations to validate their performance in a more realistic setting. These simulations showed both controllers performed close to identical to the desired response, with the SF controller performing slightly better than the SOF.

Bibliography

[1] Octávio Alves, Eliseu Monteiro, Paulo Brito, and Pedro Romano. Measurement and classification of energy efficiency in hvac systems. *Energy and Buildings*, 130: 408–419, 2016. ISSN 0378-7788. doi: https://doi.org/10.1016/j.enbuild.2016.08.070. URL `https://www.sciencedirect.com/science/article/pii/S0378778816307800`.

[2] Carsten Kallesøe, Brian Nielsen, and Agisilaos Tsouvalas. Heat balancing in cooling systems using distributed pumping. *IFAC-PapersOnLine*, 53:3292–3297, 01 2020. doi: 10.1016/j.ifacol.2020.12.1139.

[3] John Leth and Carsten Kallesøe. Stability of distributed pump configuration for cooling systems. In *European Control Conference Sweden*, June 2022.

[4] Fernando D. Bianchi, H. De Battista, and Ricardo Mantz. *Wind turbine control systems: Principles, modelling and gain scheduling design.* Advances in Industrial Control series. Springer-Verlag London Ltd., London, 2007. ISBN 978-1846284922.

[5] Sigurd Skogestad and Ian Postlethwaite. *Multivariable Feedback Control: Analysis and Design.* John Wiley & Sons, Inc., Hoboken, NJ, USA, 2005. ISBN 0470011688.

[6] Carsten W. Scherer. Theory of robust control. `https://www.imng.uni-stuttgart.de/mst/files/RC.pdf`, 03 24. (Accessed on 03/07/2024).

[7] C. Briat. *Linear Parameter-Varying And Time-Delay Systems.* Springer, 2014. ISBN 9783662440506.

[8] Grundfos, 2024. URL `https://product-selection.grundfos.com/dk/products/magna/magna3/magna3-100-120-f-97924315?pumpsystemid=2336567952&tab=variant-curves`. accesed on 05-03-24.

[9] Robert E. Benton and Dirk Smith. A non-iterative lmi-based algorithm for robust static-output-feedback stabilization. *International Journal of Control*, 72(14): 1322–1330, 1999. doi: 10.1080/002071799220290.

[10] Mahdieh S. Sadabadi and Dimitri Peaucelle. From static output feedback to structured robust static output feedback: A survey. *Annual Reviews in Control*, 42:11–26, 2016. ISSN 1367-5788. doi: https://doi.org/10.1016/j.arcontrol.2016.09.014. URL `https://www.sciencedirect.com/science/article/pii/S1367578816300852`.

[11] Brian DO Anderson and John B Moore. Linear system optimisation with prescribed degree of stability. In *Proceedings of the Institution of Electrical Engineers*, volume 116, pages 2083–2087. IET, 1969.

[12] YONG-YAN CAO, JAMES LAM, and YOU-XIAM SUN. Static output feedback stabilization: An ilmi approach. *Automatica*, 34(12):1641–1645, 1998. ISSN 0005-1098. doi: https://doi.org/10.1016/S0005-1098(98)80021-6. URL `https://www.sciencedirect.com/science/article/pii/S0005109898800216`.

[13] R.E. Benton and D. Smith. Output-feedback stabilisation with prescribed degree of stability. In *Proceedings of the 1997 American Control Conference (Cat. No.97CH36041)*, volume 1, pages 499–504 vol.1, 1997. doi: 10.1109/ACC.1997.611849.

[14] J. Löfberg. Yalmip : A toolbox for modeling and optimization in matlab. In *In Proceedings of the CACSD Conference*, Taipei, Taiwan, 2004.

Determination of controllability

I

This appendix explores the controllability of the individual WAHE's when they have been linearised using a first order Taylor approximation. To determine wether the model is controllable, the determinant of the controllability matrix is calculated to determine if the matrix has full order. The controllability matrix is defined as:

$$\mathcal{C} = \begin{bmatrix} \mathbf{B} & \mathbf{AB} & \dots & \mathbf{A}^{n-1}\mathbf{B} \end{bmatrix} \tag{I.1}$$

The matrices $\mathbf{A}$ and $\mathbf{B}$ are found from the linearised model (4.22) as:

$$\begin{aligned} \mathbf{A} &= \begin{bmatrix} -\left(\frac{q_{\mathrm{i}}^*}{V_{\mathrm{w,i}}} + \frac{B_{\mathrm{i}}}{C_{\mathrm{w}}\rho_{\mathrm{w}}V_{\mathrm{w,i}}}\right) & \frac{B_{\mathrm{i}}}{C_{\mathrm{w}}\rho_{\mathrm{w}}V_{\mathrm{w,i}}} & 0 \\ \frac{B_{\mathrm{i}}}{C_{\mathrm{a}}\rho_{\mathrm{a}}V_{\mathrm{a,i}}} & -\left(\frac{Q_{\mathrm{i}}}{V_{\mathrm{a,i}}} + \frac{B_{\mathrm{i}}}{C_{\mathrm{a}}\rho_{\mathrm{a}}V_{\mathrm{a,i}}}\right) & 0 \\ 0 & 1 & 0 \end{bmatrix} \\ \mathbf{B} &= \begin{bmatrix} \left(\frac{T_{\mathrm{w,c}} - T_{\mathrm{w,i}}^*}{V_{\mathrm{w,i}}}\right) \\ 0 \\ 0 \end{bmatrix} \end{aligned} \tag{I.2}$$

The individual columns of the controllability matrix is calculated individually to simplify the process. Note that $\mathbf{B}$ only has a value on the first entry, which means that only the first column in $\mathbf{A}$ and $\mathbf{A}^2$ will have an influence in the controllability matrix, and as such only these columns are found. In the case of $\mathbf{A}$ the first column is already derived, and therefore the first column ($\mathbf{A}_1^2$) of $\mathbf{A}^2$ is calculated.

$$\mathbf{A}_1^2 = \begin{bmatrix} \left(\frac{q_{\mathrm{i}}^*}{V_{\mathrm{w,i}}} + \frac{B_{\mathrm{i}}}{C_{\mathrm{w}}\rho_{\mathrm{w}}V_{\mathrm{w,i}}}\right)^2 + \frac{B_{\mathrm{i}}}{C_{\mathrm{w}}\rho_{\mathrm{w}}V_{\mathrm{w,i}}}\frac{B_{\mathrm{i}}}{C_{\mathrm{a}}\rho_{\mathrm{a}}V_{\mathrm{a,i}}} \\ \frac{B_{\mathrm{i}}}{C_{\mathrm{a}}\rho_{\mathrm{a}}V_{\mathrm{a,i}}}\left(-\left(\frac{q_{\mathrm{i}}^*}{V_{\mathrm{w,i}}} + \frac{B_{\mathrm{i}}}{C_{\mathrm{w}}\rho_{\mathrm{w}}V_{\mathrm{w,i}}}\right) - \left(\frac{Q_{\mathrm{i}}}{V_{\mathrm{a,i}}} + \frac{B_{\mathrm{i}}}{C_{\mathrm{a}}\rho_{\mathrm{a}}V_{\mathrm{a,i}}}\right)\right) \\ \frac{B_{\mathrm{i}}}{C_{\mathrm{a}}\rho_{\mathrm{a}}V_{\mathrm{a,i}}} \end{bmatrix} \tag{I.3}$$

With $\mathbf{A}_1^2$ derived, the controllability matrix can be expressed as:

$$\boldsymbol{\mathcal{C}} = \begin{bmatrix} \left(\frac{T_{\mathrm{w,c}}-T^*_{\mathrm{w,i}}}{V_{\mathrm{w,i}}}\right) & -\left(\frac{q^*_{\mathrm{i}}}{V_{\mathrm{w,i}}}+\frac{B_{\mathrm{i}}}{C_{\mathrm{w}}\rho_{\mathrm{w}}V_{\mathrm{w,i}}}\right)\left(\frac{T_{\mathrm{w,c}}-T^*_{\mathrm{w,i}}}{V_{\mathrm{w,i}}}\right) & \left(\left(\frac{q^*_{\mathrm{i}}}{V_{\mathrm{w,i}}}+\frac{B_{\mathrm{i}}}{C_{\mathrm{w}}\rho_{\mathrm{w}}V_{\mathrm{w,i}}}\right)^2+\frac{B_{\mathrm{i}}}{C_{\mathrm{w}}\rho_{\mathrm{w}}V_{\mathrm{w,i}}}\frac{B_{\mathrm{i}}}{C_{\mathrm{a}}\rho_{\mathrm{a}}V_{\mathrm{a,i}}}\right)\left(\frac{T_{\mathrm{w,c}}-T^*_{\mathrm{w,i}}}{V_{\mathrm{w,i}}}\right) \\ 0 & \frac{B_{\mathrm{i}}}{C_{\mathrm{a}}\rho_{\mathrm{a}}V_{\mathrm{a,i}}}\left(\frac{T_{\mathrm{w,c}}-T^*_{\mathrm{w,i}}}{V_{\mathrm{w,i}}}\right) & \frac{B_{\mathrm{i}}}{C_{\mathrm{a}}\rho_{\mathrm{a}}V_{\mathrm{a,i}}}\left(-\left(\frac{q^*_{\mathrm{i}}}{V_{\mathrm{w,i}}}+\frac{B_{\mathrm{i}}}{C_{\mathrm{w}}\rho_{\mathrm{w}}V_{\mathrm{w,i}}}\right)-\left(\frac{Q_{\mathrm{i}}}{V_{\mathrm{a,i}}}+\frac{B_{\mathrm{i}}}{C_{\mathrm{a}}\rho_{\mathrm{a}}V_{\mathrm{a,i}}}\right)\right)\left(\frac{T_{\mathrm{w,c}}-T^*_{\mathrm{w,i}}}{V_{\mathrm{w,i}}}\right) \\ 0 & 0 & \frac{B_{\mathrm{i}}}{C_{\mathrm{a}}\rho_{\mathrm{a}}V_{\mathrm{a,i}}}\left(\frac{T_{\mathrm{w,c}}-T^*_{\mathrm{w,i}}}{V_{\mathrm{w,i}}}\right) \end{bmatrix} \tag{I.4}$$

From this the determinant is calculated using the co-factor method which results in the determinant:

$$\det(\boldsymbol{\mathcal{C}}) = \left(\frac{T_{\mathrm{w,c}}-T^*_{\mathrm{w,i}}}{V_{\mathrm{w,i}}}\right)^3\left(\frac{B_{\mathrm{i}}}{C_{\mathrm{a}}\rho_{\mathrm{a}}V_{\mathrm{a,i}}}\right)^2 \tag{I.5}$$

For a system to be controllable the determinant must be different from zero. From (I.5) the specific heat capacity (C_{a}) and density (ρ_{a}) are physical constants which are different from zero, in addition the heat transfer coefficient (B_i) is different from zero, since there is always an exchange of heat between air and water. The presence of the WAHE implies the volumes $V_{\mathrm{w,i}}$ and $V_{\mathrm{a,i}}$ are different from zero. This means that that the determinant is zero only when the temperature of the water is the same as the temperature of the chiller.

Given the operating point of the water is found from the operating point of the air temperature, it is investigated for which values of $T^*_{\mathrm{a,i}}$ the determinant becomes zero. Using (4.21) where $T^*_{\mathrm{w,i}} = T_{\mathrm{w,c}}$ and isolating for the air temperature results in:

$$T^*_{\mathrm{a,i}} = \frac{T_{\mathrm{w,c}}B_{\mathrm{i}} + C_{\mathrm{a}}\rho_{\mathrm{a}}Q_{\mathrm{i}}T_{\mathrm{a,amb}}}{(B_{\mathrm{i}} + C_{\mathrm{a}}\rho_{\mathrm{a}}Q_{\mathrm{i}})} \tag{I.6}$$

For the four WAHEs and their parameters found on table 6.1, the temperatures resulting in singularities are:

$$T_{\mathrm{a}} = \begin{bmatrix} 289.4 \\ 289.4 \\ 289.4 \\ 289.4 \end{bmatrix} \tag{I.7}$$

YALMIP II

This appendix briefly gives an introduction to the software used to solve the optimisation problems and issues regarding this.

II.1 YALMIP

To solve the problems a toolbox for MATLAB called YALMIP is utilized. YALMIP is a modelling and optimisation toolbox that is capable of solving a variety of optimisation problems. YALMIP does not exactly solve the problems itself, instead it is a general interface to multiple solvers that can be installed [14]. This means that the same definitions and notation can be used for every solver supported by YALMIP, and then YALMIP will figure out the translation to the specific solver. For this project a solver called MOSEK is utilized. As mentioned YALMIP mainly functions as a interface, and as such explanations of its definitions and structure is necessary.

II.1.1 Variables

When defining optimisation variables the *sdpvar(n,m,type,field)* function is called. This function then generates a variable of the size and type defined by the input parameters. The first two parameters indicate the size of the variable, while the type referees to the structure of the variable either 'symmetric' or 'full' and the last referees to the variable being complex or real. It is worth noting the function can be overloaded when creating symmetric matrices, and as such a symmetric $n \times n$ matrix can be defined as either:

```
1 p=sdpvar(n);
2 p=sdpvar(n,n);
3 p=sdpvar(n,n,'symmetric');
```

In the case a specific structure of the variable is desired, such as an diagonal matrix, the variable can be declared as above and then used as an input parameter to the normal MATLAB diag function:

```
1 X = diag(sdpvar(n,1));
```

II.1.2 Constraints

In YALMIP constraints are interpreted depending on the context in which it is written. In the case where both the left-and right-hand side are Hermitian, then the constraint is interpreted as the definiteness, while in other cases it is interpreted as element-wise constraints. Therefore the two different types of constraints can be declared as:

```
n = 3;
P = sdpvar(n);
C1 = [P >= 0];          % Definitness
C2 = [P(:,1) >= 0];     % Element-wise
```

When multiple constraints is present within the same problem, these can be combined by concatenating them as:

```
C = [C1, C2];
```

It is worth noting that YALMIP returns an error if a strict inequality is used and advises that non-strict inequality should be used instead. In practice, the change from strict to non-strict has no actual impact when applied to numerical solvers, as solvers applies tolerances when solving, and as such only return a solution within some threshold of the actual solution [14].

II.1.3 Objective function and solving

The objective function is declared as traditionally in MATLAB. The solution to the problem is found by using the *optimize(Constraints,Objective,options)* function. This function solves the objective function subject to the constraints using the options specified. This function assumes the objective is a minimisation problem, which means that if the problem is to maximize an objective, the objective should be multiplied by -1. The options parameter is where the user can specify the, among other things, which solver should be used. As the MOSEK solver is used, the options is specified as:

```
options = sdpsettings('solver','mosek');
```

When YALMIP/mosek has found a solution, the numeric from the optimisation variable can be retrieved by calling *value(var)*. Furthermore if the constraints is of interest, a function called *check(constraints)*, can be called to retrieve the solved information of the constraints.